Advancements in decadal climate predictability: the role of nonoceanic drivers

AGU PUBLICATIONS

Reviews of Geophysics

REVIEW ARTICLE
10.1002/2014RG000473

Key Points:
- Numerous extraoceanic processes active over the decadal scale are established
- Current ESMs underrepresent processes relevant for decadal predictability
- Predictive skill assessment is hampered by lack of observations

Correspondence to:
A. Bellucci,
alessio.bellucci@cmcc.it

Citation:
Bellucci, A., et al. (2015), Advancements in decadal climate predictability: The role of nonoceanic drivers, *Rev. Geophys.*, *53*, 165–202, doi:10.1002/2014RG000473.

Received 3 OCT 2014
Accepted 27 JAN 2015
Accepted article online 30 JAN 2015
Published online 1 APR 2015

Advancements in decadal climate predictability: The role of nonoceanic drivers

A. Bellucci[1], R. Haarsma[2], N. Bellouin[3], B. Booth[4], C. Cagnazzo[5], B. van den Hurk[2], N. Keenlyside[6], T. Koenigk[7], F. Massonnet[8], S. Materia[1], and M. Weiss[2]

[1]Centro Euro-Mediterraneo sui Cambiamenti Climatici, Bologna, Italy, [2]Royal Netherlands Meteorological Institute, De Bilt, Netherlands, [3]Department of Meteorology, University of Reading, Reading, Berkshire, UK, [4]Met Office Hadley Centre, Exeter, UK, [5]Istituto di Scienze dell'Atmosfera e del Clima, Consiglio Nazionale delle Ricerche, Rome, Italy, [6]Geophysical Institute University of Bergen, Bergen, Norway, [7]Swedish Meteorological and Hydrological Institute, Norrköping, Sweden, [8]Université Catholique de Louvain, Louvain-la-Neuve, Belgium

Abstract We review recent progress in understanding the role of sea ice, land surface, stratosphere, and aerosols in decadal-scale predictability and discuss the perspectives for improving the predictive capabilities of current Earth system models (ESMs). These constituents have received relatively little attention because their contribution to the slow climatic manifold is controversial in comparison to that of the large heat capacity of the oceans. Furthermore, their initialization as well as their representation in state-of-the-art climate models remains a challenge. Numerous extraoceanic processes that could be active over the decadal range are proposed. Potential predictability associated with the aforementioned, poorly represented, and scarcely observed constituents of the climate system has been primarily inspected through numerical simulations performed under idealized experimental settings. The impact, however, on practical decadal predictions, conducted with realistically initialized full-fledged climate models, is still largely unexploited. Enhancing initial-value predictability through an improved model initialization appears to be a viable option for land surface, sea ice, and, marginally, the stratosphere. Similarly, capturing future aerosol emission storylines might lead to an improved representation of both global and regional short-term climatic changes. In addition to these factors, a key role on the overall predictive ability of ESMs is expected to be played by an accurate representation of processes associated with specific components of the climate system. These act as "signal carriers," transferring across the climatic phase space the information associated with the initial state and boundary forcings, and dynamically bridging different (otherwise unconnected) subsystems. Through this mechanism, Earth system components trigger low-frequency variability modes, thus extending the predictability beyond the seasonal scale.

1. Introduction

Delivering trustworthy climate predictions beyond the seasonal-to-interannual time scale limit is one of the grand challenges currently faced by the climate science community [*Meehl et al.*, 2014a]. While the praxis of seasonal forecast (nowadays routinely operated by several climate centers) is entering into a mature phase, decadal prediction is a relatively novel field of investigation, often referred to as being in its infancy [*Goddard et al.*, 2012; *Cane*, 2010]. Despite its young age, decadal prediction is rooted in a rather longer history of efforts devoted to understand the sources of low-frequency decadal variability found in both observational and model records.

In his seminal analysis of the observed ocean-atmosphere interactions over the midlatitude Atlantic, *Bjerknes* [1964] identified the ocean as a primary driver of decadal and multidecadal climate variability. Bjerknes' results were later corroborated by extended observations [*Gulev et al.*, 2013] and several model-based studies, highlighting the predominant role of ocean dynamics in setting the detected decadal-scale variability, mainly associated with fluctuations in the strength of the Atlantic thermohaline circulation [*Delworth et al.*, 1993; *Delworth and Greatbatch*, 2000; *Griffies and Tziperman*, 1995] and of the wind-driven gyre circulation (as postulated for the extratropical North Pacific; see *Latif and Barnett* [1994] and *Latif* [2006]). The identification in model results of physical mechanisms able to sustain low-frequency variability modes acting at the decadal time scale suggested that similar dynamics might operate in the real world, potentially leading to a consistent degree of predictability in the climate system.

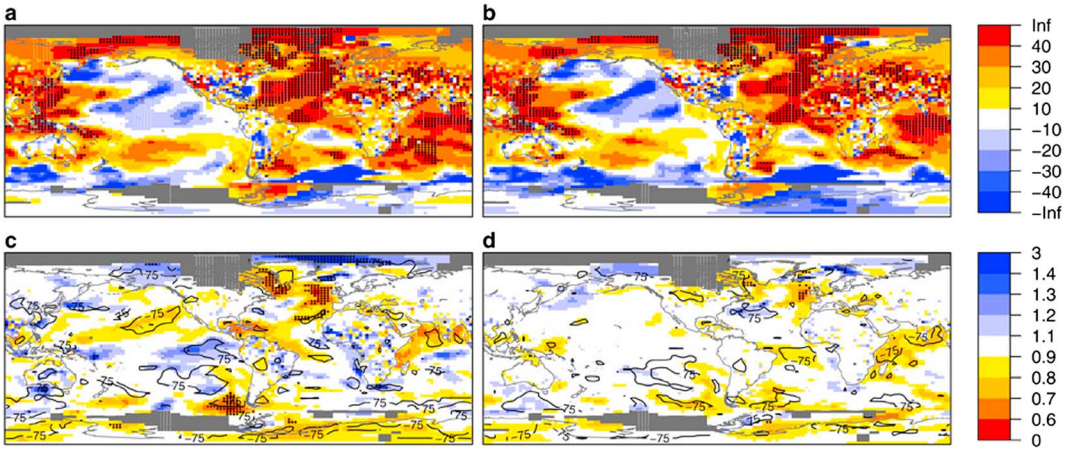

Figure 1. (a, b) Root-mean-square skill score (multiplied by 100) of the ensemble mean of a multimodel set of CMIP5 decadal hindcasts averaged over the forecast years 2–5 (Figure 1a) and 6–9 (Figure 1b). Black dots correspond to the points where the skill score is statistically significant with 95% confidence using a one-sided *F* test taking into account the autocorrelation of the observation minus prediction time series. (c, d) Ratio of root-mean-square errors between the decadal hindcasts and a twin multimodel set of noninitialized historical simulations averaged over the lead years 2–5 (Figure 1c) and 6–9 (Figure 1d). Contours are used for areas where the ratio of at least 75% of the individual forecast systems has a value above or below 1 in agreement with the multimodel ensemble mean result. Dots are used for the points where the ratio is statistically significantly above or below 1 with 90% confidence using a two-sided *F* test that takes into account the autocorrelation of the observation minus prediction time series. Poorly observationally sampled areas are masked in gray. From *Doblas-Reyes et al.* [2013]. Reprinted by permission from Macmillan Publishers Ltd.

The intrinsic predictive capabilities of coupled atmosphere-ocean general circulation models (AOGCMs) have been explored in a number of model-based studies, addressing the predictability of climate state variables using a number of different approaches [*Griffies and Bryan*, 1997; *Boer*, 2000, 2004; *Boer and Lambert*, 2008; *Pohlmann et al.*, 2004; *Collins et al.*, 2006]. These investigations paved the way to the first attempts at real decadal climate prediction, based on the use of AOGCMs initialized with realistic estimates of the oceanic and atmospheric state, and integrated forward for a few decades thus providing a near-term forecast of the climate evolution [*Smith et al.*, 2007; *Keenlyside et al.*, 2008; *Pohlmann et al.*, 2009; *Mochizuki et al.*, 2010].

Our observational knowledge of the ocean state is ever improving and was recently enhanced by the launch of the global Array for Real-Time Geostrophic Oceanography (ARGO) autonomous floats system. There is also increase in confidence in the overall performance of AOGCMs. This perspective has led the climate science community to foster several coordinated efforts aiming at a systematic exploitation of the predictive skill featured by current climate models over interannual to decadal time scales. The multimodel decadal prediction experiments performed as part of the forerunner European Union (EU)-funded ENSEMBLES (ENSEMBLE-based Predictions of Climate Changes and their Impacts) project [*van Oldenborgh et al.*, 2012; *Garcia-Serrano and Doblas-Reyes*, 2012], in particular, were conducive to the design of a specific set of near-term predictions, later included as core experiments in the CMIP5 (Fifth Coupled Model Intercomparison Project) [*Meehl et al.*, 2009b].

The quality of the forecasts delivered by the current generation of decadal prediction systems is illustrated in Figure 1 [*Doblas-Reyes et al.*, 2013], showing patterns of root-mean-square skill score from a multimodel ensemble of CMIP5 near-term predictions (Figures 1a and 1b), and the relative merits and deficiencies with respect to a twin set of noninitialized projections (Figures 1c and 1d). The emerging picture reveals that climate forecast systems have skills in retrospectively predicting temperatures for the past 50 years over vast portions of the Earth's surface. This appears to be primarily determined by changes in the prescribed radiative forcing (in turn associated with changes in the atmospheric composition), but there is also evidence of enhanced skill due to the realistic initialization of the forecast system [*Kirtman et al.*, 2013].

While the impact of ocean state initialization on decadal climate predictability is beginning to be extensively investigated [*Meehl et al.*, 2013; *Hazeleger et al.*, 2013; *Bellucci et al.*, 2014], the additional skill associated with the representation and/or initialization of other components of the climate system, such as the cryosphere, the land surface, the stratosphere, and the aerosols, has received little attention. The underlying reasons for this can be traced back to (i) a lack of an adequate set of observations enabling the initialization of

these components; (ii) the relatively poor understanding of the processes involved within these components that makes it difficult to represent them in models; and (iii) the perception that there is much less potential, compared to the ocean, for the existence of mechanisms involving these components that could contribute to decadal time scale variability and predictability.

There is an ongoing transition from standard AOGCMs to a new generation of enhanced complexity Earth system models (ESMs) that include better resolved scale interactions (e.g., eddy-permitting ocean components and high-top stratosphere-resolving atmospheres), new model components (e.g., marine biogeochemistry, terrestrial vegetation, and atmospheric chemistry), and improved representation of physical processes (e.g., ocean mixing, sea ice physics, and aerosols-clouds interaction). This is resulting in the explicit inclusion of a new set of feedbacks and a considerable extension of the spectrum of model-resolved processes. These, in turn, introduce additional time scales and "memory reservoirs" in the coupled system that ultimately impacts the overall predictability of the climate system over different temporal scales. The progressive enhancement of climate models' complexity and the related emergence of new processes and interactions within and across individual subsystems disclose new opportunities for advancing the predictive capabilities of climate prediction systems beyond the limit currently set by the ocean predictability.

As climate forecast systems lag behind the most recent model developments, the benefits for predictive skill stemming from using higher complexity dynamical models has been poorly explored. Yet there has recently been substantial progress in understanding several extraoceanic mechanisms that may potentially strengthen the predictive capabilities of the next generation of climate forecast systems over the multiyear/decadal range. It is therefore timely to review the current knowledge of these climate processes and mechanisms. Clearly, trustworthy decadal climate predictions are only feasible if supported by a reliable (and, in the perspective of moving to an operational phase, ideally real-time) observational infrastructure, enabling a realistic model initialization and validation.

The aim of this paper is to provide an overview of the state-of-the-art knowledge of the processes that may potentially enhance the decadal-scale predictability of the climate state, focusing in particular on the role of the sea ice, land surface (including soil moisture and vegetation), stratosphere, and aerosols. Also, an overview of the relevant observing systems and the perspectives for making useful decadal predictions by including and initializing these components in the current generation of Earth system models are provided.

The paper structure reflects this concept. Individual sections describe the role of sea ice (section 2), land surface (section 3), stratosphere (section 4), and aerosols (section 5) on decadal-scale predictability. Individual sections are further partitioned into subsections overviewing the corresponding mechanisms relevant for decadal predictability, available observational data sets viable for model initialization, and the perspectives for improving the current decadal forecast systems. Finally, conclusive remarks are provided in section 6.

2. Sea Ice

The rather thin layer of sea ice plays an important role in the climate system. It controls the transfers of heat, momentum, and matter between ocean and atmosphere. It effectively reflects the incoming solar radiation but acts as an almost perfect black body for the outgoing long-wave radiation. Sea ice contributes to a colder local climate and stabilizes the atmospheric stratification. Persistence of sea ice could therefore contribute to improved climate prediction skill. The transport of sea ice is determined by wind forcing, ocean currents, and sea surface gradient, and it affects climate downstream. Melting and freezing, controlled by the surface energy budget, are associated with freshwater and salt fluxes into the ocean, respectively, and can strongly affect the ocean stratification and circulation. This and the export of sea ice and freshwater out of the Arctic can affect the global ocean circulation and contribute to predictability on decadal to multidecadal time scales.

Given the importance of sea ice for both oceanic and atmospheric processes, the accurate initialization and representation of sea ice in climate prediction models will potentially result in largely improved predictions. A fundamental limitation for assessing sea ice prediction skill is the lack of observations to perform adequately initialized hindcasts to robustly quantify predictability. The hindcasts performed for CMIP5 start with 1960 as the initial year. However, satellite retrievals of sea ice concentration have been

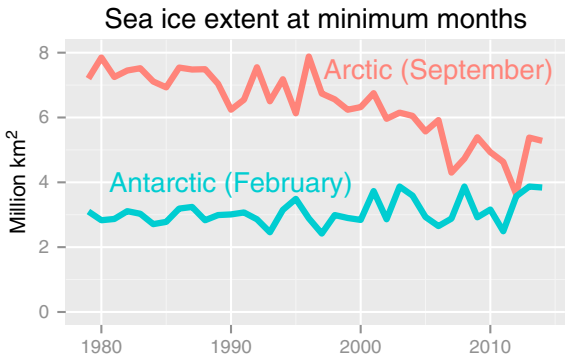

Figure 2. Arctic and Antarctic Sea Ice Extent, 1979–2014. Courtesy of National Snow and Ice Data Center (NSIDC), *Fetterer et al.* [2014].

available from the late 1970s, and sea ice thickness data are widely considered to be inadequate for most CMIP5 hindcast period. New satellite products of sea ice thickness will improve the situation in the future.

In the following, we will highlight sea ice-related processes that may be a source of interannual to decadal predictability, followed by a discussion of the availability of sea ice observations and the perspectives for future decadal predictions.

2.1. Mechanisms

2.1.1. Predictability in the Arctic

The Arctic has been rapidly warming in the last decades at a rate of about twice the global mean warming. Likely sources for the Arctic temperature amplification are the ice albedo feedback [*Serreze et al.*, 2009], enhanced meridional energy transports [*Graversen et al.*, 2008], changes in cloud and water vapor [*Graversen and Wang*, 2009], and enhanced ocean heat transports particularly into the Barents Sea [*Smedsrud et al.*, 2013; *Koenigk and Brodeau*, 2014]. Concurrently, Arctic sea ice area observations indicate strong negative trends in the last decades [*Comiso et al.*, 2008] (Figure 2). The mechanisms behind the trend in sea ice do not only give rise to predictability of the ice itself but potentially also predictability for other variables like air temperature, precipitation and atmospheric circulation, and also Arctic flora and fauna as well as socioeconomic factors [*Meier et al.*, 2014]. Despite the complex nature of the coupled ice-ocean-atmosphere Arctic climate system, it remains debated whether the Arctic climate change exhibits a linear behavior.

Winton [2008] showed that the large-scale Arctic temperature change in the Coupled Model Intercomparison Project Phase 3 (CMIP3) models remains linear well after the complete loss of September sea ice. However, locally, the atmospheric response to sea ice loss might be nonlinear as argued by *Petoukhov and Semenov* [2010]. Furthermore, the Arctic climate is subject to large interannual to decadal variations, which cannot be captured by simplistic statistical models. Therefore, fully coupled dynamical models are essential to represent these complex interactions and to improve predictions of the Arctic climate system.

Predictability studies indicate that sea ice anomalies can persist for up to a few years [*Holland et al.*, 2011; *Koenigk and Mikolajewicz*, 2009; *Tietsche et al.*, 2013], enabling the prediction of both ice and partly also local atmosphere conditions [*Koenigk et al.*, 2009]. *Blanchard-Wrigglesworth et al.* [2011] and *Chevallier and Salas-Melia* [2012] analyzed the persistence of the Arctic sea ice area in observations and models and found a decorrelation time of 2–5 months but a reemergence of summer ice area anomalies in the next year. They suggested that reduced ice area leads to reduced albedo and consequently later freeze up and thinner ice, and thus, the summer ice area signal is stored in the ice thickness. Although these processes are not directly contributing to decadal predictions, they could affect long-term oceanic processes or be part of coupled decadal atmosphere-ocean-sea ice modes in the Arctic, as discussed below.

The transport of sea ice can also contribute to predictability. This is particularly the case in the East Greenland Current: sea ice anomalies that propagate south from Fram Strait in the East Greenland Current, melt, and enter the Labrador Sea after about 2 years as freshwater anomalies. Positive freshwater anomalies reduce the deep water convection in the Labrador Sea, and this might affect the meridional overturning circulation in the North Atlantic. The ocean surface in the Labrador Sea stays also cooler because of less ocean mixing, which prevents warmer water from the deeper ocean reaching the surface. Consequently, more sea ice is formed, air temperature is reduced, and also the large-scale atmospheric circulation might be affected [*Alexander et al.*, 2004; *Kvamstö et al.*, 2004; *Magnusdottir et al.*, 2004]. This entire process is well documented in both observations [*Dickson et al.*, 1988; *Belkin et al.*, 1998] and a number of modeling studies [*Häkkinen*, 1999; *Haak et al.*, 2003; *Koenigk et al.*, 2006]. Prominent examples are the so-called "Great Salinity Anomalies" in the Labrador Sea. Figure 3 shows a clear connection between salinity and ocean temperature in observations. In observations the salinity anomalies can be further traced around the entire subpolar gyre and back into the Nordic Seas, over a period of about 10 years [*Belkin et al.*, 1998].

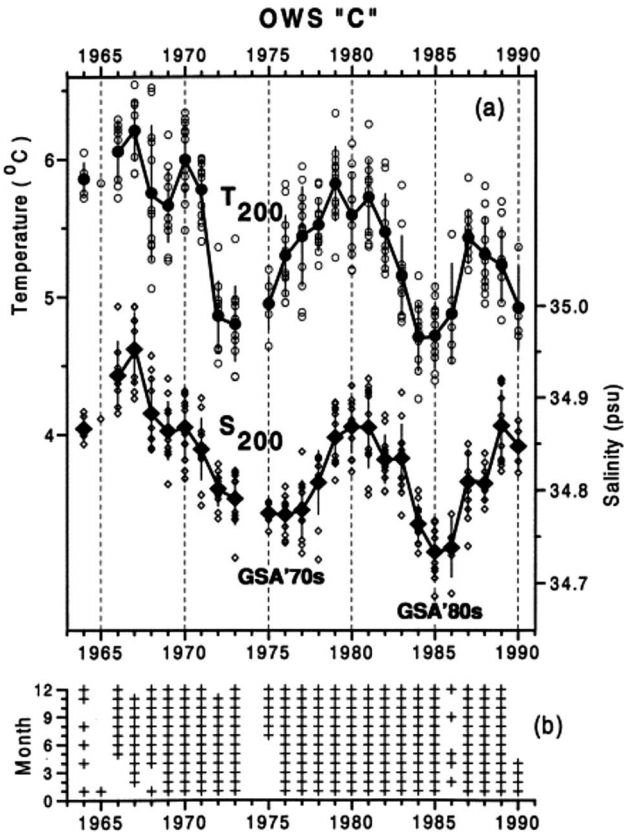

Figure 3. (a) Temperature (circles) and salinity (diamonds) at the 200 m depth at Ocean Weather Station "C" (52°45′N, 35°30′W). Open (solid) symbols show monthly (annual) means. Bars show standard deviations about annual means. (b) Availability of monthly means. From *Belkin et al.* [1998]. Reprinted with permission from Elsevier.

Observations and reconstructions of the Arctic sea ice indicate large decadal variations of Arctic ice extent [*Vinje*, 2001; *Johannessen et al.*, 2004; *Venegas and Mysak*, 2000]. A number of studies suggest Arctic climate modes with time scales of 10–15 years, which fit well to the observed ice variations [*Mysak and Venegas*, 1998; *Proshutinsky and Johnson*, 1997; *Polyakov and Johnson*, 2000; *Arfeuille et al.*, 2000].

However, the explanations for the oscillation period of 10–15 years differ. *Mysak and Venegas* [1998] suggested a negative feedback between Arctic sea ice cover and the Arctic Oscillation (AO) whereby the sea ice area in the Greenland Sea is decisive for switching the sign of the (AO). Similar to this, *Proshutinsky and Johnson* [1997] found cyclonic and anticyclonic atmospheric circulation regimes in the Arctic switching sign every 5–7 years. They argue that negative sea surface temperature (SST) anomalies over the northeastern North Atlantic lead to cyclonic circulation in the Arctic, and this in turn increases ice and freshwater exports out of the Arctic, leading to negative SST anomalies in the northern North Atlantic. *Goosse et al.* [2002] and *Goosse and Holland* [2005] pointed out the importance of meridional ocean and atmosphere heat exchanges between Arctic and North Atlantic for decadal variability in the Arctic. Variations in the Arctic on multidecadal time scales are likely dominated by variations in the oceanic heat transport into the Arctic, modifying Arctic ice volume, sea level gradient, and the export of freshwater into the deep water convection areas, which then modulates the meridional overturning circulation [*Jungclaus et al.*, 2005; *Polyakov et al.*, 2004].

Results from a potential predictability study indicate that decadal averages of Arctic sea ice thickness and area are well predictable along the ice edges in the North Atlantic ice sector [*Koenigk et al.*, 2012] (Figure 4). Connected to the ice variations, air temperature and precipitation show a high potential predictability, particularly in the Labrador and Barents/Kara Seas regions. The predictability was linked to variations in the meridional overturning circulation. First results from decadal hindcasts following the CMIP5 protocol show only limited decadal prediction skill in the Arctic [*Bellucci et al.*, 2014]. However, sea ice initialization in these predictions was based on simple approaches and not consistent with the ocean initialization. Evidence is accumulating that Arctic sea ice and midlatitude atmospheric variability are associated (*Overland and Wang* [2010] and *Budikova* [2009] for a comprehensive review). Whether the recent chain of extreme winters and summers in midlatitudes [*Overland*, 2014] is a direct consequence of the rapid, Arctic sea ice decline remains controversial and highly debated [*Francis and Vavrus*, 2012; *Screen*, 2014; *Thomas*, 2014; *Barnes*, 2013; *Barnes et al.*, 2014]. It has been argued that, in response to Arctic sea ice retreat, the lower atmosphere layers at high latitudes increase in thickness because of anomalous heating of the lower troposphere. This relaxes the poleward temperature gradient between midlatitudes and high latitudes [*Francis et al.*, 2009; *Budikova*, 2009], and this would in turn increase the amplitude of Rossby waves and slow down their progression, favoring theoccurrence of blocking patterns [*Francis and Vavrus*, 2012] and extreme weather conditions. It is, however, not clear whether blocking frequency has actually risen over recent years [*Barnes et al.*, 2014]. In addition,

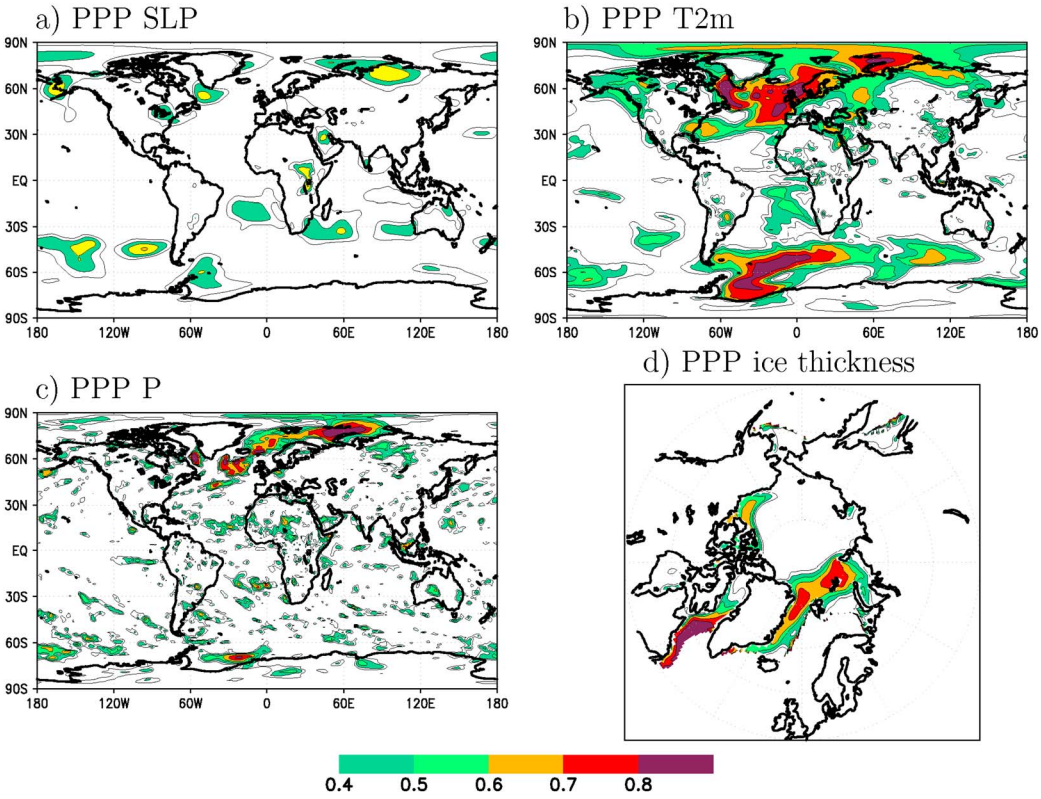

Figure 4. Potential prognostic predictability (PPP) of first decade means of (a) sea level pressure, (b) 2 m air temperature (T2m), (c) precipitation (P), and (d) sea ice thickness from perfect ensemble experiments with the global coupled model EC-Earth. All colored values are significant at 95% level. From *Koenigk et al.* [2012]. PPP is defined as one minus the ratio between the variance among ensemble members at a given time and the variance of a control simulation over time. The smaller the spread among ensemble members compared to the variability of the control simulation, the higher the prognostic potential predictability.

the negative North Atlantic Oscillation (NAO) signature, implied by this proposed mechanism is not clearly found in all model experiments [e.g., *Blüthgen et al.*, 2012; *Wallace et al.*, 2014]. Finally, factors other than sea ice may play an important role in shaping midlatitude weather (e.g., snow: *Cohen et al.* [2012]; see section 4.1), complicating the analysis. Thus, whether sea ice is a source of predictability for lower latitude climate on decadal time scales remains an open question.

2.1.2. Predictability in the Antarctic

One of the dominating climate modes in the Southern Ocean region is the Southern Annular Mode (SAM), which is often defined as the difference of normalized sea level pressure anomalies between 40°S and 65°S [*Gong and Wang*, 1999]. The sign and amplitude of the SAM are a measure of the strength of the westerlies north of the Antarctic. These westerlies strongly affect Antarctic sea ice [*Hall and Visbeck*, 2002]. The Southern Oscillation also significantly influences Antarctic sea ice [*Simmonds and Jacka*, 1995]. In contrast to the Arctic, trends in Antarctic sea ice extent are positive (Figure 2) but with large interregional differences. There are several different explanations for the Antarctic sea ice trends, including local trends in surface winds [*Holland and Kwok*, 2012], positive trends in the precipitation regimes [*Zhang*, 2007], subsurface ocean warming that leads to increased melting of the Antarctic ice shelf, and a cooling and freshening of the ocean surface [*Bintanja et al.*, 2013], and they may simply be a manifestation of low-frequency sea ice decadal variability [*Polvani and Smith*, 2013]. A review of past, recent, and possible future climate conditions is presented by *Mayewski et al.* [2009].

Most of the interest in polar prediction concentrates on the Arctic and much less on the Antarctic. Nonetheless, a few recent studies discuss Antarctic predictability too. Under perfect-model assumptions—i.e., a model is taken to represent reality and used to predict its own climate—Southern Ocean sea ice extent exhibits

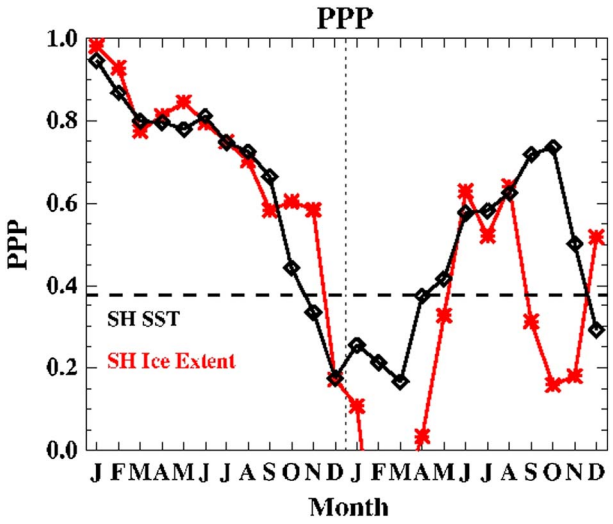

Figure 5. The PPP of surface temperature (black) averaged over the high-latitude southern ocean (south of 60°S) and total Southern Hemisphere sea ice extent (red) for the 2 years of integration. The horizontal dashed line indicates the 95% significance level. From *Holland et al.* [2013].

predictability beyond a year in the Community Climate System Model 3 [*Holland et al.*, 2013] (Figure 5). In perfect-model experiments with a model of intermediate complexity, *Zunz* [2014] found that the model was not able to replicate the short-term (lead time of several years) sea ice extent anomalies but well reproduced the longer-term (10–30 year), lower frequency variability and trends in Southern Ocean sea ice extent. *Koenigk et al.* [2012] showed in a perfect model experiment with EC-Earth that significant decadal predictability of sea ice thickness exists in the Weddell Sea. Their study also shows a high decadal predictability of 2 m temperatures north of the Weddell Sea. However, the processes leading to this predictability remain unclear. *Latif et al.* [2006] argued that the multidecadal variability of SST in the Southern Ocean is anticorrelated with SST in the North Atlantic. However, the connection with the North Atlantic is weak in *Koenigk et al.* [2012].

The inability of current general circulation models (GCMs) to simulate the observed increase in Antarctic sea ice extent, even in ocean-initialized experiments [*Zunz et al.*, 2009], indicates there is a large room for improvement in the simulation of the physical processes and/or in the ocean-sea ice initialization in this hemisphere. To the authors' knowledge, the role of sea ice initialization on the predictability of Southern Ocean climate has not been investigated yet, and research efforts similar to those for the Arctic should be undertaken to bring the research on Antarctic sea ice predictability up-to-date with its northern hemispheric counterpart.

2.2. Observations

In the general context of decadal predictability, observations are extremely valuable in two respects. First, they are used for data assimilation and initialization purposes. That is, a full hybrid state of the studied system can be derived by combining model and observed estimations of the same, unknown, real state. This hybrid state is then used as an initial condition for a prediction: more advanced data assimilation methods are expected to enhance prediction skill. Second, observations serve as a product for model evaluation. Through qualitative and/or quantitative assessment, the model systematic biases can be identified, so that improving the model physics where this is particularly needed can hopefully enhance predictability. Besides, observations are needed for verification of retrospective decadal forecasts and are the ultimate means of evaluating the skill of the decadal forecast systems. In the polar regions where observations are by nature scarce, continued efforts to monitor the ocean, atmosphere, and sea ice conditions therefore hold great promise for increasing the reliability of decadal predictions.

2.2.1. Data Assimilation and Initialization

Various sea ice data assimilation approaches follow different statistical techniques: nudging [*Tietsche et al.*, 2013], optimal interpolation [*Zhang et al.*, 2003; *Dulière and Fichefet*, 2007], and ensemble Kalman filtering [*Lisaeter et al.*, 2007; *Mathiot et al.*, 2012; *Massonnet et al.*, 2013]. Assimilated variables include sea ice concentration, sometimes ice thickness and drift. A critical point in sea ice data assimilation is the treatment of the ocean, e.g., the update in modeled salinity and temperature profiles after sea ice observations are assimilated. Without a proper ocean update, there is a risk that some of the predictability gained by ice initialization will be lost after a few time steps of the forecast due to undesirable spurious adjustments induced by inconsistencies between the sea ice and the ocean states (see also discussion on physical consistency in section 2.3).

2.2.2. Model Evaluation

In climate models, the simulated sea ice pack is traditionally compared against observations of sea ice concentration/extent/area, sea ice thickness distribution/volume, sea ice drift, and export. These metrics provide quantitative and qualitative insight on the role played by physics and parameters in current sea ice models [*Massonnet et al*., 2011; *Miller et al*., 2006]. Further small-scale observations, such as local atmosphere-ice and ice-ocean heat, mass and momentum fluxes, and deformation rates, could better constrain the development of sea ice models, resulting in a more faithful physical basis for decadal predictions. Regarding the validation of decadal forecast systems for sea ice, one is mainly concerned with the ability of models to forecast ice concentration, its geographical distribution in space and time being, for example, relevant for navigability in the Arctic.

2.3. Perspectives

Decadal sea ice prediction and predictability is a very active topic. Despite significant advances made in the past years, several challenges remain open to research. We list hereunder several of them.

2.3.1. Actual Decadal Forecasts With Initialized Ice

A number of process-based mechanisms for decadal sea ice predictability are arguably established. Some of these processes are simulated by current climate models, and reanalyses now provide a realistic estimate for sea ice cover that is suitable for model initialization but has not been used in actual prediction experiments. In other words, the potential for sea ice initialization is known through potential prognostic predictability (PPP) experiments, but this potential has not been explored yet in practical decadal predictions initialized from real sea ice observations.

2.3.2. Physical Consistency

Particular care should be paid to ensure consistency among sea ice, atmosphere, and ocean initial conditions. The inherent predictability in sea ice derived in perfect-model experiments will inevitably be degraded when switching to actual forecasts, e.g., due to the initial shock among ice, ocean, and atmosphere if those are not initialized in a consistent way. If the system is not in a balanced state at the time of initialization, the benefits from initialization may be lost in a few time steps.

2.3.3. Predictability in a Changing Climate

With nonstationary systems such as Arctic sea ice, seasonal predictions based on past, statistical relationships may be of limited use [*Holland and Stroeve*, 2011]. Resorting to dynamical model forecasting is a practical and promising alternative. However, because of increased year-to-year summer sea ice variability in a warmer climate [*Goosse et al*., 2009], the use of a large number of ensemble members will be necessary in order to predict large anomalies. Typically, recommendations for the minimum number of ensemble members necessary to distinguish signal from noise in sea ice predictions would be useful information.

2.3.4. Importance of Sea Ice Physics on Predictability

Sea ice predictability studies use sea ice models with various complexities, from simple sea ice models with no heat capacity [e.g., *Tietsche et al*., 2013] to comprehensive sea ice representation with several sea ice thickness categories [*Blanchard-Wrigglesworth et al*., 2011; *Chevallier et al*., 2013]. The dependence of forecast skill on sea ice model complexity is to our knowledge not clearly established but could guide model development.

2.3.5. Improved Understanding of Physical Processes

A number of important processes in the Arctic are not fully understood yet. One example is the atmospheric response to sea ice reductions and variations. Also, the processes governing the decadal-scale variations in the Arctic are still only poorly understood. Better knowledge of the processes behind the leading physical modes of the Arctic climate system is mandatory to further improve both climate models and climate predictions.

3. Land Surface

There is evidence that oceanic low-frequency variations propagate into the atmosphere and further onto land areas affecting precipitation, river flow, surface temperature variations, and hurricane activity over land [*Enfield et al*., 2001; *Knight et al*., 2006; *Zhang and Delworth*, 2006; *Sutton and Hodson*, 2005; *Smith et al*., 2010]. Despite this, the skill of decadal predictions over land is generally low [*Smith et al*., 2007] or drops drastically when linear temperature trends (which are fairly well predictable when greenhouse gas concentrations can be considered to remain increasing) are removed [*van Oldenborgh et al*., 2012;

Corti et al., 2012; *Bellucci et al*., 2014]. Yet the oceans and external forcing might not be the only source of predictability over land at time scales longer than 1 or 2 weeks. Various studies suggest the existence of physical processes capable of providing detectable forecast skill in continental areas. For example, the relevance of realistic soil moisture initialization for skillful prediction of precipitation and temperature variations up to 2 months ahead has been shown by *Koster et al*. [2011], *Van den Hurk et al*. [2012], and *Conil et al*. [2007], with snow mass further enhancing boreal summer predictability [*Douville*, 2010].

Many components of the land surface display temporal variability that varies across a range of time scales, from seconds for the surface skin temperature, to seasonal or multiannual time scales for vegetation, snow and (deep) soil moisture, and temperature. The components that have longer memory may be a meaningful source of information for predictability at decadal time scales. Mechanisms similar to those found for seasonal time scale may be relevant for the decadal scale: it is likely that climate persistence induced by soil moisture memory and coupling between land vegetation and atmosphere is amplified and extended through feedback mechanisms. Furthermore, variables with fluctuations at long time scales are able to absorb systematic forecasting errors occurring at shorter time scales, and this may give rise to forecast degrading drift [*Betts et al*., 1998]. An accurate initialization constrained by observations is then required. In this section we will review those land surface variables that have been explored for their potential to contribute to enhance the predictive skill of decadal forecasting systems: soil moisture and vegetation cover.

3. 1. Mechanisms

3.1.1. Soil Moisture

3.1.1.1. Basic Mechanisms

The water stored between the ground surface and the water table is known as soil moisture [*Bonan*, 2008] and represents a key variable of the land energy and water balance. Soil moisture is a large water reservoir for land surface and embodies the continental boundary condition for the atmosphere, controlling the partition of surface heat fluxes and modulating thermal properties at the land-air interface [*Dirmeyer et al*., 2006]. In addition, soil moisture provides the atmosphere with water by soil evaporation and plant transpiration, returning almost 60% of precipitation falling over land [*Oki and Kanae*, 2006, see their Figure 1].

The land water balance can be expressed as

$$\frac{dS}{dt} = P - E - R - B \tag{1}$$

where P is precipitation, E is evapotranspiration, R is the surface runoff, and B is the base flow (subsurface runoff). The rate of change in water storage is represented by dS/dt, which includes soil moisture, snow and ice mass, surface, and groundwater.

Similarly, we can define the land energy balance as:

$$\frac{dH}{dt} = R_n - \lambda E - H_s - G \tag{2}$$

where dH/dt is the rate of change of energy in a given soil layer, R_n is the net radiation, composed of incoming and outgoing longwave and shortwave radiation, λE is the latent heat flux, H_s is the sensible heat flux, and G is the heat flux stored in the soil by conduction.

Land-atmosphere *coupling*, which is the mutual interaction between land surface and atmosphere, plays an important role in the predictability of the climate system by transferring and modulating soil state anomalies to the atmosphere. As demonstrated more than 30 years ago by the experiments of *Shukla and Mintz* [1982] and strongly restated in the 2001 American Meteorological Society Council [*American Meteorological Society Statement*, 2001], knowledge of land surface initial condition is imperative for subseasonal [*Guo et al*., 2011] and seasonal [*Materia et al*., 2014] predictions.

A large fraction of the predictability imparted by land surface can be ascribed to soil moisture: water in the soil may allow the persistence of an anomalous state by up to several months [*Seneviratne et al*., 2006]. This land surface *memory* contributes to increase predictability at the seasonal time scale [*Ferranti and Viterbo*, 2006] and longer, as hypothesized by a few recent studies [e.g., *Langford et al*., 2014], and provides soil moisture with an additional element, besides coupling, that increases the potential predictability of the climate system [*Guo et al*., 2012]. Predictability arising from anomalous soil moisture differs across regions and generally tends to be higher

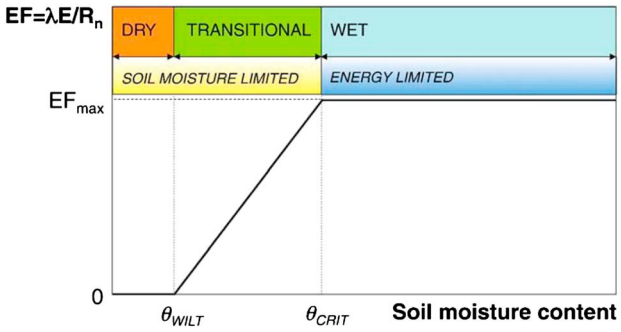

Figure 6. Definition of soil moisture regimes and corresponding evapotranspiration regimes. EF denotes the evaporative fraction (ratio of latent heat to net radiation), EF_{max} its maximum value. Reprinted from *Seneviratne et al.* [2010] with permission from Elsevier.

where memory and land-atmosphere coupling combine, such as in the Mediterranean and the Danube region [*Seneviratne et al.*, 2006].

3.1.1.2. Soil Moisture-Atmosphere Coupling

Combination of equations (1) and (2) shows that energy and water balance on land are linked by the evapotranspiration term, whose interaction with soil moisture is a key process in the land-atmosphere interface [*Seneviratne et al.*, 2010]. Two distinct hydroclimatic regimes characterize evaporation: an energy-limited regime, identified by high wetness fraction, in which surface evaporation is not constrained by limited soil water availability, and a water-limited regime, in dry regions where soil moisture provides a strong constraint to evapotranspiration [*Budyko*, 1974; *Eagleson*, 1978]. Below a threshold called *wilting point*, the amount of water in the soil is too low to become accessible to plants, and evapotranspiration stops completely. This conceptual framework, illustrated in Figure 6 [*Seneviratne et al.*, 2010, their Figure 5], gives a representative portrait of the coupling between land and atmosphere.

In a multimodel study, *Koster et al.* [2004] identified hot spots of particularly strong land-atmosphere coupling, located in transitional zones between dry and wet climates. Recently, *Santanello et al.* [2013] analyzed soil moisture-atmosphere coupling during case studies of extremely dry and wet climate conditions and found large mutual interactions between the land surface and the atmosphere. Observation-derived coupling diagnostics [*Miralles et al.*, 2012] support the finding of *Koster et al.* [2004] of a strong coupling in transitional climate regimes.

While land surface-temperature coupling has only recently received considerable attention [*Fischer et al.*, 2007; *Miralles et al.*, 2012], the soil moisture-precipitation coupling has been investigated since the 1990s, with many studies emphasizing the capability of soil moisture to alter the boundary layer properties, creating favorable conditions for precipitation [*Betts and Ball*, 1995; *Eltahir*, 1998; *Schär et al.*, 1999].

The process driving this interaction includes three main connected players: soil moisture, evaporation, and precipitation. The way rainfall affects soil moisture is trivial: unless the ground is saturated or the infiltration rate is exceeded, rainfall increases soil moisture. On the other hand, the fraction of net radiation converted to latent heat (thus evapotranspiration) generally increases with wetter soils, destabilizing the boundary layer and favoring conditions for precipitation.

Under specific conditions, land-atmosphere coupling was found to affect predictability at the multiannual time scale. In the U.S. Great Plains, changes in long-term predictability are primarily driven by modification of the soil moisture-atmosphere coupling [*Schubert et al.*, 2008]. This interaction must be considered when evaluating the predictability of recurring droughts in this area and potentially in other regions of substantial land-atmosphere interaction. With a modeling study, *Schubert et al.* [2004] have shown that disabling the interaction between land and air does not allow the reproduction of the 1930s Dust Bowl, highlighting the importance of such a mechanism for the self-sustenance of the multiyear drought. These studies point out that the big drought was triggered mostly by atmospheric variability, inducing low soil moisture that possibly initiated positive feedbacks with the land surface maintaining the dry condition [*Hoerling et al.*, 2009]. The mutual interaction among land surface constituents may generate mechanisms of drought maintenance. In the Sahel, for instance, prolonged droughts may generate anomalous dust loadings, both mineral-based and generated by biomass burning, that may impact the atmospheric radiation budget [*Nicholson*, 2013] by warming the midtroposphere and cooling the surface [*Reale et al.*, 2011] for longer than a year.

3.1.1.3. Soil Moisture Memory

Since *Fennessy and Shukla* [1999] pioneering work, which suggested that a realistic initial state of soil wetness would enhance seasonal forecast skill, initialization of land surface state has become an imperative requirement

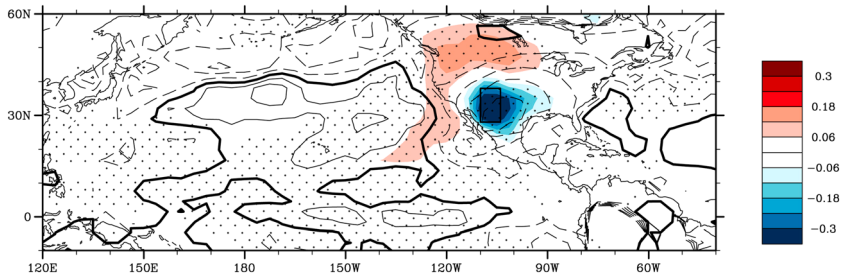

Figure 7. Simultaneous regression of area-averaged monsoon (in the black rectangle) region standardized precipitation anomaly onto surface temperature anomalies over land and sea (°C per standard deviation of monsoon precipitation), for 5 year running means of July-August-September (JAS). The color contours indicate the average of 20 CMIP5 simulations. The stippling indicates that more than two thirds of the models agree on the sign of the regression. From *Langford et al.* [2014], © American Meteorological Society. Used with permission.

in climate prediction systems based on fully coupled models [*Paolino et al.*, 2012]. In fact, medium- and long-term forecasts cannot rely on the initialization of the atmosphere alone, because the time scales over which tropospheric anomalies dissipate are too short [*Koster and Suarez*, 2001]. *Dirmeyer* [2003] estimates the contribution to forecast skill from the atmospheric state in a coupled land-atmosphere model with prescribed (time varying) SSTs decays in less than a month. Instead, soil moisture anomalies may persist for several months, and this "memory" of initial states has promising implications for climate prediction.

Langford et al. [2014] examine the mechanisms of decadal variability in precipitation over southwestern North America, in the CMIP5 models and observations. The simultaneous regression pattern of precipitation anomalies over the south-west U.S. onto surface temperatures at the multiannual (5 year) time scale highlights, in both historical CMIP5 simulations and observations, a relatively weak relation with tropical and extratropical North Pacific SSTs (explaining only 20% of the total variance), while most of the variability appears to be explained by local anomalies, associated with land-atmosphere feedbacks (Figure 7). This result points to a potentially relevant role of land surface state in long-term (decadal-scale) forecasts of drought-like conditions in the south-west US.

Moreover, soil moisture memory may provide predictability at multiyear time scales through the information stored in the slowly varying components of the soil system, such as the groundwater. Although state-of-the-art climate models with a coupling to a dynamic groundwater reservoir exist [*Fan and Miguez-Macho*, 2010], exploration of the contribution of this component to decadal time scale predictability with such models has not yet been carried out. *Bierkens and Van den Hurk* [2007] used a conceptual model of the coupled land-atmosphere system and demonstrated that in semiarid conditions groundwater convergence may introduce multiyear variability in precipitation, implying potential predictability over the same time scale.

3.1.2. Vegetation

The distribution of natural vegetation, its phenology, and development state are largely controlled by climate [*Koeppen*, 1884], but in turn vegetation systematically affects regional climate [*Pielke et al.*, 2011; *Arora*, 2002]. *Weiss et al.* [2012] illustrated the beneficial impact of a realistic observation-based vegetation state on the potential predictability and skill of a climate model. Remotely sensed leaf area index (LAI) and albedo products were used to examine the role of vegetation in the coupled land-atmosphere system. Perfect-model experiments were performed to determine the impact of realistic temporal variability of vegetation on potential predictability of evaporation and temperature, as well as model skill in coupled model simulations. While a realistic representation of vegetation positively influences the simulation of evaporation and its potential predictability, a positive impact on surface air temperature is of smaller magnitude, regionally confined and more pronounced in climatically extreme years.

Various studies have elaborated on the importance of vegetation-atmosphere feedbacks at decadal time scales. An iconic study by *Zeng et al.* [1999] illustrated the contribution of vegetation dynamics to reinforce the late 1980s drought in the Sahel, where different feedbacks are evident at different time scales. Correlation and potential predictability studies exploring the relation between vegetation dynamics and climatic indicators, such as rainfall anomalies, have been carried out for various climatic zones and regions, including the Tibetan plateau [*Wang et al.*, 2010], the Amazon [*Wang et al.*, 2011a], and the Asian monsoon [*Li et al.*, 2009]. To our

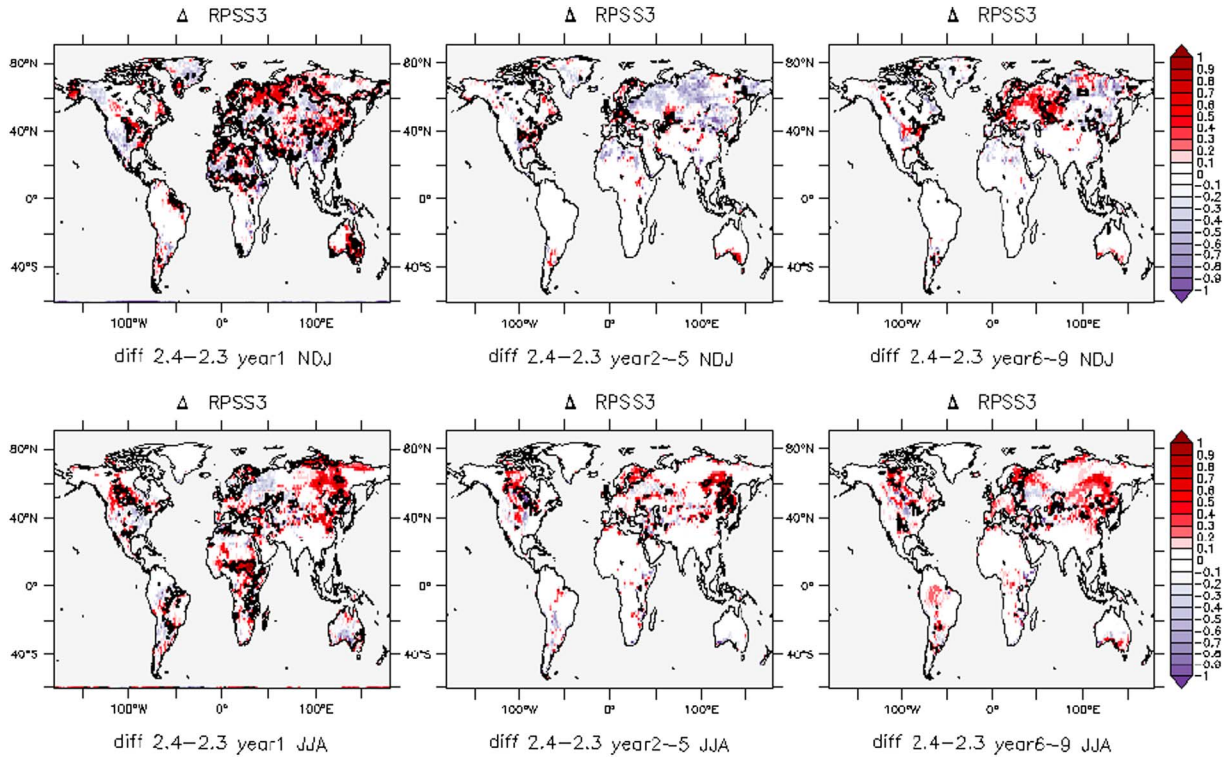

Figure 8. Difference in Ranked Probability Skill Score (RPSS), comparing decadal hindcasts performed with the EC-Earth model, with and without dynamic vegetation for June, July, August (JJA), and November, December, January (NDJ) for lead times of 1 year, 2–5 years, and 6–9 years. RPSS is calculated with respect to ERA40 climatology. From *Weiss et al.* [2014], © American Meteorological Society. Used with permission.

knowledge, the first study investigating the impact of vegetation on decadal predictions using a prognostic model setup is by *Weiss et al.* [2014]. In their approach the initial state of the vegetation is based on long off-line spin-up runs with a dynamic vegetation model driven by observed climate. Coupling the vegetation and atmospheric modules allows a two-way interaction between the vegetation state and the climate system beyond the initialization phase. Vegetation is characterized solely by a variable value of LAI for high and low vegetation, replacing the default configuration using a static prescribed LAI value in the land surface model. Decadal hindcasts were carried out following the CMIP5 decadal forecasting protocol, using a fully coupled atmosphere-land-ocean-sea-ice model and including the vegetation coupling.

The results of *Weiss et al.* [2014] indicate a reduction of the surface air temperature bias in many regions and slightly more reliable forecasts. The ranked probability skill score (RPSS) is found to increase in a few regions, especially in the first year after initialization (Figure 8). However, only a very few areas demonstrated to have higher skill than climatology. Moreover, the additional degrees of freedom introduced by the interactive vegetation generate supplementary noise to the model that does not necessarily translate into improved skill.

The regions with the greatest bias improvement were found in the tropical Sahel and India and at high latitudes in boreal Russia and North America. These results are in agreement with former studies by *Douville* [2010], *Koster et al.* [2011], and *Seneviratne et al.* [2010]. As for soil moisture at the seasonal time scale, the main gain for decadal predictions from vegetation appears to be in regions exposed to shifts in the Intertropical Convergenze Zone (ITCZ) and monsoon cycles, consistently with the transitional dry-to-wet climate zones that expose a strong land-atmosphere coupling.

The study of *Weiss et al.* [2014] was carried out with a suboptimal system setup. To avoid potentially unstable feedbacks between the vegetation and atmosphere, the list of exchanged variables was limited, thereby accepting certain inconsistencies between models. One consequence of this approach is that drifts in LAI were generated in the coupled system. They likely bear their origin in an inconsistent (and high) soil moisture availability in the vegetation model due to a systematic precipitation bias in the climate model. A lesson to be learned from this is that vegetation and climate consistency in different hydroclimatic regimes needs to

be ensured by exchanging information on the vegetation transpiration stress between the modules. This ensures that vegetation dynamics in the coupled model exhibits a realistic variability that is also generated when forced with observations. Based on the observed correlation between LAI and moisture supply in most regions of the world, a revision of the soil moisture information exchange has the potential to greatly improve the representation of memory in the vegetation state and its associated predictability.

Also, in order to explore the added value of a realistic initialization for vegetation, start dates other than November (as prescribed by the CMIP5 protocol) should be considered in the experimental design. Probably the initial vegetation state in early Northern Hemisphere spring contains a lot more useful information, for both the seasonal and the decadal time scales.

3.2. Observations

3.2.1. Soil Moisture

As already mentioned, the scarcity of soil moisture observations is the most significant limitation to the understanding of land surface-atmosphere interaction. Available in situ measurements have been gathered using a standardization protocol for a comprehensive harmonized global database into the International Soil Moisture Network database [*Dorigo et al*., 2011]. Its limitations reside in the lack of station data over several areas, including the Arctic, Africa, and South America. In fact, the high costs and the large efforts required to put instruments in place only allow a sparse coverage, with the exception of some regional networks [*Robock et al*., 2000]. Besides, soil moisture field campaigns suggest that upscaling via simple spatial averaging of data acquired from randomly distributed sites results in large errors, unless high sampling densities are maintained [*Crow et al*., 2012].

On the other hand, indirect estimates of soil moisture, such as remote sensing measurements [*de Jeu et al*., 2008], still have several limitations (e.g., the lack of information on deep soil water) and gaps in key regions due to the shading exerted by vegetation [*Wagner et al*., 2007]. The most complete and, to date, reliable data set of this kind was developed as part of the European Space Agency program Climate Change Initiative and was initiated in 2010 for a period of 6 years [*Liu et al*., 2011]. It blends active and passive microwave satellite estimates, producing a global database of soil moisture from 1979 to 2010. However, spatial gaps are still substantial in densely forested areas and in snow-covered regions during winter, and temporal gaps are present as well.

Land surface models forced with meteorological observations supply global estimates at a fairly high resolution (e.g., Global Soil Wetness Project 2 (GSWP-2) at 1°) [*Dirmeyer et al*., 2006], but regional tuning [*Guo and Dirmeyer*, 2006]. However, discrepancies among models [*Materia et al*., 2010] and a high dependency on the quality of forcing data [*Guo et al*., 2006] represent large sources of uncertainty. Recent reanalyses of the land surface have improved upon the output of the atmospheric forced land surface models through the inclusion of observed precipitation data into the data assimilation system [*Balsamo et al*., 2012], but even these data rely still heavily on the (limited) skill of land surface models. Improving details in the parameterization of these models does not seem to guarantee enhanced predictability results [*Dirmeyer et al*., 2013]. Other model-derived soil moisture products can be retrieved from atmospheric global models constrained with monthly SST observations [*Koster et al*., 2006]. *Seneviratne et al*. [2010] describe several validation data sets of soil moisture, analyzing pros and cons of each methodology.

3.2.2. Vegetation

Many global vegetation data sets currently exist. A full review of these is beyond the scope of this paper, but they can generally be discerned in products representing vegetation type distributions (see *Xie et al*. [2008] for a review), or aiming at monitoring the state of the aboveground biomass or leaf area index [*Zhu et al*., 2013]. A pioneering product was the normalized difference vegetation index (NDVI) [*Tucker*, 1979], for which routine databases are available since 1982. Moderate Resolution Imaging Spectroradiometer products based on Fraction of Absorbed Radiation are available since 2002 [*Myneni et al*., 2002], including postprocessing routines generating LAI estimates and other vegetation indicators.

Application of LAI databases is currently being explored for seasonal predictions [*Boussetta et al*., 2013]. For this a climatologically stable and well-interpretable data set is required. Major issues with NDVI and LAI databases are sensitivity to sensor degradation and platform replacement, cloud screening and atmospheric absorption, and translation of the remotely sensed radiances into a geophysical product that can be interpreted by the assimilating model.

3.3. Perspectives

Only very few sensitivity experiments were carried out to assess the role of soil moisture on decadal predictability. However, the works mentioned in section 3.1.1 have triggered discussion about its possible impacts on multiannual time scales. It is argued that climate persistence induced by soil moisture memory and land-atmosphere coupling is amplified and extended through feedback mechanisms. These findings state the importance of a realistic representation of the land surface component, besides its initialization, to improve our chance of obtaining effective decadal predictions on land regions where SST forcing is limited.

In addition, recent investigations have highlighted the importance of land management forcing for resulting effects on the climate system, mainly through changes in soil albedo [*Luyssaert et al*., 2014]. *Cook et al*. [2009] find that SST changes are not sufficient to explain the Dust Bowl: human-induced land degradation has played a crucial role in the formation and amplification of the drought, as a result of land surface feedbacks. *Dirmeyer et al*. [2013] detected a change in the predictability of precipitation and temperature anomalies in response to major land use conversions in the U.S. Great Plains area. Predictable trends in deforestation may provide a source of predictability over the areas affected [e.g., *Sampaio et al*., 2007]. Obviously, these studies must take into consideration the model-specific features that may affect the results, but they represent an important step in defining the role of anthropogenic land modifications on decadal predictability.

The importance of vegetation for decadal predictions has not been thoroughly investigated, and one of the main reasons is the short record of available observational products (as discussed in section 3.2.2). The documented impact of vegetation on regional climate and the low skill of current operational decadal predictions over land warrant the need for further investigation. The few studies that have addressed the potential and actual decadal predictability do show limited increase in predictability and skill for the first few (2–5) years for most land regions. Largest increase in decadal prediction skill appears to be gained in regions with large interannual variations in surface conditions related to strongly varying precipitation forcing, and regions situated in the transitional dry-to-wet climate zones, characterized by strong land-atmosphere coupling. First studies have indicated that capturing the potential predictability associated with vegetation requires that the coupling among the atmosphere, vegetation, and land surface is consistent with a closed water and energy cycle. Utilizing the predictability from vegetation should thus be accompanied with a proper treatment of the soil moisture impact on vegetation dynamics. Furthermore, additional gain of skill during the first forecast year can be expected when start dates are used that coincide with the part of the seasonal cycle where vegetation has a strong effect on the successive hydroclimatic conditions. This requires experiments that deviate from the CMIP5 protocol, where the November start date is recommended. Additionally, adequately large ensembles are required to extract the relatively small (deterministic) signal from the considerable noise that exists both in the real world and the modeling systems. These limitations will be likely overcome in the new experimental setup for near-term predictions, currently being designed for Coupled Model Intercomparison Project Phase 6 (CMIP6).

4. Stratosphere

At decadal time scales, both changes in external forcing (greenhouse gases (GHGs), stratospheric aerosols, and solar forcing) and internal factors affect climate variations. The stratospheric flow presents interdecadal variability that can be dynamically driven [*Butchart et al*., 2000] but also a response to low-frequency variations of external forcing. Indeed, at multidecadal time scales, the stratosphere responds to the radiative forcing of anthropogenic compounds, of natural solar cycle variations and of the aerosol loading following large volcanic eruptions [*Shindell et al*., 2001; *Meehl et al*., 2009a]. Furthermore, low-frequency stratospheric variations can influence tropospheric circulation [*Scaife et al*., 2005]. In the last decade it has been suggested that knowing the state of the stratosphere can result in enhanced predictability at seasonal time scales in the extratropics [*Baldwin et al*., 2003]; indeed, recent research works have demonstrated that seasonal forecast systems initialized during stratospheric sudden warmings lead to significantly larger forecast skill in the extratropics [*Kuroda*, 2008; *Marshall and Scaife*, 2010; *Sigmond et al*., 2013]. The dynamical link between the stratosphere and the troposphere is found at midlatitudes in winter in the Northern Hemisphere and in spring/summer in the Southern Hemisphere. Therefore, these are the seasons where there is a potential role for the stratosphere in surface climate predictability. To this regard, the stratosphere may also play an integral role in decadal variability of climate [*Schimanke et al*., 2011; *Reichler et al*., 2012]. However, the link

between the stratosphere and the troposphere is not only of dynamical origin: stratospheric background aerosols other than volcanic eruptions and variations in stratospheric water vapor have been recently recognized to be important drivers of decadal variations of surface warming [*Joshi et al*., 2006; *Solomon et al*., 2010; *Solomon et al*., 2011]. The stratosphere-troposphere-ocean coupled system has to be considered as a whole for its role in both internally generated and externally forced climate variability. Its proper representation will likely enhance decadal prediction skill, as it has contributed to enhance seasonal prediction skill [*Scaife et al*., 2014a].

4.1. Mechanisms

The dynamical coupling between the stratosphere and the troposphere occurs through variations in the strength of the polar vortex. Anomalies in the stratospheric flow can propagate downward and affect the weather and climate in the troposphere, lasting up to 2 months [*Baldwin and Dunkerton*, 2001; *Thompson et al*., 2002]. Different mechanisms have been proposed to explain the involved pathways of the stratosphere-troposphere connection [*Gerber et al*., 2012]; however, a better understanding of the coupling between the stratosphere and the different components of the climate system is still needed. The proposed mechanisms include, among others, a remote response of the troposphere to stratospheric potential vorticity anomalies [*Hartley et al*., 1998; *Black*, 2002], a local tropospheric response maintained by feedbacks with transient eddies [*Song and Robinson*, 2004], vertical reflection of planetary waves [*Perlwitz and Harnik*, 2003] and refraction of synoptic waves [*Simpson et al*., 2009], and linear interference between the climatological waves in the stratosphere and the wave response to a tropospheric forcing [*Fletcher and Kushner*, 2011]. Impact of stratospheric changes on baroclinic instability [*Rivière*, 2011] and wave breaking into the troposphere [*Kunz et al*., 2009] has also been invoked.

At the surface, extreme events of the stratospheric circulation modulate the NAO polarity with a positive/negative phase of the NAO preceded by strong/weak vortex anomalies. This dynamical connection between the stratosphere and the troposphere is the basis for potential enhanced predictability of the stratosphere-troposphere coupled system. On monthly to seasonal time scales, the slow radiative relaxation rates in the lower stratosphere provide additional predictive skill to tropospheric patterns of circulation from the longer stratospheric memory [*Baldwin et al*., 2003; *Sigmond et al*., 2013]. At interannual time scales, predictability can originate not only from surface ocean conditions in the Atlantic that can impact the frequency of atmospheric blocking [*Maidens et al*., 2013] but also from stratospheric processes with long time scale. For example, the quasi-biennial oscillation (QBO) has a period of about 2–3 years and is predictable for 1–2 cycles, and having a persistent teleconnection to the winter surface climate, it appears to offer midlatitude surface climate predictability [*Marshall and Scaife*, 2009; *Thompson et al*., 2002], even though recently *Scaife et al*. [2014b] have shown a limited predictability of the extratropical winter teleconnection associated to the QBO. A few studies also pointed out the possibility of a remote influence of the QBO on the subtropical circulation [*Giorgetta et al*., 1999] and tropical cyclones [*Ho et al*., 2009]. Moreover, teleconnections via the stratosphere between El Niño–Southern Oscillation (ENSO), a predictable tropical mode of variability, and European climate in late winter can be considered a potential source of predictability at this time scale [*Ineson and Scaife*, 2009; *Cagnazzo and Manzini*, 2009]; if it holds at interannual time scales, it is also possible that it holds at longer time scales: at decadal time scales climate variations over the Pacific Ocean and area surroundings are strongly related to the Pacific Decadal Oscillation that has a certain degree of predictability [*Mochizuki et al*., 2010; *Lienert and Doblas-Reyes*, 2013; *Ding et al*., 2013; *Meehl and Teng*, 2014; *Meehl et al*., 2014b]. At interannual time scales, it is also recognized the existing link between the variability in the Siberian snow cover and the AO [*Cohen et al*., 2007], and this knowledge has been used to improve seasonal time scale winter forecasts; however, this coupling may be also modulating the winter warming trend, with implications for decadal-scale temperature projections [*Schimanke et al*., 2011].

At the decadal time scales, it has been recently shown, using a stratosphere-resolving atmosphere-ocean general circulation model, that the frequency of stratospheric sudden warmings (SSW) varies on decadal and multidecadal time scales. This is reflected in long lasting anomalies of the stratospheric polar vortex that are in turn connected to variations in the Atlantic Ocean [*Schimanke et al*., 2011]. This analysis suggests that enhanced wave flux entering the lower stratosphere (associated to positive heat flux anomalies from the North Atlantic into the atmosphere, to enhanced snow cover over Eurasia and more blocking activity) leads to a larger number of SSWs; stratospheric anomalies can in turn impact surface weather in the following

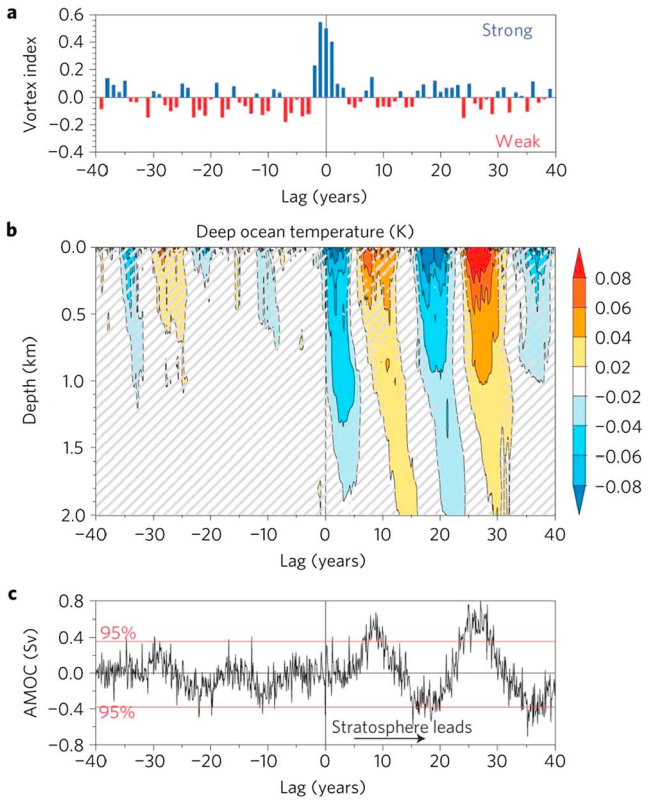

Figure 9. Geophysical Fluid Dynamics Laboratory Climate Model version 2.1 derived composites of periods during which the polar vortex was either persistently strong (75 events) or persistently weak (70 events, multiplied by −1). (a) Composite time series of the vortex index, measuring the likelihood that a vortex event happens during a given year. The index represents a composite and therefore varies smoothly between +1 and −1. (b) Corresponding monthly time-depth development of ocean temperature anomalies (K) over the study region (15°W–60°W, 45°N–65° N); hatching shows insignificant (95%) results. (c) Corresponding monthly anomalies in Atlantic meridional overturning circulation (AMOC) strength (Sv). From *Reichler et al.* [2012]. Reprinted by permission from Macmillan Publishers Ltd.

weeks and may potentially enhance multidecadal variations of the coupled ocean-atmosphere system in the Atlantic. Indeed, recent studies [*Manzini et al.*, 2012; *Reichler et al.*, 2012] have shown that sequence of circulation anomalies propagating down from the stratosphere in a climate model, in turn, affect decadal variations of the North Atlantic Ocean (Figure 9).

On the other hand, the tropospheric and stratospheric anomalies appear to be partly driven by North Atlantic SST changes; a result that appears to depend on accurate representation of stratosphere-troposphere interaction in atmospheric general circulation models [*Omrani et al.*, 2014]. In particular, *Omrani et al.* [2014] investigated the period 1951–1960 during which North Atlantic SSTs were anomalously warm (Figure 10a), associated with the observed Atlantic multidecadal variability. During this period the NAO tended to be in its negative phase during the late winter (Figure 10b) and were connected to weak polar stratospheric vortex in the early winter. The tropospheric (Figures 10c and 10d) and stratospheric changes could be largely simulated, but only in a stratospheric resolving model configuration. Thus, resolving stratosphere-troposphere interaction appears key to simulating the large-scale atmospheric response to North Atlantic SST changes.

At the decadal time scale, the 11 year solar cycle is a driver of stratospheric variability. Although total solar irradiance perturbations at the Earth surface are small, variations in the UV part of the spectrum are larger (though with a great uncertainty in their magnitude) and cause a substantial and well-documented perturbation in ozone [*Soukharev and Hood*, 2006; *Randel and Wu*, 2007] and temperature [*Gray et al.*, 2010; *Frame and Gray*, 2010] of the upper stratosphere and lower mesosphere with an amplification of the signal in the lower stratosphere [*Haigh*, 1996]. It has been shown that such variations affect background stratospheric winds, therefore impacting wave propagation in the winter stratosphere [*Kodera and Kuroda*, 2002]. Evidence of a solar signal at surface from observations and model simulations is also documented in upper oceanic temperature and heat storage [*White et al.*, 1997], in the tropical Pacific sea level pressure and sea surface temperatures, where the effect of solar forcing resembles La Niña events [*van Loon and Meehl*, 2008], then followed by a warm El Niño event with a lag of a few years [*Meehl and Arblaster*, 2009]. Impact of solar variations on climate has also been identified on tropical convection [*van Loon and Labitzke*, 2000; *Balachandran et al.*, 1999] with an increase in off-equatorial precipitation [*Meehl et al.*, 2009a], a weakening of the Hadley cell [*Kodera and Shibata*, 2006] and a modulation of the Indian Monsoon system [*Kodera*, 2004]. Statistical analyses [*Lockwood et al.*, 2010] and climate modeling studies have linked low solar activity to low temperatures over Northern Europe and North Atlantic [*Ineson et al.*, 2011] (Figure 11), with a more robust lagged response [*Gray et al.*, 2013] possibly due to ocean-atmosphere interactions [*Scaife et al.*,

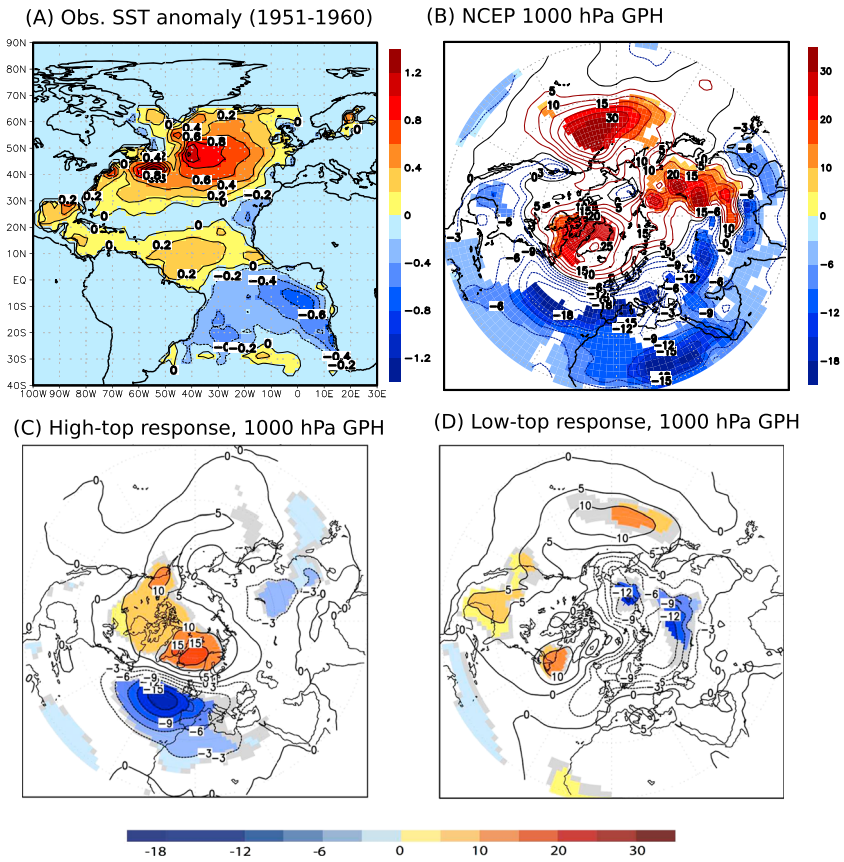

Figure 10. (a) SST and (b) 1000 hPa geopotential height anomalies for the period 1951–1960 relative to 1961–1990 for January-February-March (JFM) from observations [*Rayner et al.*, 2003] and reanalysis [*Kalnay et al.*, 1996], respectively. The 1000 hPa geopotential height response to the anomalous SST changes in Figure 10a simulated by the European Centre Hamburg Model version 5 in (c) high-top and (d) low-top configurations. Only differences significant at the 90% level are plotted in Figures 10b–10d. Adapted from *Omrani et al.* [2014]. With kind permission from Springer Science and Business Media.

2013], through a "top-down" mechanism: variations in stratospheric ozone due to solar variability in the ultraviolet (UV) spectrum range result in dynamical responses in the stratosphere and troposphere [*Haigh*, 1996; *Balachandran et al.*, 1999; *Shindell et al.*, 1999]. In the Pacific, it has been shown that the impact of solar variability on climate occurs through a "bottom-up" mechanism acting together with the top-down pathway: air-sea radiative coupling at the surface in the tropics, modulated by cloud distribution, could initiate a set of processes linking the solar forcing to its tropospheric response through coupled atmosphere-ocean dynamical feedbacks [*Meehl et al.*, 2003, 2008, 2009a]. Moreover, some observational [*Labitzke*, 1987] and modeling [*Schmidt et al.*, 2010] studies suggest a possible modulation of the stratospheric solar cycle signal by the QBO. A correct simulation of the connection between solar variations and regional climate variability could provide predictability at the decadal scale. However, it has proved difficult for climate models to consistently reproduce solar cycle signal in the stratosphere and the troposphere [*Schmidt et al.*, 2010; *Tsutsui et al.*, 2009], even though some of them have been successful [*Matthes et al.*, 2006; *Shindell et al.*, 2001].

Unpredictable explosive volcanic eruptions can inject large amounts of sulfur into the lower stratosphere where they form aerosol particles, which are transported by large-scale circulations and stay up to about 2 years. The radiative forcing from these events can be substantial [*Robock*, 2000], with a cooling of the troposphere due to scattering of solar radiation and a warming of the lower stratosphere due to enhanced absorbing of infrared radiation [*Angell*, 1997]. The radiative impact of volcanic aerosols can impact ozone and induce a stronger polar vortex [*Kodera*, 1994; *Perlwitz and Graf*, 1995; *Kodera and Kuroda*, 2000a, 2000b; *Shindell et al.*, 2001], potentially shifting the tropospheric jet stream and producing a response that generally

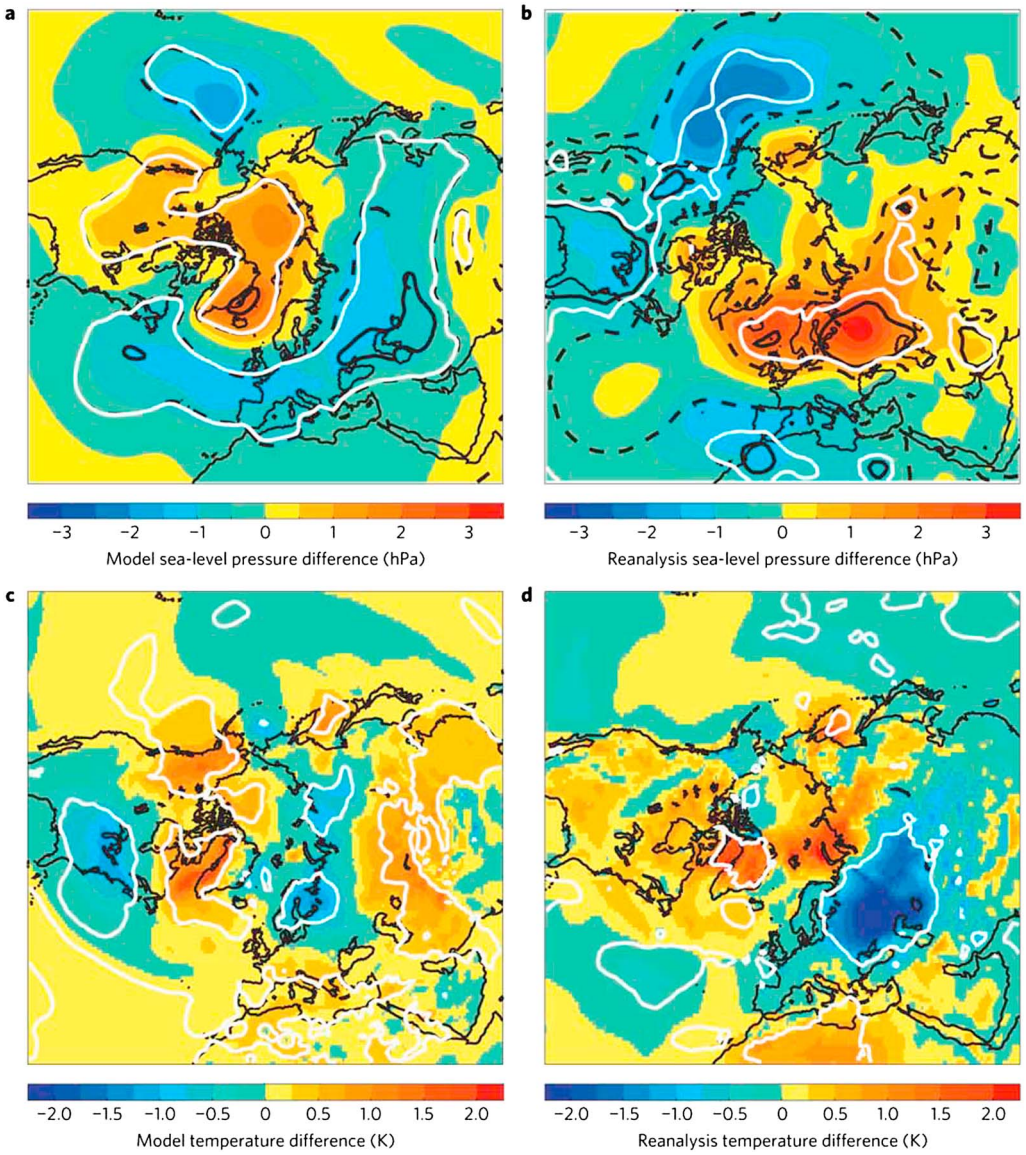

Figure 11. Sea level pressure difference for (a) model and (b) ERA-40/ERA-Interim reanalysis. Near-surface temperature difference for (c) model and (d) reanalysis. The differences are for December to February mean fields. The dashed (solid) black contours show the sea level pressure difference relative to the interannual standard deviation at 25% (50%). The solid white contours indicate significance at the 95% confidence level for the model (Figures 11a and 11c) and 90% for reanalyses (Figures 11b and 11d). All panels are centered around the North Pole. From *Ineson et al.* [2010]. Reprinted by permission from Macmillan Publishers Ltd.

includes an anomalously positive phase of the AO, more pronounced in the boreal winter but only partially simulated in models [*Stenchikov et al.*, 2006].

At multidecadal time scales, external forcing (anthropogenic and natural) and unforced internal variability both contribute to explain climate variations. The boundary condition forcings from anthropogenic ozone depletion and greenhouse gas increases can therefore be important sources of predictability. A clear example is found in the Southern Hemisphere. Long-term changes associated to the ozone depletion over Antarctica have dominated climate change in austral spring and summer over the past few decades [*Thompson and Solomon*, 2002; *Thompson et al.*, 2011]. The cooling of the lower stratosphere of radiative and dynamical origin (up to about 10 K) has led to a strengthening of the polar vortex, with a delayed transition from winter westerlies to summer easterlies and an impact on the shift of the tropospheric jet

stream [*Son et al*., 2010]. Stratospheric changes have projected onto the positive polarity of the Southern Annular Mode (SAM) [*Thompson and Solomon*, 2002] with possible impact on oceanic circulation [*Cai*, 2006], hydrological cycle [*Kang et al*., 2012], sea ice (though controversial) [*Turner et al*., 2009; *Sigmond and Fyfe*, 2010; *Sigmond and Fyfe*, 2014], and air-sea carbon fluxes [*Lenton et al*., 2009]. Recently, it has been shown the importance of including a proper representation of stratospheric dynamics in order to obtain more reliable long-term climate simulations and projections in the Southern Hemisphere circulation patterns and air-sea fluxes [*Cagnazzo et al*., 2013]. If in the past, the increase in GHG and the stratospheric ozone depletion have both contributed to the observed changes in the Antarctic region, in the future because of the ozone recovery, it is expected that GHG change and the stratospheric ozone change will no longer combine to produce a positive SAM trend at the surface. It is therefore essential to properly represent chemistry-radiative and dynamical stratospheric changes and their feedbacks in future climate projections.

In the Northern Hemisphere (NH), it is expected that the polar vortex will continue to respond to radiative cooling and to changes in tropospheric wave activity, as a result of greenhouse gas forcing [*McLandress and Shepherd*, 2009; *Calvo and Garcia*, 2009]. Projected changes of the polar vortex winds are consistent with a strengthening of the Brewer-Dobson circulation due to climate change (see *Butchart* [2014] for a review; [*Butchart and Scaife*, 2001; *Butchart et al*., 2006]). These low-frequency stratospheric changes can influence trends in tropospheric temperatures and precipitations [*Scaife et al*., 2005]. Recent numerical experiments have also demonstrated that stratospheric changes can be different in models with a better representation of stratospheric dynamical processes and that details of regional climate change in NH winter may depend on the representation of the stratosphere in climate models [*Scaife et al*., 2012; *Karpechko and Manzini*, 2012].

4.2. Observations

At the global scale, stratospheric radiosonde observations exist since the late 1950s [*Pawson and Fiorino*, 1998]. Satellite observations of the lower stratosphere have global coverage from the late 1970s [*Bailey et al*., 1993], and from the early 1990s, data assimilation has been used to produce comprehensive stratospheric analyses [*Swinbank and O'Neill*, 1994]. Stratospheric reanalyses can be used to initialize the stratosphere in models extending up in the middle atmosphere. Those include National Centers for Environmental Prediction/National Center for Atmospheric Research reanalysis [*Kalnay et al*., 1996] available from 1948 to present, Modern-Era Retrospective Analysis for Research and Applications [*Rienecker et al*., 2011] covering the period from 1979 to the present, the European Centre for Medium-Range Weather Forecasts ERA-40 [*Uppala et al*., 2005] available from September 1957 to August 2002 and ERA-Interim [*Simmons et al*., 2007] from 1979 to the present. If initialization of the polar stratosphere during SSWs events has been demonstrated to enhance forecast skills at seasonal time scales [*Sigmond et al*., 2013], it may have limited skills at the decadal time scale because of the limited polar vortex strength predictability. Initialization in the tropics could instead be beneficial for representing the correct phase and amplitude of the QBO, at least for a few years following the initialization [*Marshall and Scaife*, 2009; *Scaife et al*., 2014b].

4.3. Perspectives

Assessing to what extent the representation of the stratospheric processes illustrated in section 4.1 is key to improved decadal predictions does necessarily require a better understanding of the mechanisms governing the stratospheric impact on climate at different time scales. The representation of the stratosphere itself and therefore of the stratosphere-troposphere-ocean-sea ice coupling could lead to improved prediction skill at the decadal time scale, because of the dynamical mechanism linking the stratosphere to troposphere and possibly to oceanic circulation in the extratropics. It can enhance dynamical feedbacks, but also amplify the impact of external forcing. Therefore, a requirement for better skill at the decadal time scale is to have a model that realistically simulates the stratospheric response to tropospheric variations and the tropospheric response to polar vortex changes, in general, occurring in models with a well-represented stratosphere [*Hardiman et al*., 2012]. This can be achieved by raising the model lid, increasing model stratospheric resolution, and improving representation of stratospheric dynamics and thermodynamics. All these ingredients have been recently recognized as essential for extended-range forecast skill at the seasonal time scale [*Roff et al*., 2011; *Sigmond et al*., 2013; *Scaife et al*., 2014a]. These works have pointed out the importance of a proper stratospheric initialization in order to perform skillful seasonal predictions. At interannual time scales the initialization of the tropical stratosphere can be relevant for the QBO; *Scaife et al*. [2014b] have demonstrated predictability of the QBO up to a few years into the future suggesting

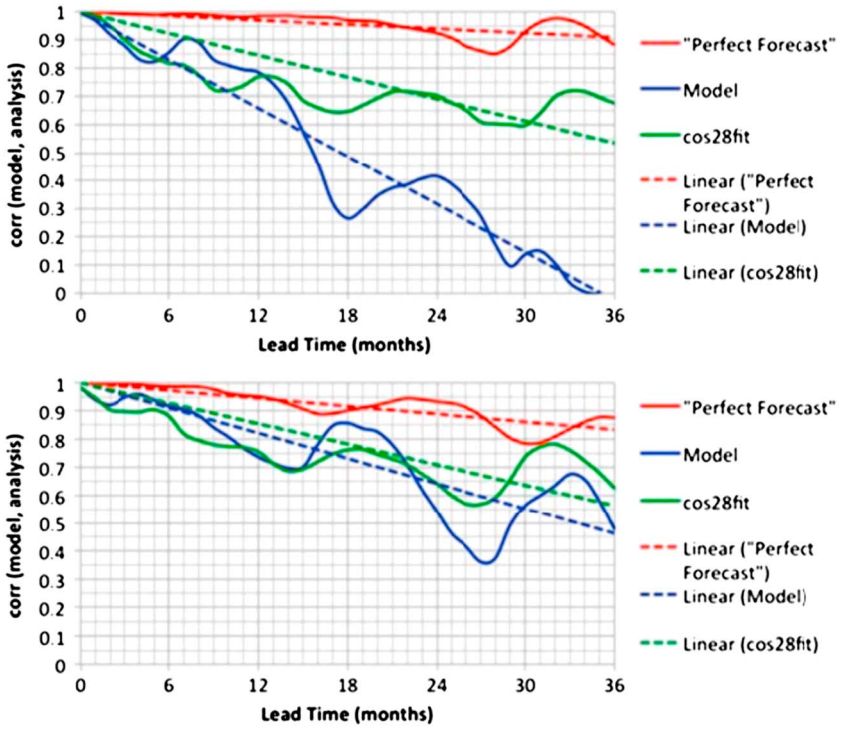

Figure 12. Correlation scores for monthly and zonally averaged values of equatorial wind at 30 hPa as a function of lead time, indicating predictability of the QBO in the (top) UKMO and (bottom) MiKlip decadal forecast systems, using decadal forecasts over 1960–2006, verified against observational analyses (blue). Dashed lines show linear least squares fits. Skill predictions is high at very long lead times (larger than 0.8 at lead times up to 6 months; above 0.7 at 12 months; significant out to 4 years ahead in the MiKlip forecasts) and is larger than other modes of variability such as ENSO. From *Scaife et al*. [2014b].

possible higher skills with improved initialization and modeling of the QBO (Figure 12). However, at longer time scales, improving the stratospheric initial conditions may have a negligible impact on forecast skills, as SSWs are highly nonlinear events and it is not possible to predict polar vortex anomalies beyond a week or two. Moreover, a skillful prediction of the QBO itself does not guarantee predictability of the extratropical winter teleconnection [*Scaife et al*., 2014b].

On longer time scales, accurate representation of stratosphere-troposphere interaction may be critical in capturing atmospheric teleconnections to variations in tropical and extratropical SST [*Ineson and Scaife*, 2009; *Omrani et al*., 2014], Eurasian snow cover [*Hardiman et al*., 2008], and Arctic sea ice [*Jaiser et al*., 2013], all of which exhibit predictability on seasonal-to-decadal time scales.

A better dynamical stratosphere includes an improved model vertical resolution in the upper troposphere and lower stratosphere, a model top higher than 1 hPa (this definition has been used in *Charlton-Perez et al*. [2013] and is based on previous literature showing that models with a top below the stratopause fail to properly simulate SSWs), the representation of momentum conserving orographic and nonorographic subgrid-scale gravity wave drag, necessary for reproducing realistic winds and temperatures [*Shaw and Shepherd*, 2007; *Shaw et al*., 2009]. The vertical resolution and parameterization of gravity waves also play a role in the representation of the QBO in models [*Giorgetta et al*., 2006], a phenomenon not resolved by almost all of the CMIP5 models. However, uncertainties still derive from parameterized processes in current models, such as the gravity wave parameterizations that are indeed highly idealized and poorly constrained to observations [*Geller et al*., 2013].

Stratospheric chemistry and microphysics processes are also missing in most models. The impact of stratospheric ozone loss and recovery on past and projected climate change in the Southern Hemisphere derived from model simulations could be sensitive to the use of a fully interactive stratospheric ozone

chemistry scheme [*Gerber et al*., 2012]. The transport of water vapor into the stratosphere plays a key role in modulating climate change at surface therefore acting as a source of unforced decadal variability, or as a feedback coupled to climate change [*Solomon et al*., 2010]; its representation in current climate models has large biases, and it is dependent on the representation of microphysical processes in the tropical tropopause layer [*Fueglistaler et al*., 2009; *Randel and Jensen*, 2013], on the representation of the tropopause temperature [*Gettelman et al*., 2010] as well as on the representation of the large-scale circulation. Moreover, climate models are not able to fully simulate the observed positive AO signature following a large volcanic eruption, therefore limiting their predictive skills.

Concerning the solar cycle effect on climate, some radiation schemes in current climate models have been off-line validated against line-by-line models to estimate how sensitive the radiation codes are to changes in solar irradiance and ozone and how well the 11 year solar signature is reproduced [*Forster et al*., 2011]. Results indicate that some current state-of-the-art models cannot properly simulate solar-induced variations in stratospheric temperature. Moreover, the indirect dynamical effects in the tropical lower stratosphere and extratropical stratosphere and the extension of the signal into the troposphere are more challenging to reproduce [*SPARC-CCMVal*, 2010].

5. Aerosols

Aerosols, the small liquid or solid particles suspended in the atmosphere, have three properties that make them of particular interest within the context of decadal projections: their potentially large radiative impact on global and regional scales, the strongly heterogeneous nature of this impact, and the potential for aerosol concentrations to change rapidly over decadal time scales as a result of policy or socioeconomic drivers. Accounting for aerosols processes, and the future emissions scenarios that they will respond to, could therefore represent an important component of future decadal predictability. Here we discuss this potential alongside some of the current challenges, not least the difficulty in representing the complex mechanisms involved, which range from the cloud droplet scale to synoptic transport. Given the peculiar nature of aerosols, essentially acting on boundary (rather than initial-)-value predictability, no specific section is devoted to available observational data sets, usable to realistically constrain model initialization. The role of observations of aerosol properties in the context of models development and evaluation is briefly discussed in section 5.2.

5.1. Mechanisms

Aerosols contribute to the Earth's radiative budget by scattering and absorbing solar and thermal radiation, and providing cloud condensation and ice nuclei, thus playing an important role in the formation of clouds. Changes in aerosol concentrations thus exert a radiative forcing, which over the industrial era is negative at the top of the atmosphere and surface on a global scale, but can be of either sign regionally [*Boucher et al*., 2013]. Figure 13 shows distributions of radiative forcing from aerosol-radiation and aerosol-cloud interactions, simulated by the Hadley Centre climate model Hadley Centre Global Environmental Model version 2 (HadGEM2) between the years 1860 and 1980, and 1980 and 2000. Radiative forcing patterns are partly driven by changes in aerosol concentrations and hence tend to be located close to and downwind from anthropogenic emissions sources. Locally, the magnitude and sign of aerosol radiative forcing are determined by three factors. First is the varying degree of competition between scattering and absorption processes, because aerosol-radiation interactions by absorbing carbonaceous and mineral aerosols exert a positive radiative forcing at the top of the atmosphere, which is stronger when aerosols are located above bright surfaces such as deserts and clouds [*Boucher et al*., 2013]. Second is the concentration of aerosols in pristine regions, because aerosol-cloud interactions are nonlinear with stronger radiative effects in cleaner environments. So continental emissions can have their stronger impacts in maritime regions with low-level cloud such as in the North Atlantic and Pacific Ocean, away from their emission sources. Third is the sign of the trend in aerosol concentrations. Regions where anthropogenic aerosol concentrations have decreased (for example, North America and Europe between 1980 and 2000) are associated with a positive radiative forcing that is the symptom of the suppression of an earlier negative radiative forcing. Conversely, regions where anthropogenic aerosol concentrations have increased are associated with a strengthening negative radiative forcing.

Aerosol radiative forcing triggers a redistribution of radiative fluxes within the atmosphere. Recent frameworks [*Hansen et al*., 2005; *Boucher et al*., 2013] distinguish the fast adjustments that operate on atmospheric time

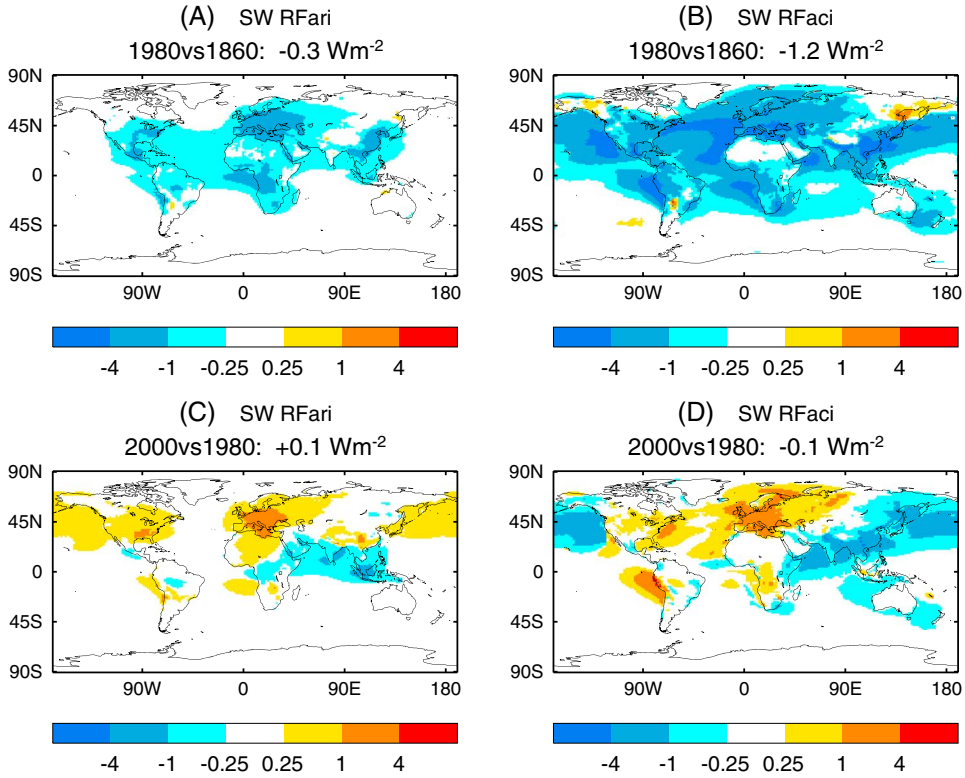

Figure 13. Shortwave top of atmosphere radiative forcing, in W m^{-2}, exerted by (a and c) direct aerosol-radiation and (b and d) aerosol-cloud albedo interactions between 1860 and 1980 (Figures 13a and 13b) and 1980 and 2000 (Figures 13c and 13d), as diagnosed from the Hadley Centre climate model HadGEM2.

scales, from the longer-term climate feedbacks that operate through changes in sea surface temperatures. Fast adjustments are local in nature and stem from the compensation of changes in the surface and atmospheric radiative budgets by changes in latent heat flux, in first approximation. The subsequent changes in moisture and temperature profiles affect cloud formation and the timing, intensity, and location of precipitation. This is particularly important for absorbing aerosols, which cause warming aloft and, depending on the cloud regime and the relative position of aerosols and clouds, lead to increased or decreased rainfall [*Bond et al*., 2013]. Modeling studies have suggested that on a global scale, the rainfall suppression from increases in sulfate aerosols is dominated by the longer-term global surface temperature increase rather than by the fast adjustments [*Andrews et al*., 2010; *Ming et al*., 2010]. Fast adjustments to aerosol-cloud interactions also perturb precipitation: the formation of smaller cloud droplet may delay precipitation and, in regimes where precipitation regulates the cloud life cycle, increase cloud cover and thickness, although strong buffering mechanisms may exist to dampen the cloud response to aerosol changes [*Stevens and Feingold*, 2009].

Climate feedbacks stem from large-scale changes in surface temperature and operate on oceanic time scales. Scattering aerosols, which exert a negative radiative forcing and lead to a cooling of the climate system, are associated with precipitation changes of typically 2–3% per degree of temperature change, in common with most other radiative drivers [*Andrews et al*., 2010]. Increases in scattering aerosols would therefore cause a long-term suppression of rainfall and for this reason marked decadal variations in global precipitation have been linked to decadal changes in aerosol amount [*Wu et al*., 2013]. The strongly regional or hemispheric nature of anthropogenic aerosols also leads to feedbacks on atmospheric circulation and the associated rainfall patterns. Such dynamical links between aerosol changes and rainfall are found on a range of spatial and temporal scales. To illustrate the differences in scale, on the local regional end of the spectrum, *Lau et al*. [2006] illustrate links between Himalayan dust and the timing of the Indian Monsoon onset. On a broader scale, *Chung and Seinfeld* [2005] suggest that interactions between North Hemisphere black carbon aerosols

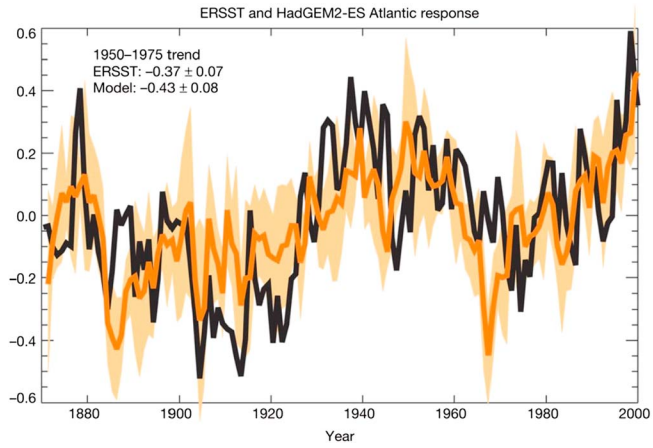

Figure 14. Comparison of basinwide (0–60 N) North Atlantic SSTs from observations (Extended Reconstructed Sea Surface Temperature (ERSST), black) and simulations of HadGEM2-ES (orange) for the historical (1860–2000) period. The ensemble average from four simulations (each starting from ocean states chosen to sample different phases in the internal ocean driver Atlantic variability) is shown (solid orange line) with the spread (1 standard deviation) indicated by the lighter orange region. On decadal time scales, common covariation of all four ensemble members, which matches a number of features of the observed variability, is evident—highlighting the potential forced role in decadal changes (industrial and volcanic aerosols in this case). Adapted from *Booth et al*. [2012]. Reprinted by permission from Macmillan Publishers Ltd.

and radiation shifts the ITCZ northward, while *Teng et al*. [2012] propose that enhanced black carbon absorption of solar radiation over Asia has the potential to trigger increases in surface temperature in North America through large-scale circulation changes. On a global scale, the strong hemispheric gradient in aerosol radiative forcing are linked to the position of the Asian monsoon system [*Bollasina et al*., 2011] and Sahel precipitation [*Ackerley et al*., 2011; *Haywood et al*., 2013]. Finally, the same hemispheric gradient explains why transient climate sensitivity is larger for anthropogenic aerosol changes than long-lived greenhouse gas changes, because the land-dominated North Hemisphere, where aerosols are located, responds faster than the ocean-dominated Southern Hemisphere [*Shindell*, 2014].

The North Atlantic Ocean and South Asia are two prominent regions where aerosol radiative effects and forcing may impact regional and global climate via circulation changes. The strongly heterogeneous nature of North Atlantic SST (NASST) variations relative to the neighboring South Atlantic or Pacific Ocean has been linked to large decadal climate changes worldwide: African Sahel drought in observations [*Folland et al*., 1986; *Hoerling et al*., 2006] and physical models [*Zhang and Delworth*, 2006; *Knight et al*., 2006]; rainfall in the Amazon region [*Knight et al*., 2006; *Good et al*., 2008]; Atlantic hurricanes [*Goldenberg et al*., 2001; *Trenberth and Shea*, 2006; *Zhang and Delworth*, 2006]; North American mean rainfall changes [*Enfield et al*., 2001] and rainfall extremes [*Curtis*, 2008]; European summer climate [*McCabe et al*., 2004; *Sutton and Hodson*, 2005; *Sutton and Dong*, 2012]; Indian monsoon rainfall [*Goswami et al*., 2006; *Zhang and Delworth*, 2006; *Lu et al*., 2006]; Arctic and Antarctic temperatures [*Chylek et al*., 2010]; Hadley circulation [*Baines and Folland*, 2007]; and ENSO [*Dong et al*., 2006] and ENSO-Asian monsoon relationships [*Chen et al*., 2010]. Crucially, those studies can be interpreted in an aerosol radiative forcing context. Radiative effects of aerosol-cloud interactions project strongly onto NASSTs [*Williams et al*., 2001; *Rotstayn and Lohmann*, 2002] because the clean maritime environment makes boundary layer cloud particularly sensitive to changes in aerosol amount. This can be seen in Figure 13b, where the North Atlantic is associated with strong aerosol-cloud radiative forcing in spite of the continental origin of anthropogenic aerosol changes. Indeed, an analysis of CMIP3 models shows that aerosol-cloud interactions need to be represented in models in order to simulate the observed trend in North and South Atlantic temperature contrast [*Chang et al*., 2011].

Past and future changes in aerosol emissions have, therefore, the potential to be one of the key decadal drivers of regional climate change, acting through NASST changes. *Booth et al*. [2012] using Hadley Centre Global Environmental Model version 2 Earth System configuration (HadGEM2-ES), a model with relatively strong aerosol-cloud radiative forcing, suggest that past aerosols changes are capable of explaining much of the temporal and spatial variability in NASSTs on multidecadal time scales, as illustrated in Figure 14. Atlantic aerosols have similarly been linked to Sahel drought [*Ackerley et al*., 2011; *Martin et al*., 2014], the Amazon dry season [*Cox et al*., 2008], Arctic temperature variability [*Fyfe et al*., 2013], a forced component to the Atlantic Meridional Ocean Circulation [*Cheng et al*., 2013] and hurricanes and tropical storms [*Villarini et al*., 2011; *Dunstone et al*., 2013]. Figure 15 [*Dunstone et al*., 2013] illustrates how a climate model, HadGEM2-ES, is able to capture the observed interdecadal changes in North Atlantic storm frequency when driven by aerosol emission changes. In both illustrations (Figures 14 and 15) the strong model-observed agreement

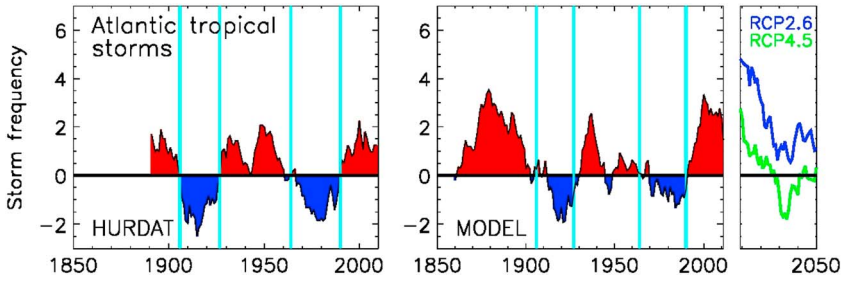

Figure 15. The change in (left) the North Atlantic Hurricane Database (HURDAT) tropical storm count and the equivalent indices calculated from the model ((middle) historical and (right) future). The model changes are based on the average of four ensemble members, with different initial ocean states. This emphasizes the common, forced changes in the model. The future-projected changes in the tropical storm count are shown for two Representative Concentration Pathway (RCP) scenarios: RCP2.6 and RCP4.5. Adapted from *Dunstone et al.* [2013]. Reprinted by permission from Macmillan Publishers Ltd.

highlights why there is current interest in capturing aerosol processes within near-term projection systems. Furthermore, aerosol-driven SST responses are not limited to the Atlantic Ocean: for example, *Xie et al.* [2013] used CMIP5 simulations by three global models to highlight robust responses to aerosol radiative forcing in the Pacific Ocean.

The growing body of studies focusing on aerosol impacts on the South Asian Monsoon can also be seen within the context of aerosol-driven hydrological mechanisms. Mineral dust [*Lau and Kim*, 2006; *Gautam et al.*, 2010] and mineral dust and black carbon [*Lau and Kim*, 2006] absorbing aerosols act via local processes in Tibet and India, causing warming that leads to a dynamically driven increase in rainfall. In fully coupled simulations, *Meehl et al.* [2008] suggest that it is the large-scale aerosol cooling over India that drives reductions in precipitation. Other studies suggest that remote sulfate aerosol forcing drives dynamical changes via changes in the Hadley circulation [*Kim et al.*, 2007; *Bollasina et al.*, 2011]. It is worth noting that aerosol-climate interactions are a two-way coupled system, where precipitation and circulation changes can equally feedback on local aerosol concentrations. There is currently no agreement on the net aerosol impact, with some studies suggesting that an increase in aerosols weakens [*Ramanathan et al.*, 2005; *Meehl et al.*, 2008; *Liu*, 2009; *Bollasina et al.*, 2011; *Shindell*, 2012] or strengthens [*Menon et al.*, 2002; *Lau and Kim*, 2006] the Asian monsoon. However, this disagreement relates partly to differences in experimental design, where atmosphere-ocean coupled experiments are compared to fixed SST experiments that do not capture SST-driven dynamical changes. Differences in process complexity (comparing impact of single versus multiple aerosol species) and differences in temporal (intraseasonal, seasonal, and interannual to decadal) and spatial scales also play a role.

Although we have so far focused on anthropogenic aerosol changes as potential drivers of decadal climate change, natural aerosols also play a role, including in the Atlantic and monsoon regions discussed above. Natural aerosols respond to either human (such as land use and wildfires) or climate drivers (moisture, temperature, and wind speed). *Wang et al.* [2012] illustrate how multidecadal changes in Sahel mineral dust correlate strongly with Sahel rainfall which is itself linked to NASST changes. As *Lau and Kim* [2007] and *Evan et al.* [2009, 2011] illustrate, these dust trends contribute to further cooling of Atlantic SSTs and as such are important feedback mechanisms within the climate system, which are important to represent in decadal prediction systems. In addition, emissions of sulfur dioxide by large volcanic eruptions can exert a strong negative radiative forcing that last several years, as demonstrated by the eruption of Mount Pinatubo in 1991 [*Dhomse et al.*, 2014]. Eruptions that load the two hemispheres asymmetrically, such as the eruption of El Chichon in 1982, may have contributed to Sahel droughts through changes in the Hadley circulation [*Haywood et al.*, 2013].

5.2. Perspectives

We have highlighted above an increasing body of literature that links aerosols to historical climate changes on decadal scales. There is a potential, therefore, for future emission changes to play an important role in regional and global climate. Figure 15 illustrates how sulfate aerosol differences (driven by different CO_2 mitigation pathways) imply two markedly different projected future changes in Atlantic tropical storms, in the HadGEM2 model [*Dunstone et al.*, 2013]. Under a scenario with aggressive mitigation of CO_2 emissions

(RCP2.6) this model projects a record increase in tropical storm frequency over the next decade. The higher future sulfur emissions associated with a more modest CO_2 mitigation pathway (RCP4.5), on the other hand, point to a steady decline in tropical storms over the same period. However, the degree to which aerosols will do so is linked to the magnitude of their radiative forcing, an aspect of climate models which is currently uncertain. Lack of process understanding is a severe limitation to modeling aerosols on the global scale, and the key elements for progress in modeling aerosol effects are better observations and improved understanding. Those improvements are happening, and processes behind interactions between aerosols and radiation and liquid clouds are getting better understood. Mechanisms of interactions between aerosols and mixed-phase and ice clouds remain poorly known, however [*Boucher et al*., 2013]. In the meantime, decadal projections need to be seen within the context of aerosol uncertainty. Aerosol processes complexity has increased in many GCMs [*Wang et al*., 2011a, 2011b], although the level of complexity needed to represent aerosol-cloud interactions with fidelity remains unclear. The diversity in aerosol distributions simulated by the state-of-the-art models that participated in CMIP5 simulations is very large, in spite of sharing the same aerosol emission data sets [*Wilcox et al*., 2013]. This diversity betrays the lack of knowledge and observational constraints on aerosol processes and arises not only from differences in aerosol representation [*Storelvmo et al*., 2009] but also from different simulations of atmospheric or cloud processes [*Haerter et al*., 2009; *Golaz et al*., 2013]. CMIP5 models cover a broad range of process complexity. For example, only two models represent nitrate aerosols. Nitrate aerosol formation competes with that of sulfate, so decreases in sulfur dioxide emissions in Europe and North America have been partly offset by increased nitrate aerosol arising from increased ammonia emissions. The omission of nitrate aerosols is therefore likely to lead to an underestimate of aerosol radiative forcing in models [*Bellouin et al*., 2011]. Carbonaceous aerosols are also treated differently across models, and the omission of complex ageing processes, in many models, is likely to lead to suppressed cloud condensation nucleus and overestimated black carbon aerosol lifetimes [*Spracklen et al*., 2011]. The challenge for decadal projection systems is that as process understanding develops so does our understanding of the role of near-term aerosol changes on the climate system. Importantly, models with stronger total aerosol forcing show more marked climate impacts [*Dunstone et al*., 2013]. The Geophysical Fluid Dynamics Laboratory coupled model 3.0 (GFDL-CM3), whose globally averaged aerosol radiative forcing is at the higher end of the –0.7 to –1.5 W m^{-2} range given by *Shindell et al*. [2013], links sulfate aerosol increases to large reductions in South Asian monsoon [*Bollasina et al*., 2011]. Similarly, anthropogenic aerosols in HadGEM2, another model with a strong globally averaged radiative forcing, explain 66% of past multidecadal NASST variability [*Booth et al*., 2012].

Given the potential for aerosol changes to drive substantial regional responses in models with stronger aerosol radiative forcing, it will be important to identify metrics that can validate these processes, although what these metrics will be remains an open question. *Zhang et al*. [2013], for example, highlight that the deep ocean North Atlantic heat uptake, a property influenced by the aerosol forced changes, is underestimated in HadGEM2. At the same time, *Haywood et al*. [2011] show that this same model is able to capture the observed decline and recovery in surface shortwave over the nearby land stations, which is the key mechanism via which aerosols drive variations in surface temperature. Open questions remain, therefore, on how to reconcile these conflicting inferences, and this will be an area that the community will need to make progress on before we can be more confident of the actual aerosols play in decadal changes. On the other end of the spectrum, models with smaller radiative effects are likely to explain a smaller fraction and hence capture weaker connections between future aerosol changes and climate response. It should be noted, however, that even models whose aerosol radiative forcing is comparatively weak at the global scale may still simulate strong local radiative forcing in key regions such as the North Atlantic [*Szopa et al*., 2013].

Observations of aerosol properties play an important role in model development and evaluation but can only provide an imperfect snapshot of the large number of aerosol and cloud properties involved in aerosol-radiation [*Kahn*, 2012] and aerosol-cloud interactions [*Stevens and Feingold*, 2009]. Simulated aerosol-radiation interactions can be benchmarked against a range of observational estimates [*Bellouin et al*., 2008; *Myhre et al*., 2013], although estimates of aerosol radiative forcing need to rely at least partly on global numerical modeling, where unobserved preindustrial aerosol concentrations dominate uncertainties [*Carslaw et al*., 2013]. There are also open questions about how to reconcile simulated aerosol absorption optical depth with ground-based retrievals [*Bond et al*., 2013]. The degree to which cloud albedo and life cycle are influenced by changes in aerosol number is similarly debated, because of inherent difficulties in distinguishing

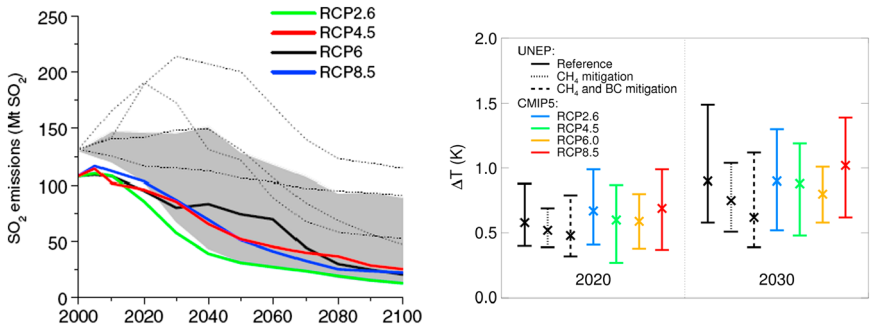

Figure 16. (left) Emissions of SO_2 for the future RCP scenarios (colors) with the 90% spread from the larger family of scenarios (22 members, which the RCPs were drawn from) in gray. SRES SO_2 emissions, the previous generation of socioeconomic pathways, are indicated by the dotted lines. From *van Vuuren* [2011]. (right) Globally averaged surface temperature change (K) in (left) 2016–2025 and (right) 2026–2035 relative to 1986–2005, according to multimodel United Nations Environment Programme (UNEP) and CMIP5 simulations with various emission scenarios of long- and short-lived climate forcers. Whiskers show the full model range. Crosses indicate the multimodel average. Adapted from Figure 11.24a of *Kirtman et al*. [2013].

aerosol-cloud interactions from thermodynamically driven cloud properties, such as changes in liquid water path [*Loeb and Schuster*, 2008]. Aircraft observations have provided strong evidence for aerosol-cloud interactions, but scaling those temporally and spatially sparse relationships up to regional and global scales remains challenging. Next-generation satellite retrieval algorithms are, however, promising, because they should be able to retrieve cloud droplet number concentrations and cloud updraft velocities at the same time, thus offering the prospect of distinguishing in observations aerosol influences on cloud properties from meteorological variability [*Rosenfeld et al*., 2014].

The other aspect of potential predictability is tied to future emissions scenarios, because aerosols are short lived and have the potential to respond rapidly to policy or socioeconomic changes. Near-term projections are remarkably insensitive to existing scenario differences in greenhouse gas emissions, which are more keenly felt as the century progresses [*Hawkins and Sutton*, 2009; *Booth et al*., 2013]. Decadal prediction systems have traditionally made use of Special Report on Emissions Scenarios (SRES) or RCP scenarios for near-term projections, and yet there are reasons why new scenarios need to be explored. First, aerosol emission differences between current RCPs arise from different assumptions about carbon dioxide mitigation, with a focus on the radiative forcing exerted in 2100. While the associated difference on sulfur dioxide emissions can have an appreciable climate impact [*Chalmers et al*., 2012], future aerosol emissions have the potential to respond to a wider range of drivers. The RCPs make common assumptions for all scenarios that air quality measures are rapidly, aggressively, and universally adopted [*van Vuuren et al*., 2011]. While sulfur dioxide emission reductions since the start of the 21st century have confirmed RCP assumptions [*Klimont et al*., 2013], whether similar reduction rates will be sustained for another decade is unknown and merits exploring in decadal scenarios. To give an example of the consequences of RCP assumptions, the aerosol emission differences that drive the two projections of future Atlantic tropical storms [*Dunstone et al*., 2013] (Figure 15) arise solely from differences in CO_2 mitigation pathways, not air quality measures. This can be illustrated by comparing the range of projected future SO_2 emissions presented in the current RCPs (Figure 16). Year 2000 baseline differences aside, the narrow distribution of future trends compared to the spread in the wider RCP storylines and early SRES scenarios (Figure 16, left) arise from the assumption of a common air quality approach, across the RCPs. In doing so they underestimate the spread of decadal forcing that would arise if such measures are delayed. Alternative emission storylines, such as the UNEP reference scenario [*Shindell et al*., 2012] make more conservative assumptions, based on only those emission cuts already subject to international agreements, and obtain a quite different picture for near-term aerosol concentrations. Differences in 2020 and 2030 mean estimates of projected warming, and lower bounds, are evident between the UNEP scenario and the RCP scenarios (Figure 16, right). The point that air quality mitigation assumptions can represent a first-order impact on these time scales, even for global average changes, is emphasized by *Kloster et al*. [2010] who show that by 2030, globally averaged temperature change can double (from 1° to over 2°) if a maximum feasible aerosol abatement scenario was followed. Decadal

projections based solely on existing RCP scenarios are therefore likely to be biased warm as RCPs overestimate decreases in aerosol emission. Fortunately, those limitations of the RCP framework have been identified and the sixth phase of the CMIP activity introduces the concept of Shared Socio-economic Pathways (SSPs) [*O'Neill et al*., 2014]. Combined with RCPs, SSPs form a matrix which explores both possible future radiative forcing trajectories and socioeconomic storylines [*van Vuuren et al*., 2014].

Second, given the potential of aerosols to drive regional climate change and their ability to respond rapidly to socioeconomic or policy drivers, aerosols are on the policy agenda. Decadal emission scenarios that span the range of possible aerosol changes over the next two decades need to be developed. For example, the use of black carbon aerosols to mitigate short-term global warming was recently discussed at G8 and Council of the Arctic meetings and is mooted as a potentially more tractable way to reduce near-term warming than greenhouse gas mitigation. According to *United Nations Environment Programme and World Meteorological Organization* [2011], decreases in black carbon emissions have the potential to mitigate 0.5° of warming up to 2050, with a large fraction of this realized within 10 to 30 years [*Shindell et al*., 2012]. Such a mitigation approach would significantly change the pattern and nature of emissions of aerosols and their precursors, raising questions about local impacts, especially on monsoon systems, and coemitted scattering aerosols [*Bond et al*., 2013]. Another example is the tension between economic expansion and air quality in East Asia. Chinese sulfur dioxide emissions, originating mainly from coal combustion, increased by up to 7% per year for the first part of the last decade [*Lu et al*., 2010]. While the introduction of chimney-scrubbing technologies since 2006 has lessened the rate of increase, further decreases could be achieved rapidly in response to worsening air quality in the main Chinese cities. Such decisions would again have important implications for regional aerosol concentrations, with associated impacts on the climate, both locally and remotely. Decadal projection systems are uniquely placed for exploring relationships between potential aerosol mitigation pathways and their associated climate impacts. Such an approach, taken by different modeling groups, would provide insight into the implication of any uncertainties inherent with our current modeling understanding. Testing a range of near-term aerosol emission scenarios would lessen the likelihood of systematically overestimating or underestimating future radiative forcing and in turn would inform socioeconomic and policy decisions in an analogous way that current RCPs inform longer-term climate mitigation decisions. To that end, CMIP6 includes simulations dedicated to short-lived climate forcers, which include aerosols and their gaseous precursors, within its ongoing Aerosols Chemistry Model Intercomparison Project. (AerChemMIP)

6. Conclusions

Recent research on decadal-scale predictability has mostly focused on the impact of ocean initialization [*Meehl et al*., 2009b, 2013; *Branstator et al*., 2012]. This stems from the ocean's large heat capacity that results in a slow manifold of the climate system and decadal predictability, arising from the initial state. Other constituents of the climate system have received relatively less attention because their contribution to the slow manifold is less obvious and the initialization as well as the representation of these components in state-of-the-art climate models are still very challenging. This is further exacerbated by a lack of adequate observations.

Here we present an overview of the most recent progress in understanding the potential role of sea ice, land surface, stratosphere, and aerosols in decadal-scale climate predictability. These (scarcely observed/poorly modeled) components act over different time scales and contribute to the overall predictability of the climate system following very different routes.

Strengthening the initial-value predictability through an improved initialization appears to be a viable option for the land surface (through soil moisture or vegetation initialization), sea ice, and, marginally, the stratosphere (possibly through the initialization of the QBO phase). On the other hand, realistically capturing future aerosol emission and land use storylines acts on the boundary-value predictability, both aerosols and land cover representing a key near-term forcing agent with the potential to drive both global and regional changes over the decadal time frame.

In addition to the obvious benefits stemming from the refinement of the initial- and boundary-value predictability, the overall predictive ability of ESMs is expected to depend on accurate representation/inclusion of climate feedback processes associated with specific components (and related interactions with other subsystems), regardless of their initialization and/or impact exerted as a forcing agent. Being associated with

process representation, this additional source of predictive skill—next referred to as *systemic buffering*—is active across various components of the Earth system and can potentially extend their intrinsic memory beyond the seasonal time scale, as illustrated in the following examples.

As documented in section 2.1.1, decadal variations in North Atlantic Ocean circulation affect the transport of sea ice through the Fram Strait, and this can subsequently modify deep water formation in the Labrador basin, ultimately influencing the meridional overturning circulation strength and heat transport. A more accurate model representation of this feedback loop, based on better quality observations and improved understanding of the mechanisms underlying the complex ocean-sea ice interaction, will therefore extend and amplify the intrinsic predictability associated with ocean initialization. Similarly, the inclusion of a well-resolved stratosphere in a dynamical model may represent, via the coupling with the troposphere and, possibly, the underlying ocean and sea ice, an additional source of predictability, dynamically bridging subsystems typically weakly (or not at all) connected in the previous generations of coupled AOGCMs. As reported in section 4.3, several studies suggest that the stratosphere can play an important role in modulating the low-frequency ocean-induced variability, such as the SST-forced NAO/AO response. The mechanism by which prolonged droughts over Sahel, through anomalous dust loadings, may affect the atmospheric radiation budget for longer than 1 year (discussed in section 3.3) is another example of systemic buffering, associated with land surface processes. An ocean-driven example (not discussed in this review) is provided by the analysis of *Stenchikov et al*. [2009]. The authors of this work show that the transient climate perturbation associated with the emission of volcanic sulfate aerosols during particularly vigorous eruptions is potentially able to persist well beyond the typical 2–3 years lower stratosphere residence time scale, thanks to the buffering effect of the oceans, responding to the volcanic-induced radiative cooling over the multidecadal time range. In all of these examples, the involved components of the climate system act as a "signal carrier," transferring and propagating information associated with the seeds of predictability embedded in the initial state and/or in the boundary forcings, through the full climatic phase space.

Potential predictability experiments designed for specific climate components provide a powerful diagnostic tool to sort out which variables, areas, seasons, and time scales are predictable and to focus further research. *Koenigk et al*. [2012] for instance indicate that decadal averages of Arctic sea ice thickness and area are well predicted along the ice edges in the North Atlantic sector. Whereas *Weiss et al*. [2012] suggest that the main gain in decadal predictions appear to be in regions exposed to shifts in the ITCZ and monsoon cycles, consistently with the transitional dry-to-wet climate zones that expose a strong land-atmosphere coupling. The use of the potential predictability experimental framework might be usefully extended to other processes, not yet explored through this approach. For instance, several studies indicate that the dynamical coupling of the stratosphere with snow and sea ice cover in the Arctic features potential decadal predictability (section 4.3). Similarly, the Asian monsoon system and Sahel rainfall appear to be sensitive to aerosol concentrations and might have potential decadal predictability (section 5.1).

Obvious and crucial requirements of these new components are internal consistency and conservation of mass and energy. Although this may sound trivial, it is not easily accomplished. These components are often developed off-line and use different variables. Future developments should therefore also focus on the coherent and consistent incorporation of these components into climate models. Pioneering decadal simulations with a dynamic vegetation model revealed the importance of consistency in hydroclimatic regimes between the vegetation and climate models [*Weiss et al*., 2014]. Coherence and consistency are also required for the initialization. Decadal sea ice predictions have shown that a balanced initial state between the different components is required to avoid an initial shock that ruins all the benefits that might come from including these new components (section 2.3).

The inclusion of new components introduces additional degrees of freedom that result in additional skill only if the fundamental processes, from large-scale dynamics to microphysics, are accurately simulated. In addition to model development, it is equally important to recognize that a thorough exploitation of the predictive ability of Earth system models is only possible if supported by adequate observational networks and computational resources. Concerning observations, for many climate constituents progress is hampered by the scarcity of data. For instance, sea ice and soil moisture cannot be adequately initialized due to the lack of reliable data. Similarly, insufficient data are available to validate and calibrate stratospheric chemistry

and the impact of aerosols on cloud formation. In addition, some areas that might exhibit potential predictability, such as Antarctica and the surrounding ocean, experience harsh weather conditions year-round, resulting in scarcity of data. The inherently low signal-to-noise ratio characterizing the predictable fraction of the full signal requires the use of large-sized ensembles. This in turn calls for suitable computational resources, which are currently still out of reach for most of the modeling groups. Future investments in computational and observational infrastructures will be therefore strategic to improve the quality and trustworthiness of decadal climate forecasts.

Acknowledgments

Data supporting Figure 2 are available at National Snow and Ice Data Center (NSIDC), *Fetterer et al*. [2014], Sea ice index, Electronic, available at http://nsidc.org/data/seaice_index. The authors wish to thank the EU Joint Programme Initiative-Climate for hosting, fostering, and stimulating the discussions that led to conceive this work. Comments from Adam Scaife, Doug Smith, Silvio Gualdi, Gerald Meehl, Mark Moldwin, and an anonymous reviewer are also gratefully acknowledged. A.B. and S.M. received support from the Italian Ministry of Education, University and Research and Ministry for Environment, Land and Sea through the Project GEMINA.

The Editor on this paper was Alan Robock. He thanks Gerald Meehl, Mark Moldwin, and one anonymous reviewer for their review assistance on this manuscript.

References

Ackerley, D., B. B. B. Booth, S. H. E. Knight, E. J. Highwood, D. J. Frame, M. R. Allen, and D. P. Rowell (2011), Sensitivity of twentieth-century Sahel rainfall to sulfate aerosol and CO_2 forcing, *J. Clim.*, *24*, 4999–5014, doi:10.1175/JCLI-D-11-00019.1.

Alexander, M., U. Bhatt, J. Walsh, M. Timlin, J. Miller, and J. Scott (2004), The atmospheric response to realistic Arctic sea ice anomalies in an AGCM during winter, *J. Clim.*, *17*, 890–905.

American Meteorological Society Statement (2001), Seasonal to interannual climate prediction (adopted by AMS Council 14 January 2001), *Bull. Am. Meteorol. Soc.*, *82*, 701–703.

Andrews, T., P. M. Forster, O. Boucher, N. Bellouin, and A. Jones (2010), Precipitation, radiative forcing and global temperature change, *Geophys. Res. Lett.*, *37*, L14701, doi:10.1029/2010GL043991.

Angell, J. K. (1997), Stratospheric warming due to Agung, E1 Chichon, and Pinatubo taking into account the quasi-biennial oscillation, *J. Geophys. Res.*, *102*, 9479–9485, doi:10.1029/96JD03588.

Arfeuille, G., L. A. Mysak, and L. B. Tremblay (2000), Simulation of the interannual variability of the wind-driven Arctic sea-ice cover during 1958–1998, *Clim. Dyn.*, *16*, 107–121.

Arora, V. (2002), Modeling vegetation as a dynamic component in soil-vegetation-atmosphere transfer schemes and hydrological models, *Rev. Geophys.*, *40*(2), 1006, doi:10.1029/2001RG000103.

Bailey, M., A. O'Neill, and V. D. Pope (1993), Stratospheric analyses produced by the UK Meteorological Office, *J. Appl. Meteorol.*, *32*, 1472–1483.

Baines, P. G., and C. K. Folland (2007), Evidence for a rapid global climate shift across the late 1960s, *J. Clim.*, *20*, 2721–2744.

Balachandran, N., D. Rind, P. Lonergan, and D. Shindell (1999), Effects of solar cycle variability on the lower stratosphere and the troposphere, *J. Geophys. Res.*, *104*, 27,321–27,339, doi:10.1029/1999JD900924.

Baldwin, M. P., and T. J. Dunkerton (2001), Stratospheric harbingers of anomalous weather regimes, *Science*, *294*, 581–584.

Baldwin, M. P., D. B. Stephenson, D. W. J. Thompson, T. J. Dunkerton, A. J. Charlton, and A. O'Neill (2003), Stratospheric memory and extended-range weather forecasts, *Science*, *301*, 636–640.

Balsamo, G., et al. (2012), ERA-Interim/Land: A global land-surface reanalysis based on ERA-Interim meteorological forcing, *ERA-Report series*, 13.

Barnes, E. A. (2013), Revisiting the evidence linking Arctic amplification to extreme weather in midlatitudes, *Geophys. Res. Lett.*, *40*, 4734–4739, doi:10.1002/grl.50880.

Barnes, E. A., E. Dunn-Sigouin, G. Masato, and T. Woollings (2014), Exploring recent trends in Northern Hemisphere blocking, *Geophys. Res. Lett.*, *41*, 638–644, doi:10.1002/2013GL058745.

Belkin, I., S. Levitus, J. Antonov, and S. A. Malmberg (1998), "Great Salinity Anomalies" in the North Atlantic, *Prog. Oceanogr.*, *41*, 1–68.

Bellouin, N., A. Jones, J. Haywood, and S. A. Christopher (2008), Updated estimate of aerosol direct radiative forcing from satellite observations and comparison against the Hadley Centre climate model, *J. Geophys. Res.*, *113*, D10205, doi:10.1029/2007JD009385.

Bellouin, N., et al. (2011), Aerosol forcing in the Climate Model Intercomparison Project (CMIP5) simulations by HadGEM2-ES and the role of ammonium nitrate, *J. Geophys. Res.*, *116*, D20206, doi:10.1029/2011JD016074.

Bellucci, A., et al. (2014), An assessment of a multi-model ensemble of decadal climate predictions, *Clim. Dyn.*, doi:10.1007/s00382-014-2164-y.

Betts, A. K., and J. H. Ball (1995), The FIFE surface diurnal cycle climate, *J. Geophys. Res.*, *100*(D12), 25,679–25,693, doi:10.1029/94JD03121.

Betts, A. K., P. Viterbo, A. Beljaars, H.-L. Pan, S.-Y. Hong, M. Goulden, and S. Wofsy (1998), Evaluation of land-surface interaction in ECMWF and NCEP/NCAR reanalysis models over grassland (FIFE) and boreal forest (BOREAS), *J. Geophys. Res.*, *103*(D18), 23,079–23,085, doi:10.1029/98JD02023.

Bierkens, M. P., and B. J. J. M. van den Hurk (2007), Groundwater convergence as a possible mechanism for multi-year persistence in rainfall, *Geophys. Res. Lett.*, *34*, L02402, doi:10.1029/2006GL028396.

Bintanja, R., G. J. van Oldenborgh, S. S. Drijfhout, B. Wouters, and C. A. Katsman (2013), Important role for ocean warming and increased ice-shelf melt in Antarctic sea-ice expansion, *Nat. Geosci.*, *6*(5), 376–379, doi:10.1038/ngeo1767.

Bjerknes, J. (1964), Atlantic air-sea interaction, *Adv. Geophys.*, *10*, 1–82.

Black, R. X. (2002), Stratospheric forcing of surface climate in the Arctic Oscillation, *J. Clim.*, *15*, 268–277.

Blanchard-Wrigglesworth, E., K. C. Armour, C. M. Bitz, and E. DeWeaver (2011), Persistence and inherent predictability of Arctic sea ice in a GCM ensemble and observations, *J. Clim.*, *24*, 231–250.

Blüthgen, J., R. Gerdes, and M. Werner (2012), Atmospheric response to the extreme Arctic sea ice conditions in 2007, *Geophys. Res. Lett.*, *39*, L02707, doi:10.1029/2011GL050486.

Boer, G. J. (2000), A study of atmosphere–ocean predictability on long time scales, *Clim. Dyn.*, *16*, 469–472.

Boer, G. J. (2004), Long timescale potential predictability in an ensemble of coupled climate models, *Clim. Dyn.*, *23*, 29–44.

Boer, G. J., and S. J. Lambert (2008), Multi-model decadal potential predictability of precipitation and temperature, *Geophys. Res. Lett.*, *35*, L05706, doi:10.1029/2008GL033234.

Bollasina, M., Y. Ming, and V. Ramaswamy (2011), Anthropogenic aerosols and the weakening of the South Asian summer monsoon, *Science*, *334*(6055), 502–505, doi:10.1126/science.1204994.

Bonan, G. B. (2008), *Ecological Climatology*, 552 pp., Cambridge Univ. Press, Cambridge, U. K.

Bond, T. C., et al. (2013), Bounding the role of black carbon in the climate system: A scientific assessment, *J. Geophys. Res. Atmos.*, *118*, 5380–5552, doi:10.1002/jgrd.50171.

Booth, B. B. B., N. J. Dunstone, P. R. Halloran, T. Andrews, and N. Bellouin (2012), Aerosols implicated as a prime driver of twentieth-century North Atlantic climate variability, *Nature*, *484*, 228–232, doi:10.1038/nature10946.

Booth, B. B. B., D. Bernie, D. McNeall, E. Hawkins, J. Caesar, C. Boulton, P. Friedlingstein, and D. M. H. Sexton (2013), Scenario and modelling uncertainty in global mean temperature change derived from emission-driven global climate models, *Earth Syst. Dyn.*, *4*, 95–108, doi:10.5194/esd-4-95-2013.

Boucher, O., et al. (2013), Clouds and Aerosols, in *Climate Change 2013: The Physical Science Basis. Contribution of Working Group I to the Fifth Assessment Report of the Intergovernmental Panel on Climate Change*, edited by T. F. Stocker et al., Cambridge Univ. Press, Cambridge, U. K., and New York.
Boussetta, S., et al. (2013), Natural land carbon dioxide exchanges in the ECMWF Integrated Forecasting System: Implementation and offline validation, *J. Geophys. Res. Atmos.*, *118*, 5923–5946, doi:10.1002/jgrd.50488.
Branstator, G., H. Teng, G. Meehl, M. Kimoto, J. Knight, M. Latif, and A. Rosati (2012), Systematic estimates of initial value decadal predictability for six AOGCMs, *J. Clim.*, *25*, 1827–1846.
Budikova, D. (2009), Role of Arctic sea ice in global atmospheric circulation: A review, *Global Planet. Change*, *68*, 149–163, doi:10.1016/j.gloplacha.2009.04.001.
Budyko, M. I. (1974), *Climate and Life*, 508 pp., Academic Press, New York.
Butchart, N. (2014), The Brewer-Dobson circulation, *Rev. Geophys.*, *52*, 157–184, doi:10.1002/2013RG000448.
Butchart, N., and A. Scaife (2001), Removal of chlorofluorocarbons by increased mass exchange between the stratosphere and troposphere in a changing climate, *Nature*, *410*, 799–802.
Butchart, N., J. Austin, J. Knight, A. Scaife, and M. L. Gallani (2000), The response of the stratospheric climate to projected changes in the concentrations of the well-mixed greenhouse gases from 1992–2051, *J. Clim.*, *13*, 2142–2159.
Butchart, N., et al. (2006), Simulations of anthropogenic change in the strength of the Brewer-Dobson circulation, *Clim. Dyn.*, *27*, 727–741, doi:10.1007/s00382-006-0162-4.
Cagnazzo, C., and E. Manzini (2009), Impact of the stratosphere on the winter tropospheric teleconnections between ENSO and the North Atlantic and European region, *J. Clim.*, *22*, 1223–1238.
Cagnazzo, C., E. Manzini, P. G. Fogli, M. Vichi, and P. Davini (2013), Role of stratospheric dynamics in the ozone–carbon connection in the Southern Hemisphere, *Clim. Dyn.*, *41*, 3039–3054, doi:10.1007/s00382-013-1745-5.
Cai, W. (2006), Antarctic ozone depletion causes an intensification of the Southern Ocean super-gyre circulation, *Geophys. Res. Lett.*, *33*, L03712, doi:10.1029/2005GL024911.
Calvo, N., and R. R. Garcia (2009), Wave forcing of the tropical upwelling in the lower stratosphere under increasing concentrations of greenhouse gases, *J. Atmos. Sci.*, *66*, 3184–3196, doi:10.1175/2009JAS3085.1.
Cane, M. (2010), Climate science: Decadal predictions in demand, *Nat. Geosci.*, *3*, 231–232, doi:10.1038/ngeo823.
Carslaw, K. S., et al. (2013), Large contribution of natural aerosols to uncertainty in indirect forcing, *Nature*, *503*, 67–71, doi:10.1038/nature12674.
Chalmers, N., E. J. Highwood, E. Hawkins, R. T. Sutton, and L. J. Wilcox (2012), Aerosol contribution to the rapid warming of near-term climate under RCP 2.6, *Geophys. Res. Lett.*, *39*, L18709, doi:10.1029/2012GL052848.
Chang, C. Y., J. C. H. Chiang, M. F. Wehner, A. Friedman, and R. Ruedy (2011), Sulfate aerosol control of tropical Atlantic climate over the 20th century, *J. Clim.*, *24*, 2540–2555.
Charlton-Perez, A. J., et al. (2013), On the lack of stratospheric dynamical variability in low-top versions of the CMIP5 models, *J. Geophys. Res. Atmos.*, *118*, 2494–2505, doi:10.1002/jgrd.50125.
Chen, W., B.-W. Dong, and R.-Y. Lu (2010), Impact of the Atlantic Ocean on the multidecadal fluctuation of El Niño Southern Oscillation-South Asian monsoon relationship in a coupled general circulation model, *J. Geophys. Res.*, *115*, D17109, doi:10.1029/2009JD013596.
Chevallier, M., and D. Salas-Melia (2012), The role of sea ice thickness distribution in the Arctic sea ice potential predictability: A diagnostic approach with a coupled GCM, *J. Clim.*, *25*, 3025–3038.
Chevallier, M., D. Salas-Melia, A. Voldoire, M. Deque, and G. Garric (2013), Seasonal forecasts of the Pan-Arctic sea ice extent using a GCM-based seasonal prediction system, *J. Clim.*, *26*(16), 6092–6104, doi:10.1175/JCLI-D-12-00612.1.
Chung, S. H., and J. H. Seinfeld (2005), Climate response of direct radiative forcing of anthropogenic black carbon, *J. Geophys. Res.*, *110*, D11102, doi:10.1029/2004JD005441.
Chylek, P., C. K. Folland, G. Lesins, and M. K. Dubey (2010), Twentieth century bipolar seesaw of the Arctic and Antarctic surface air temperatures, *Geophys. Res. Lett.*, *37*, L08703, doi:10.1029/2010GL042793.
Cohen, J. L., M. Barlow, P. J. Kushner, and K. Saito (2007), Stratosphere–troposphere coupling and links with Eurasian land surface variability, *J. Clim.*, *20*, 5335–5343, doi:10.1175/2007JCLI1725.1.
Cohen, J. L., J. C. Furtado, M. A. Barlow, V. A. Alexeev, and J. E. Cherry (2012), Arctic warming, increasing snow cover and widespread boreal winter cooling, *Environ. Res. Lett.*, *7*, 014007, doi:10.1088/1748-9326/7/1/014007.
Collins, M., et al. (2006), Interannual to decadal climate predictability in the North Atlantic: A multimodel-ensemble study, *J. Clim.*, *19*, 1195–1203.
Comiso, J. C., C. Parkinson, R. Gersten, and L. Stock (2008), Accelerated decline in the Arctic sea ice cover, *Geophys. Res. Lett.*, *35*, L01703, doi:10.1029/2007GL031972.
Conil, S., H. Douville, and S. Tyteca (2007), The relative influence of soil moisture and SST in climate predictability explored within ensembles of AMIP type experiments, *Clim. Dyn.*, *28*(2–3), 125–145.
Cook, B. I., R. L. Miller, and R. Seager (2009), Amplification of the North American "Dust Bowl" drought through human-induced land degradation, *Proc. Natl. Acad. Sci. U.S.A.*, *106*(13), 4997–5001.
Corti, S., A. Weisheimer, T. N. Palmer, F. J. Doblas-Reyes, and L. Magnusson (2012), Reliability of decadal predictions, *Geophys. Res. Lett.*, *39*, L21712, doi:10.1029/2012GL053354.
Cox, P. M., P. P. Harris, C. Huntingford, R. A. Betts, M. Collins, C. D. Jones, T. E. Jupp, J. A. Marengo, and C. A. Nobre (2008), Increasing risk of Amazonian drought due to decreasing aerosol pollution, *Nature*, *453*, 212–215, doi:10.1038/nature06960.
Crow, W. T., A. A. Berg, M. H. Cosh, A. Loew, B. P. Mohanty, R. Panciera, P. de Rosnay, D. Ryu, and J. P. Walker (2012), Upscaling sparse ground-based soil moisture observations for the validation of coarse-resolution satellite soil moisture products, *Rev. Geophys.*, *50*, RG2002, doi:10.1029/2011RG000372.
Curtis, S. (2008), The Atlantic multidecadal oscillation and extreme daily precipitation over the US and Mexico during the hurricane season, *Clim. Dyn.*, *30*, 343–351.
De Jeu, R. A. M., W. Wagner, T. H. Holmes, A. J. Dolman, N. C. van de Giesen, and J. Friesen (2008), Global soil moisture patterns observed by space borne microwave radiometers and scatterometers, *Surv Geophys.*, *29*(4–5), 399–420.
Delworth, T., and R. J. Greatbatch (2000), Multidecadal thermohaline circulation variability driven by atmospheric surface flux forcing, *J. Clim.*, *13*, 1481–1495.
Delworth, T., S. Manabe, and R. J. Stouffer (1993), Interdecadal variations of the thermohaline circulation in a coupled ocean–atmosphere model, *J. Clim.*, *6*, 1993–2011.
Dhomse, S. S., et al. (2014), Aerosol microphysics simulations of the Mt. Pinatubo eruption with the UKCA composition-climate model, *Atmos. Chem. Phys. Discuss.*, *14*, 2799–2855, doi:10.5194/acpd-14-2799-2014.

Dickson, R., J. Meincke, and S. A. Malmberg (1988), The "Great Salinity Anomaly" in the northern North Atlantic, *Prog. Oceanogr.*, *20*, 103–151.
Ding, H., R. J. Greatbatch, M. Latif, W. Park, and R. Gerdes (2013), Hindcast of the 1976/77 and 1998/99 climate shifts in the Pacific, *J. Clim.*, *26*, 7650–7661, doi:10.1175/JCLI-D-12-00626.1.
Dirmeyer, P. A. (2003), The role of the land surface background state in climate predictability, *J. Hydrometeorol.*, *4*, 599–610.
Dirmeyer, P. A., X. Gao, M. Zhao, Z. Guo, T. Oki, and N. Hanasaki (2006), GSWP-2: Multimodel analysis and implications for our perception of the land surface, *Bull. Am. Meteorol. Soc.*, *87*, 1381–1397.
Dirmeyer, P. A., S. Kumar, M. J. Fennessy, E. L. Altshuler, T. DelSole, Z. Guo, B. A. Cash, and D. Straus (2013), Model estimates of land-driven predictability in a changing climate from CCSM4, *J. Clim.*, *26*, 8495–8512, doi:10.1175/JCLI-D-13-00029.1.
Doblas-Reyes, F. J., I. Andreu-Burillo, Y. Chikamoto, J. García-Serrano, V. Guemas, M. Kimoto, T. Mochizuki, L. R. L. Rodrigues, and G. J. van Oldenborgh (2013), Initialized near-term regional climate change prediction, *Nat. Comm.*, *4*, 1715, doi:10.1038/ncomms2704.
Dong, B., R. T. Sutton, and A. A. Scaife (2006), Multidecadal modulation of El Niño–Southern Oscillation (ENSO) variance by Atlantic Ocean sea surface temperatures, *Geophys. Res. Lett.*, *33*, L08705, doi:10.1029/2006GL025766.
Dorigo, W. A., et al. (2011), The International Soil Moisture Network: A data hosting facility for global in situ soil moisture measurements, *Hydrol. Earth Syst. Sci.*, *15*(5), 1675–1698, doi:10.5194/hess-15-1675-2011.
Douville, H. (2010), Relative contribution of soil moisture and snow mass to seasonal climate predictability: A pilot study, *Clim. Dyn.*, *34*(6), 797–818.
Dulière, V., and T. Fichefet (2007), On the assimilation of ice velocity and concentration data into large-scale sea ice models, *Ocean Sci.*, *3*, 321–335.
Dunstone, N. J., D. M. Smith, B. B. B. Booth, L. Hermanson, and R. Eade (2013), Anthropogenic aerosol forcing of Atlantic tropical storms, *Nat. Geosci.*, *6*, 534–539, doi:10.1038/ngeo1854.
Eagleson, P. S. (1978), Climate, soil, and vegetation: 4. The expected value of annual evapotranspiration, *Water Resour. Res.*, *14*(5), 731–739, doi:10.1029/WR014i005p00731.
Eltahir, E. A. B. (1998), A soil moisture–rainfall feedback mechanism: 1. Theory and observations, *Water Resour. Res.*, *34*(4), 765–776, doi:10.1029/97WR03499.
Enfield, D. B., A. M. Mestas-Nunez, and P. J. Trimble (2001), The Atlantic Multidecadal Oscillation and its relation to rainfall and river flows in the continental US, *Geophys. Res. Lett.*, *28*(10), 2077–2080, doi:10.1029/2000GL012745.
Evan, A. T., D. J. Vimont, A. K. Heidinger, J. P. Kossin, and R. Bennartz (2009), The role of aerosols in the evolution of tropical North Atlantic Ocean temperature anomalies, *Science*, *324*, 778–781.
Evan, A. T., G. R. Foltz, D. Zhang, and D. J. Vimont (2011), Influence of African dust on ocean-atmosphere variability in the tropical Atlantic, *Nat. Geosci.*, *4*, 762–765.
Fan, Y., and G. Miguez-Macho (2010), Potential groundwater contribution to Amazon evapotranspiration, *Hydrol. Earth. Syst. Sci.*, *14*, 2039–2056.
Fennessy, M., and J. Shukla (1999), Impact of soil wetness on seasonal atmospheric prediction, *J. Clim.*, *12*, 3167–3180.
Ferranti, L., and P. Viterbo (2006), The European summer of 2003: Sensitivity to soil water initial conditions, *J. Clim.*, *19*, 3659–3680.
Fetterer, F., K. Knowles, W. Meier, and M. Savoie (2014), Sea ice index, Electronic. [Available at http://nsidc.org/data/seaice_index/] (last access: Aug 2014).
Fischer, E. M., S. I. Seneviratne, P. L. Vidale, D. Lüthi, and C. Schär (2007), Soil moisture–atmosphere interactions during the 2003 European summer heat wave, *J. Clim.*, *20*, 5081–5099.
Fletcher, C. G., and P. J. Kushner (2011), The role of linear interference in the Annular Mode response to tropical SST forcing, *J. Clim.*, *24*, 778–794.
Folland, C. K., T. N. Palmer, and D. E. Parker (1986), Sahel rainfall and worldwide sea temperatures, 1901–85, *Nature*, *320*, 602–607.
Forster, P. M., et al. (2011), Evaluation of radiation scheme performance within chemistry climate models, *J. Geophys. Res.*, *116*, D10302, doi:10.1029/2010JD015361.
Frame, T., and L. J. Gray (2010), The 11-year solar cycle in era-40 data: An update to 2008, *J. Clim.*, *23*, 2213–2222, doi:10.1175/2009JCLI3150.1.
Francis, J. A., and S. J. Vavrus (2012), Evidence linking Arctic amplification to extreme weather in mid-latitudes, *Geophys. Res. Lett.*, *39*, L06801, doi:10.1029/2012GL051000.
Francis, J. A., W. Chan, D. Leathers, J. R. Miller, and D. E. Veron (2009), Winter Northern Hemisphere weather patterns remember summer Arctic sea ice extent, *Geophys. Res. Lett.*, *36*, L07503, doi:10.1029/2009GL037274.
Fueglistaler, S., A. E. Dessler, T. J. Dunkerton, I. Folkins, Q. Fu, and P. W. Mote (2009), Tropical tropopause layer, *Rev. Geophys.*, *47*, RG1004, doi:10.1029/2008RG000267.
Fyfe, J. C., N. P. Gillett, and F. W. Zwiers (2013), Overestimated global warming over the past 20 years, *Nat. Clim. Change*, *3*, 767–769, doi:10.1038/nclimate1972.
Garcia-Serrano, J., and F. J. Doblas-Reyes (2012), On the assessment of near-surface global temperature and North Atlantic multi-decadal variability in the ENSEMBLES decadal hindcast, *Clim. Dyn.*, *39*, doi:10.1007/s00382-012-1413-1.
Gautam, R., N. C. Hsu, and K.-M. Lau (2010), Premonsoon aerosol characterization and radiative effects over the Indo-Gangetic Plains: Implications for regional climate warming, *J. Geophys. Res.*, *115*, D17208, doi:10.1029/2010JD013819.
Geller, M. A., et al. (2013), A comparison between gravity wave momentum fluxes in observations and climate models, *J. Clim.*, *26*, 6383–6405, doi:10.1175/JCLI-D-12-00545.1.
Gerber, E. P., et al. (2012), Assessing and understanding the impact of stratospheric dynamics and variability on the Earth system, *Bull. Am. Meteorol. Soc.*, *93*, 845–859, doi:10.1175/BAMS-D-11-00145.1.
Gettelman, A., et al. (2010), Multimodel assessment of the upper troposphere and lower stratosphere: Tropics and global trends, *J. Geophys. Res.*, *115*, D00M08, doi:10.1029/2009JD013638.
Giorgetta, M. A., L. Bengtsson, and K. Arpe (1999), An investigation of QBO signals in the east Asian and Indian monsoon in GCM experiments, *Clim. Dyn.*, *15*, 435–450.
Giorgetta, M. A., E. Manzini, E. Roeckner, M. Esch, and L. Bengtsson (2006), Climatology and forcing of the quasi-biennial oscillation in the MAECHAM5 model, *J. Clim.*, *19*, 3882–3901.
Goddard, L., J. W. Hurrell, B. P. Kirtman, J. Murphy, T. Stockdale, and C. Vera (2012), Two time scales for the price of one (almost), *Bull. Am. Meteorol. Soc.*, *93*, 621–629.
Golaz, J.-C., L. W. Horowitz, and H. Levy (2013), Cloud tuning in a coupled climate model: Impact on 20th century warming, *Geophys. Res. Lett.*, *40*, 2246–2251, doi:10.1002/grl.50232.
Goldenberg, S. B., C. W. Landsea, A. M. Mestas-Nuñez, and W. M. Gray (2001), The recent increase in Atlantic hurricane activity: Causes and implications, *Science*, *293*, 474–479.
Gong, D., and S. Wang (1999), Definition of Antarctic oscillation index, *Geophys. Res. Lett.*, *26*(4), 459–462, doi:10.1029/1999GL900003.

Good, P., et al. (2008), An objective tropical Atlantic sea surface temperature gradient index for studies of south Amazon dry-season climate variability and change, *Phil. Trans. R. Soc. Biol. Sci.*, *363*, 1761–1766.
Goosse, H., and M. M. Holland (2005), Mechanisms of decadal Arctic climate variability in the Community Climate System Model, version 2 (CCSM2), *J. Clim.*, *18*, 3552–3570.
Goosse, H., F. M. Selten, R. J. Haarsma, and J. D. Opsteegh (2002), A mechanism of decadal variability of the sea-ice volume in the Northern Hemisphere, *Clim. Dyn.*, *19*, 61–83.
Goosse, H., O. Arzel, C. M. Bitz, A. de Montety, and M. Vancoppenolle (2009), Increased variability of the Arctic summer ice extent in a warmer climate, *Geophys. Res. Lett.*, *36*, L23702, doi:10.1029/2009GL040546.
Goswami, B. N., M. S. Madhusoodanan, C. P. Neema, and D. Sengupta (2006), A physical mechanism for North Atlantic SST influence on the Indian summer monsoon, *Geophys. Res. Lett.*, *33*, L02706, doi:10.1029/2005GL024803.
Graversen, R. G., and M. Wang (2009), Polar amplification in a coupled climate model with locked albedo, *Clim. Dyn.*, *33*, 629–643, doi:10.1007/s00382-002-0290-4.
Graversen, R. G., T. Mauritsen, M. Tjernström, E. Källen, and G. Svensson (2008), Vertical structure of recent Arctic warming, *Nature*, *541*, 53–56, doi:10.1038/nature06502.
Gray, L. J. J., et al. (2010), Solar influences on climate, *Rev. Geophys.*, *48*, RG4001, doi:10.1029/2009RG000282.
Gray, L. J., et al. (2013), A lagged response to the 11 year solar cycle in observed winter Atlantic/European weather patterns, *J. Geophys. Res. Atmos.*, *118*, 13,405–13,420, doi:10.1002/2013JD020062.
Griffies, S. M., and K. Bryan (1997), A predictability study of simulated North Atlantic multidecadal variability, *Clim. Dyn.*, *13*, 459–488.
Griffies, S. M., and E. Tziperman (1995), A linear thermohaline oscillator driven by stochastic atmospheric forcing, *J. Clim.*, *8*, 2440–2453.
Gulev, S. K., M. Latif, N. Keenlyside, W. Park, and K. P. Koltermann (2013), North Atlantic Ocean control on surface heat flux on multidecadal timescales, *Nature*, *499*(7459), 464–467, doi:10.1038/nature12268.
Guo, Z., and P. A. Dirmeyer (2006), Evaluation of the Second Global Soil Wetness Project soil moisture simulations: 1. Intermodel comparison, *J. Geophys. Res.*, *111*, D22S02, doi:10.1029/2006JD007233.
Guo, Z., et al. (2006), GLACE: The Global Land–Atmosphere Coupling Experiment. Part II: Analysis, *J. Hydrometeorol.*, *7*, 611–625.
Guo, Z., P. A. Dirmeyer, and T. DelSole (2011), Land surface impacts on subseasonal and seasonal predictability, *Geophys. Res. Lett.*, *38*, L24812, doi:10.1029/2011GL049945.
Guo, Z., P. A. Dirmeyer, T. DelSole, and R. D. Koster (2012), Rebound in atmospheric predictability and the role of the land surface, *J. Clim.*, *25*, 4744–4749.
Haak, H., J. Jungclaus, U. Mikolajewicz, and M. Latif (2003), Formation and propagation of great salinity anomalies, *Geophys. Res. Lett.*, *30*(9), 1473, doi: 10.1029/2003GL017065.
Haerter, J. O., et al. (2009), Parametric uncertainty effects on aerosol radiative forcing, *Geophys. Res. Lett.*, *36*, L15707, doi:10.1029/2009GL039050.
Haigh, J. D. (1996), The impact of solar variability on climate, *Science*, *272*, 981–984, doi:10.1126/science.272.5264.981.
Häkkinen, S. (1999), A simulation of thermohaline effects of a great salinity anomaly, *J. Clim.*, *6*, 1781–1795.
Hall, A., and M. Visbeck (2002), Synchronous variability in the Southern Hemisphere atmosphere, sea ice and ocean resulting from the Annular Mode, *J. Clim.*, *15*, 3043–3057.
Hansen, J., et al. (2005), Efficacy of climate forcings, *J. Geophys. Res.*, *110*, D18104, doi:10.1029/2005JD005776.
Hardiman, S. C., P. J. Kushner, and J. Cohen (2008), Investigating the ability of general circulation models to capture the effects of Eurasian snow cover on winter climate, *J. Geophys. Res.*, *113*, D21123, doi:10.1029/2008JD010623.
Hardiman, S. C., N. Butchart, T. J. Hinton, S. M. Osprey, and L. J. Gray (2012), The effect of a well-resolved stratosphere on surface climate: Differences between CMIP5 simulations with high and wow top versions of the Met Office climate model, *J. Clim.*, *25*, 7083–7099, doi:10.1175/JCLI-D-11-00579.1.
Hartley, D. E., J. T. Villarin, R. X. Black, and C. A. Davis (1998), A new perspective on the dynamical link between the stratosphere and troposphere, *Nature*, *391*, 471–474.
Hawkins, E., and R. Sutton (2009), The potential to narrow uncertainty in regional climate predictions, *Bull. Am. Meteorol. Soc.*, *90*(8), 1095–1107.
Haywood, J. M., N. Bellouin, A. Jones, O. Boucher, M. Wild, and K. P. Shine (2011), The roles of aerosol, water vapor and cloud in future global dimming/brightening, *J. Geophys. Res.*, *116*, D20203, doi:10.1029/2011JD016000.
Haywood, J. M., A. Jones, N. Bellouin, and D. Stephenson (2013), Asymmetric forcing from stratospheric aerosols impacts Sahelian rainfall, *Nat. Clim. Change*, *3*, 660–665, doi:10.1038/nclimate1857.
Hazeleger, W., V. Guemas, B. Wouters, S. Corti, I. Andreu-Burillo, F. J. Doblas-Reyes, K. Wyser, and M. Caian (2013), Multiyear climate predictions using two initialization strategies, *Geophys. Res. Lett.*, *40*, 1794–1798, doi:10.1002/grl.50355.
Ho, C.-H., H.-S. Kim, J.-H. Jeong, and S.-W. Son (2009), Influence of stratospheric quasi-biennial oscillation on tropical cyclone tracks in the western North Pacific, *Geophys. Res. Lett.*, *36*, L06702, doi:10.1029/2009GL037163.
Hoerling, M., J. Hurrell, J. Eischeid, and A. Phillips (2006), Detection and attribution of twentieth-century northern and southern African rainfall change, *J. Clim.*, *19*, 3989–4008.
Hoerling, M., X. W. Quan, and J. Eischeid (2009), Distinct causes for two principal US droughts of the 20th century, *Geophys. Res. Lett.*, *36*, L19708, doi:10.1029/2009GL039860.
Holland, M. M., and J. Stroeve (2011), Changing seasonal sea ice predictor relationships in a changing Arctic climate, *Geophys. Res. Lett.*, *38*, L18501, doi:10.1029/2011GL049303.
Holland, M. M., D. A. Bailey, and S. Vavrus (2011), Inherent sea ice predictability in the rapidly changing Arctic environment of the Community Climate System Model 3, *Clim. Dyn.*, *36*, 1239–1253, doi:10.1007/s00382-010-0792-4.
Holland, M. M., E. Blanchard-Wrigglesworth, J. Kay, and S. Vavrus (2013), Initial-value predictability of Antarctic sea ice in the Community Climate System Model 3, *Geophys. Res. Lett*, *40*, 2121–2124, doi:10.1002/grl.50410.
Holland, P. R., and R. Kwok (2012), Wind-driven trends in Antarctic sea-ice drift, *Nat. Geosci.*, *5*, 872–875, doi:10.1038/ngeo1627.
Ineson, S., and A. A. Scaife (2009), The role of the stratosphere in the European climate response to El Niño, *Nat. Geosci.*, *2*, 32–36.
Ineson, S., A. A. Scaife, J. R. Knight J. C. Manners, N. J. Dunstone, L. J. Gray, and J. D. Haigh (2011), Solar forcing of winter climate variability in the Northern Hemisphere, *Nat. Geosci.*, *4*, 753–757, doi:10.1038/ngeo1282.
Jaiser, R., K. Dethloff, and D. R. Handorf (2013), Stratospheric response to Arctic sea ice retreat and associated planetary wave propagation changes, *Tellus Ser. A*, *65*, 19,375, doi:10.3402/tellusa.v65i0.19375.
Johannessen, O. M., et al. (2004), Arctic climate change: Observed and modeled temperature and sea-ice variability, *Tellus*, *56*(4), 328–341.
Joshi, M. M., A. J. Charlton, and A. A. Scaife (2006), On the influence of stratospheric water vapor changes on the tropospheric circulation, *Geophys. Res. Lett.*, *33*, L09806, doi:10.1029/2006GL025983.

Jungclaus, J. H., H. Haak, M. Latif, and U. Mikolajewicz (2005), Arctic-North Atlantic interactions and multidecadal variability of the meridional overturning circulation, *J. Clim.*, *18*, 4013–4031.
Kahn, R. A., et al. (2012), Reducing the uncertainties in direct aerosol radiative forcing, *Surv. Geophys.*, *33*, 701–721, doi:10.1007/s10712-011-9153-z.
Kalnay, E., et al. (1996), The NCEP/NCAR 40-year reanalysis project, *Bull. Am. Meteorol. Soc.*, *77*, 437–471, doi:10.1175/1520-0477(1996)077<0437:TNYRP>2.0.CO;2.
Kang, S., L. Polvani, J. C. Fyfe, and M. Sigmond (2012), Impact of Polar ozone depletion on subtropical precipitation, *Science*, *332*, 951–954, doi:10.1126/science.1202131.
Karpechko, A. Y., and E. Manzini (2012), Stratospheric influence on tropospheric climate change in the Northern Hemisphere, *J. Geophys. Res.*, *117*, D05133, doi:10.1029/2011JD017036.
Keenlyside, N., M. Latif, J. Jungclaus, L. Kornblueh, and E. Roeckner (2008), Advancing decadal-scale climate prediction in the North Atlantic sector, *Nature*, *453*(7191), 84–88.
Kim, M.-K., W. K. M. Lau, K.-M. Kim, and W.-S. Lee (2007), A GCM study of effects of radiative forcing of sulfate aerosol on large scale circulation and rainfall in East Asia during boreal spring, *Geophys. Res. Lett.*, *34*, L24701, doi:10.1029/2007GL031683.
Kirtman, B., et al. (2013), Near-term climate change: Projections and predictability, in *Climate Change 2013: The Physical Science Basis. Contribution of Working Group I to the Fifth Assessment Report of the Intergovernmental Panel on Climate Change*, edited by T. F. Stocker et al., Cambridge Univ. Press, Cambridge, U. K., and New York.
Klimont, Z., S. J. Smith, and J. Cofala (2013), The last decade of global anthropogenic sulfur dioxide: 2000–2011 emissions, *Environ. Res. Lett.*, doi:10.1088/1748-9326/8/1/014003.
Kloster, S., F. Dentener, J. Feichter, F. Raes, U. Lohmann, E. Roeckner, and I. Fischer-Bruns (2010), A GCM study of future climate response to aerosol pollution reductions, *Clim. Dyn.*, *34*(7–8), 1177–1194.
Knight, J. R., C. K. Folland, and A. A. Scaife (2006), Climate impacts of the Atlantic Multidecadal Oscillation, *Geophys. Res. Lett.*, *33*, L17706, doi:10.1029/2006GL026242.
Kodera, K. (1994), Influence of volcanic eruptions on the troposphere through stratospheric dynamical processes in the Northern Hemisphere winter, *J. Geophys. Res.*, *99*(D1), 1273–1282, doi:10.1029/93JD02731.
Kodera, K. (2004), Solar influence on the Indian Ocean monsoon through dynamical processes, *Geophys. Res. Lett.*, *31*, L24209, doi:10.1029/2004GL020928.
Kodera, K., and Y. Kuroda (2000a), Tropospheric and stratospheric aspects of the Arctic Oscillation, *Geophys. Res. Lett.*, *27*(20), 3349–3352, doi:10.1029/2000GL012017.
Kodera, K., and Y. Kuroda (2000b), A mechanistic model study of slowly propagating coupled stratosphere-troposphere variability, *J. Geophys. Res.*, *105*(D10), 12,361–12,370, doi:10.1029/2000JD900094.
Kodera, K., and Y. Kuroda (2002), Dynamical response to the solar cycle: Winter stratopause and lower stratosphere, *J. Geophys. Res.*, *107*(D24), 4749, doi:10.1029/2002JD002224.
Kodera, K., and K. Shibata (2006), Solar influence on the tropical stratosphere and troposphere in the northern summer, *Geophys. Res. Lett.*, *33*, L19704, doi:10.1029/2006GL026659.
Koenigk, T., and L. Brodeau (2014), Ocean heat transport into the Arctic in the 20th and 21st century in EC-Earth, *Clim. Dyn.*, *42*, 3101–3120, doi:10.1007/s00382-013-1821-x.
Koenigk, T., and U. Mikolajewicz (2009), Seasonal to interannual climate predictability in mid and high northern latitudes in a global coupled model, *Clim. Dyn.*, *32*, 783–798, doi:10.1007/s00382-008-0419-1.
Koenigk, T., U. Mikolajewicz, H. Haak, and J. Jungclaus (2006), Variability of Fram Strait sea ice export: Causes, impacts and feedbacks in a coupled climate model, *Clim. Dyn.*, *26*, 17–34, doi:10.1007/s00382-005-0060-1.
Koenigk, T., U. Mikolajewicz, J. Jungclaus, and A. Kroll (2009), Sea ice in the Barents Sea: Seasonal to interannual variability and climate feedbacks in a global coupled model, *Clim. Dyn.*, *32*, 1119–1138, doi:10.1007/s00382-008-0450-2.
Koenigk, T., C. König Beatty, M. Caian, R. Döscher, and K. Wyser (2012), Potential decadal predictability and its sensitivity to sea ice albedo parameterization in a global coupled model, *Clim. Dyn.*, *38*(11–12), 2389–2408, doi:10.1007/s00382-011-1132-z.
Koeppen, W. (1884), Die W ärmezonen der Erde, nach der Dauer der heissen, gem ässigten und kalten Zeit und nach der Wirkung der W ärme auf die organische Welt betrachtet (The thermal zones of the Earth according to the duration of hot, moderate and cold periods and to the impact of heat on the organic world), *Meteorol. Z.*, *1*(3), 215–226, (translated and edited by E. Volken and S. Bronnimann, *Meteorol. Z.*, 20 (2011), 351–360).
Koster, R. D., and M. J. Suarez (2001), Soil moisture memory in climate models, *J. Hydrometeorol.*, *2*, 558–570.
Koster, R. D., et al. (2004), Regions of strong coupling between soil moisture and precipitation, *Science*, *305*, 1138–1140, doi:10.1126/science.1100217.
Koster, R. D., et al. (2006), GLACE: The Global Land–Atmosphere Coupling Experiment. Part I: Overview, *J. Hydrometeorol.*, *7*, 590–610, doi:10.1175/JHM510.1.
Koster, R. D., et al. (2011), The second phase of the global land-atmosphere coupling experiment: Soil moisture contributions to subseasonal forecast skill, *J. Hydrometeorol.*, *12*(5), 805–822.
Kunz, T., K. Fraedrich, and F. Lunkeit (2009), Synoptic scale wave breaking and its potential to drive NAO-like circulation dipoles: A simplified GCM approach, *Q. J. R. Meteorol. Soc.*, *135*, 1–19.
Kuroda, Y. (2008), Effect of stratospheric sudden warming and vortex intensification on the tropospheric climate, *J. Geophys. Res.*, *113*, D15110, doi:10.1029/2007JD009550.
Kvamstö, N. G., P. Skeie, and D. B. Stephenson (2004), Large-scale impact of localized Labrador sea-ice changes on the North Atlantic Oscillation, *Int. J. Climatol.*, *24*, 603–612.
Labitzke, K. (1987), Sunspots, the QBO and the stratospheric temperature in the north polar region, *Geophys. Res. Lett.*, *14*, 535–537, doi:10.1029/GL014i005p00535.
Langford, S., S. Stevenson, and D. Noone (2014), Analysis of low-frequency precipitation variability in CMIP5 historical simulations for southwestern North America, *J. Clim.*, *27*, 2735–2756, doi:10.1175/JCLI-D-13-00317.1.
Latif, M. (2006), On North Pacific multidecadal climate variability, *J. Clim.*, *19*, 2906–2915.
Latif, M., and T. P. Barnett (1994), Causes of decadal climate variability over the North Pacific and North America, *Science*, *266*, 634–637.
Latif, M., C. Böning, J. Willebrand, A. Biastoch, J. Dengg, N. Keenlyside, U. Schweckendiek, and G. Madec (2006), Is the thermohaline circulation changing?, *J. Clim.*, *19*, 4631–4637.
Lau, K.-M., and K.-M. Kim (2006), Observational relationships between aerosol and Asian monsoon rainfall, and circulation, *Geophys. Res. Lett.*, *33*, L21810, doi:10.1029/2006GL027546.

Lau, K. M., and K. M. Kim (2007), Cooling of the Atlantic by Saharan dust, *Geophys. Res. Lett.*, *34*, L23811, doi:10.1029/2007GL031538.
Lau, K. M., M. K. Kim, and K. M. Kim (2006), Asian summer monsoon anomalies induced by aerosol direct forcing: The role of the Tibetan Plateau, *Clim. Dyn.*, *26*(7–8), 855–864, doi:10.1007/s00382-006-0114-z.
Lenton, A., F. Codron, L. Bopp, N. Metzl, P. Cadule, A. Tagliabue, and J. Le Sommer (2009), Stratospheric ozone depletion reduces ocean carbon uptake and enhances ocean acidification, *Geophys. Res. Lett.*, *36*, L12606, doi:10.1029/2009GL038227.
Li, Y., S. P. Harrison, P. Zhao, and J. Ju (2009), Simulations of the impacts of dynamic vegetation on interannual and interdecadal variability of Asian summer monsoon with modern and mid-Holocene orbital forcings, *Global Planet. Change*, *66*, 235–252, doi:10.1016/j.gloplacha.2008.12.013.
Lienert, F., and F. J. Doblas-Reyes (2013), Decadal prediction of interannual tropical and North Pacific sea surface temperature, *J. Geophys. Res. Atmos.*, *118*, 5913–5922, doi:10.1002/jgrd.50469.
Lisaeter, K. A., G. Evensen, and S. Laxon (2007), Assimilating synthetic CryoSat sea ice thickness in a coupled ice-ocean, *J. Geophys. Res.*, *112*, C07023,, doi:10.1029/2006JC003786.
Liu, Y., J. Sun, and B. Yang (2009), The effects of black carbon and sulphate aerosols in China regions on East Asia monsoons, *Tellus B*, *61*, 642–656, doi:10.1111/j.1600-0889.2009.00427.x.
Liu, Y. Y., R. M. Parinussa, W. A. Dorigo, R. A. M. De Jeu, W. Wagner, A. I. J. M. van Dijk, M. F. McCabe, and J. P. Evans (2011), Developing an improved soil moisture dataset by blending passive and active microwave satellite-based retrievals, *Hydrol. Earth Syst. Sci.*, *15*, 425–436, doi:10.5194/hess-15-425-2011.
Lockwood, M., R. G. Harrison, T. J. Woollings, and S. Solanki (2010), Are cold winters in Europe associated with low solar activity?, *Environ. Res. Lett.*, *5*, 024001, doi:10.1088/1748-9326/5/2/024001.
Loeb, N. G., and G. L. Schuster (2008), An observational study of the relationship between cloud, aerosol and meteorology in broken low-level cloud conditions, *J. Geophys. Res.*, *113*, D14214, doi:10.1029/2007JD009763.
Lu, R., B. Dong, and H. Ding (2006), Impact of the Atlantic Multidecadal Oscillation on the Asian summer monsoon, *Geophys. Res. Lett.*, *33*, L24701, doi:10.1029/2006GL027655.
Lu, Z., D. G. Streets, Q. Zhang, S. Wang, G. R. Carmichael, Y. F. Cheng, C. Wei, M. Chin, T. Diehl, and Q. Tan (2010), Sulfur dioxide emissions in China and sulfur trends in East Asia since 2000, *Atmos. Chem. Phys.*, *10*(13), 6311–6331.
Luyssaert, S., et al. (2014), Land management and land-cover change have impacts of similar magnitude on surface temperature, *Nat. Clim. Change*, *4*, 389–393, doi:10.1038/nclimate2196.
Magnusdottir, G., C. Deser, and R. Saravanan (2004), The effects of North Atlantic SST and sea ice anomalies on the winter circulation in CCM3. Part 1: Main features and storm track characteristics of the response, *J. Clim.*, *17*, 857–876.
Maidens, A., A. Arribas, A. A. Scaife, C. MacLachlan, D. Peterson, and J. Knight (2013), The influence of surface forcings on prediction of the North Atlantic Oscillation regime of winter 2010/11, *Mon. Weather Rev.*, *141*, 3801–3813.
Manzini, E., C. Cagnazzo, P. G. Fogli, A. Bellucci, and W. A. Muller (2012), Stratosphere-troposphere coupling at inter-decadal time scales: Implications for the North Atlantic Ocean, *Geophys. Res. Lett.*, *39*, L05801, doi:10.1029/2011GL050771.
Marshall, A. G., and A. A. Scaife (2009), Impact of the QBO on surface winter climate, *J. Geophys. Res.*, *114*, D18110, doi:10.1029/2009JD011737.
Marshall, A. G., and A. A. Scaife (2010), Improved predictability of stratospheric sudden warming events in an atmospheric general circulation model with enhanced stratospheric resolution, *J. Geophys. Res.*, *115*, D16114, doi:10.1029/2009JD012643.
Martin, E. R., C. Thorncroft, and B. B. B. Booth (2014), SST-Sahel rainfall teleconnection in CMIP5 simulations, *J. Clim.*, *27*, 784–806.
Massonnet, F., T. Fichefet, H. Goosse, M. Vancoppenolle, P. Mathiot, and C. König Beatty (2011), On the influence of model physics on simulations of Arctic and Antarctic sea ice, *Cryosphere*, *5*, 687–699, doi:10.5194/tc-5-687-2011.
Massonnet, F., P. Mathiot, T. Fichefet, H. Goosse, C. Koenig Beatty, M. Vancoppenolle, and T. Lavergne (2013), A model reconstruction of the Antarctic sea ice thickness and volume changes over 1980–2008 using data assimilation, *Ocean Model.*, *64*(0), 67–75.
Materia, S., P. A. Dirmeyer, Z. Guo, A. Alessandri, and A. Navarra (2010), The sensitivity of simulated river discharge to land surface representation and meteorological forcings, *J. Hydrometeorol.*, *11*, 334–351, doi:10.1175/2009JHM1162.1.
Materia, S., A. Borrelli, A. Bellucci, A. Alessandri, P. Di Pietro, P. Athanasiadis, A. Navarra, and S. Gualdi (2014), Impact of atmosphere and land surface initial conditions on seasonal forecast of global surface temperature, *J. Clim.*, *27*, 9253–9271, doi:10.1175/JCLI-D-14-00163.1.
Mathiot, P., C. König Beatty, T. Fichefet, H. Goosse, F. Massonnet, and M. Vancoppenolle (2012), Better constraints on the sea-ice state using global sea ice data assimilation, *Geosci. Model Dev.*, *5*, 1501–1515.
Matthes, K., Y. Kuroda, K. Kodera, and U. Langematz (2006), Transfer of the solar signal from the stratosphere to the troposphere: Northern winter, *J. Geophys. Res.*, *111*, D06108, doi:10.1029/2005JD006283.
Mayewski, P. A., et al. (2009), State of the Antarctic and Southern Ocean climate system, *Rev. Geophys.*, *47*, RG1003, doi:10.1029/2007RG000231.
McCabe, G. J., M. A. Palecki, and J. L. Betancourt (2004), Pacific and Atlantic Ocean influences on multidecadal drought frequency in the United States, *Proc. Natl. Acad. Sci. U.S.A.*, *101*(12), 4136–4141.
McLandress, C., and T. G. Shepherd (2009), Simulated anthropogenic changes in the Brewer-Dobson circulation, including its extension to higher latitudes, *J. Clim.*, *22*, 1516–1540.
Meehl, G. A., and J. M. Arblaster (2009), A lagged warm event-like response to peaks in solar forcing in the Pacific region, *J. Clim.*, *22*(13), 3647–3660.
Meehl, G. A., and H. Teng (2014), CMIP5 multi-model initialized decadal hindcasts for the mid-1970s shift and early-2000s hiatus and predictions for 2016–2035, *Geophys. Res. Lett.*, *41*, 1711–1716, doi:10.1002/2014GL059256.
Meehl, G. A. W. M., T. M. L. Washington, J. M. A. Wigley, and A. Dai (2003), Solar and greenhouse gas forcing and climate response in the twentieth century, *J. Clim.*, *16*, 426–444.
Meehl, G. A., J. M. Arblaster, and W. D. Collins (2008), Effects of black carbon aerosols on the Indian monsoon, *J. Clim.*, *21*(12), 2869–2882, doi:10.1175/2007jcli1777.1.
Meehl, G. A., J. M. Arblaster, K. Matthes, F. Sassi, and H. van Loon (2009a), Amplifying the Pacific climate system response to a small 11-year solar cycle forcing, *Science*, *325*, 1114–1118.
Meehl, G. A., et al. (2009b), Decadal prediction: Can it be skillful?, *Bull. Am. Meteorol. Soc.*, *90*(10), 1467–1485.
Meehl, G. A., et al. (2013), Decadal climate prediction: An update from the trenches, *Bull. Am. Meteorol. Soc.*, *95*, 243–267, doi:10.1175/BAMS-D-12-00241.1.
Meehl, G. A., R. Moss, K. E. Taylor, V. Eyring, R. J. Stouffer, S. Bony, and B. Stevens (2014a), Climate model intercomparisons: Preparing for the next phase, *Eos Trans. AGU*, *95*(9), 77–78, doi:10.1002/2014EO090001.
Meehl, G. A., H. Teng, and J. M. Arblaster (2014b), Climate model simulations of the observed early-2000s hiatus of global warming, *Nat. Clim. Change*, doi:10.1038/NCLIMATE2357.

Meier, W. N., et al. (2014), Arctic sea ice in transformation: A review of recent observed changes and impacts on biology and human activity, *Rev. Geophys.*, *52*, 185–217, doi:10.1002/2013RG000431.
Menon, S., J. Hansen, L. Nazarenko, and Y. F. Luo (2002), Climate effects of black carbon aerosols in China and India, *Science*, *297*(5590), 2250–2253.
Miller, P. A., S. W. Laxon, D. L. Feltham, and D. J. Cresswell (2006), Optimization of a sea ice model using basinwide observations of Arctic sea ice thickness, extent and velocity, *J. Clim.*, *19*, 1090–1108.
Ming, Y., V. Ramaswamy, and G. Persad (2010), Two opposing effects of absorbing aerosols on global-mean precipitation, *Geophys. Res. Lett.*, *37*, L13701, doi:10.1029/2010GL042895.
Miralles, D. G., M. J. van den Berg, A. J. Teuling, and R. A. M. deJeu (2012), Soil moisture-temperature coupling: A multiscale observational analysis, *Geophys. Res. Lett.*, *39*, L21707, doi:10.1029/2012GL053703.
Mochizuki, T., et al. (2010), Pacific decadal oscillation hindcasts relevant to near-term climate prediction, *Proc. Natl. Acad. Sci. U.S.A.*, *107*, 1833–1837.
Myhre, G., et al. (2013), Radiative forcing of the direct aerosol effect from AeroCom Phase II Simulations, *Atmos. Chem. Phys.*, *13*, 1853–1877 doi:10.5194/acp-13-1853-2013.
Myneni, R. B., et al. (2002), Global products of vegetation leaf area and fraction absorbed PAR from year one of MODIS data, *Remote Sens. Environ.*, *83*, 214–231.
Mysak, L., and S. Venegas (1998), Decadal climate oscillations in the Arctic: A new feedback loop for atmosphere-ice-ocean interactions, *Geophys. Res. Lett.*, *25*(19), 3607–3610, doi:10.1029/98GL02782.
Nicholson S. (2013), The West African Sahel: A review of recent studies on the rainfall regime and its interannual variability, *ISRN Meteorol.*, Article ID 453521, 32, doi:10.1155/2013/453521.
Oki, T., and S. Kanae (2006), Global hydrological cycles and world water resources, *Science*, *313*, 1068–1072.
Omrani, N.-E., N. S. Keenlyside, J. Bader, and E. Manzini (2014), Stratosphere key for wintertime atmospheric response to warm Atlantic decadal conditions, *Clim. Dyn.*, *42*, 649–663, doi:10.1007/s00382-013-1860-3.
O'Neill, B. C., E. Kriegler, K. Riahi, K. L. Ebi, S. Hallegatte, T. R. Carter, R. Mathur, and D. P. van Vuuren (2014), A new scenario framework for climate change research: the concept of shared socioeconomic pathways, *Clim. Change*, *122*(3), 387–400.
Overland, J. E. (2014), Atmospheric science: Long-range linkage, *Nat. Clim. Change*, *4*, 11–12.
Overland, J. E., and M. Wang (2010), Large-scale atmospheric circulation changes are associated with the recent loss of Arctic sea ice, *Tellus Ser. A*, *62*, 1–9, doi:10.1111/j.1600-0870.2009.00421.x.
Paolino, D., J. L. Kinter, B. P. Kirtman, D. Min, and D. M. Straus (2012), The impact of land surface and atmospheric initialization on seasonal forecasts with CCSM, *J. Clim.*, *25*, 1007–1021, doi:10.1175/2011JCLI3934.1.
Pawson, S., and M. Fiorino (1998), A comparison of reanalyses in the tropical stratosphere. Part 1: Thermal structure and the annual cycle, *Clim. Dyn.*, *14*, 631–644.
Perlwitz, J., and H.-F. Graf (1995), The statistical connection between tropospheric and stratospheric circulation of the Northern Hemisphere in winter, *J. Clim.*, *8*, 2281–2295.
Perlwitz, J., and N. Harnik (2003), Observational evidence of a stratospheric influence on the troposphere by planetary wave reflection, *J. Clim.*, *16*, 3011–3026.
Petoukhov, V., and V. A. Semenov (2010), A link between reduced Barents-Kara sea ice and cold winter extremes over northern continents, *J. Geophys. Res.*, *115*, D21111, doi:10.1029/2009JD013568.
Pielke, R. A., Sr., et al. (2011), Land use/land cover changes and climate: Modeling analysis and observational evidence, Wiley Interdisciplinary Reviews, WIREs, *Clim. Change*, doi:10.1002/wcc.144.
Pohlmann, H., M. Botzet, M. Latif, A. Roesch, M. Wild, and P. Tschuck (2004), Estimating the decadal predictability of a coupled AOGCM, *J. Clim.*, *17*, 4463–4472, doi:10.1175/3209.1.
Pohlmann, H., J. H. Jungclaus, A. Kohl, D. Stammer, and J. Marotzke (2009), Initializing decadal climate predictions with the GECCO oceanic synthesis: Effects on the North Atlantic, *J. Clim.*, *22*(14), 3926–3938.
Polvani, L. M., and K. L. Smith (2013), Can natural variability explain observed Antarctic sea ice trends? New modeling evidence from CMIP5, *Geophys. Res. Lett.*, *40*, 3195–3199, doi:10.1002/grl.50578.
Polyakov, I. V., and M. Johnson (2000), Arctic decadal and interdecadal variability, *Geophys. Res. Lett.*, *27*(24), 4097–4100, doi:10.1029/2000GL011909.
Polyakov, I. V., G. V. Alekssev, L. A. Timokhov, U. S. Bhatt, R. L. Colony, H. L. Simmons, D. Walsh, J. E. Walsh, and V. F. Zakharov (2004), Variability of the intermediate Atlantic water of the Arctic Ocean over the last 100 years, *J. Clim.*, *17*, 4485–4497.
Proshutinsky, A. Y., and M. A. Johnson (1997), Two circulation regimes of the wind-driven Arctic Ocean, *J. Geophys. Res.*, *102*(C6), 12,493–12,514, doi:10.1029/97JC00738.
Ramanathan, V., C. Chung, D. Kim, T. Bettge, L. Buja, J. T. Kiehl, W. M. Washington, Q. Fu, D. R. Sikka, and M. Wild (2005), Atmospheric brown clouds: Impacts on South Asian climate and hydrological cycle, *Proc. Natl. Acad. Sci. U.S.A.*, *102*(15), 5326–5333.
Randel, W., and F. Wu (2007), A stratospheric ozone profile data set for 1979–2005: Variability, trends, and comparisons with column ozone data, *J. Geophys. Res.*, *112*, D06313, doi:10.1029/2006JD007339.
Randel, W. J., and E. J. Jensen (2013), Physical processes in the tropical tropopause layer and their roles in a changing climate, *Nat. Geosci.*, *6*, 169–176, doi:10.1038/ngeo1733.
Rayner, N. A., D. E. Parker, E. B. Horton, C. K. Folland, L. V. Alexander, D. P. Rowell, E. C. Kent, and A. Kaplan (2003), Global analyses of sea surface temperature, sea ice, and night marine air temperature since the late nineteenth century, *J. Geophys. Res.*, *108*(D14), 4407, doi:10.1029/2002JD002670.
Reale, O., K. M. Lau, and A. da Silva (2011), Impact of an interactive aerosol on the African easterly jet in the NASA GEOS-5 Global Forecasting System, *Weather Forecasting*, *26*, 504–519.
Reichler, T., J. Kim, E. Manzini, and J. Kroeger (2012), A stratospheric connection to Atlantic climate variability, *Nat. Geosci.*, *5*, 783–787, doi:10.1038/ngeo1586.
Rienecker, M. M., et al. (2011), MERRA: NASA's Modern-Era Retrospective Analysis for Research and Applications, *J. Clim.*, *24*, 3624–3648, doi:10.1175/JCLI-D-11-00015.1.
Rivière, G. (2011), A dynamical interpretation of the poleward shift of the jet streams in global warming scenarios, *J. Atmos. Sci.*, *68*, 1253–1272, doi:10.1175/2011JAS3641.1.
Robock, A. (2000), Volcanic eruptions and climate, *Rev. Geophys.*, *38*(2), 191–219, doi:10.1029/1998RG000054.
Robock, A., K. Y. Vinnikov, G. Srinivasan, J. K. Entin, S. E. Hollinger, N. A. Speranskaya, S. Liu, and A. Namkhai (2000), The Global Soil Moisture Data Bank, *Bull. Am. Meteorol. Soc.*, *81*, 1281–1299, doi:10.1175/1520-0477(2000)081<1281:TGSMDB>2.3.CO;2.
Roff, G., D. W. J. Thompson, and H. H. Hendon (2011), Does increasing model stratospheric resolution improve extended-range forecast skill?, *Geophys. Res. Lett.*, *38*, L05809, doi:10.1029/2010GL046515.

Rosenfeld, D., et al. (2014), Global observations of aerosol-cloud-precipitation-climate interactions, *Rev. Geophys.*, *52*, 750–808, doi:10.1002/2013RG000441.
Rotstayn, L. D., and U. Lohmann (2002), Tropical rainfall trends and the indirect aerosol effect, *J. Clim.*, *15*, 2103–2116.
Sampaio, G., C. Nobre, M. H. Costa, P. Satyamurty, B. S. Soares-Filho, and M. Cardoso (2007), Regional climate change over eastern Amazonia caused by pasture and soybean cropland expansion, *Geophys. Res. Lett.*, *34*, L17709, doi:10.1029/2007GL030612.
Santanello, J. A., C. D. Peters-Lidard, A. Kennedy, and S. V. Kumar (2013), Diagnosing the nature of land–atmosphere coupling: A case study of dry/wet extremes in the U.S. Southern Great Plains, *J. Hydrometeorol.*, *14*, 3–24, doi:10.1175/JHM-D-12-023.1.
Scaife, A. A., J. R. Knight, G. K. Vallis, and C. K. Folland (2005), A stratospheric influence on the winter NAO and North Atlantic surface climate, *Geophys. Res. Lett.*, *32*, L18715, doi:10.1029/2005GL023226.
Scaife, A. A., et al. (2012), Climate change projections and stratosphere–troposphere interaction, *Clim. Dyn.*, *38*, 2089–2097, doi:10.1007/s00382-011-1080-7.
Scaife, A. A., S. Ineson, J. R. Knight, L. J. Gray, K. Kodera, and D. M. Smith (2013), A mechanism for lagged North Atlantic climate response to solar variability, *Geophys. Res. Lett.*, *40*, 434–439, doi:10.1002/grl.50099.
Scaife, A. A., et al. (2014a), Skillful long-range prediction of European and North American winters, *Geophys. Res. Lett.*, *41*, 2514–2519, doi:10.1002/2014GL059637.
Scaife, A. A., et al. (2014b), Predictability of the quasi-biennial oscillation and its northern winter teleconnection on seasonal to decadal timescales, *Geophys. Res. Lett.*, *41*, 1752–1758, doi:10.1002/2013GL059160.
Schär, C., D. Lüthi, U. Beyerle, and E. Heise (1999), The soil-precipitation feedback: A process study with a regional climate model, *J. Clim.*, *12*(3), 722–741.
Schimanke, S., J. Korper, T. Spangehl, and U. Cubasch (2011), Multi-decadal variability of sudden stratospheric warmings in an AOGCM, *Geophys. Res. Lett.*, *38*, L01801, doi:10.1029/2010GL045756.
Schmidt, H., G. P. Brasseur, and M. A. Giorgetta (2010), The solar cycle signal in a general circulation and chemistry model with internally generated QBO, *J. Geophys. Res.*, *115*, D00I14, doi:10.1029/2009JD012542.
Schubert, S. D., M. J. Suarez, P. J. Pegion, R. D. Koster, and J. D. Bacmeister (2004), Causes of long-term drought in the U.S. Great Plains, *J. Clim.*, *17*, 485–503, doi:10.1175/1520-0442(2004)017<0485:COLDIT>2.0.CO;2.
Schubert, S. D., M. J. Suarez, P. J. Pegion, R. D. Koster, and J. T. Bacmeister (2008), Potential predictability of long-term drought and pluvial conditions in the U.S. Great Plains, *J. Clim.*, *21*, 802–816, doi:10.1175/2007JCLI1741.1.
Screen, J. A. (2014), Arctic amplification decreases temperature variance in northern mid-to-high-latitudes, *Nat. Clim. Change*, *4*, 577–582.
Seneviratne, S. I., et al. (2006), Soil moisture memory in AGCM simulations: Analysis of Global Land–Atmosphere Coupling Experiment (GLACE) data, *J. Hydrometeorol.*, *7*, 1090–1112.
Seneviratne, S. I., T. Corti, E. L. Davin, M. Hirschi, E. B. Jaeger, I. Lehner, B. Orlowsky, and A. J. Teuling (2010), Investigating soil moisture–climate interactions in a changing climate: A review, *Earth Sci. Rev.*, *99*(3–4), 125–161.
Serreze, M. C., A. P. Barrett, J. C. Stroeve, D. N. Kindig, and M. M. Holland (2009), The emergence of surface-based Arctic amplification, *Cryosphere*, *3*, 11–19.
Shaw, T. A., and T. G. Shepherd (2007), Angular momentum conservation and gravity wave drag parameterization: Implications for climate models, *J. Atmos. Sci.*, *64*, 190–203.
Shaw, T. A., M. Sigmond, T. G. Shepherd, and J. F. Scinocca, (2009), Sensitivity of simulated climate to conservation of momentum in gravity wave drag parameterization, *J. Clim.*, *22*, 2726–2742.
Shindell, D., D. Rind, N. Balachandran, J. Lean, and J. Lonergan (1999), Solar cycle variability, ozone, and climate, *Science*, *284*, 305–308.
Shindell, D., et al. (2012), Simultaneously mitigating near-term climate change and improving human health and food security, *Science*, *335*(6065), 183–189, doi:10.1126/science.1210026.
Shindell, D. T. (2014), Inhomogeneous forcing and transient climate sensitivity, *Nat. Clim. Change*, *4*, 274–277, doi:10.1038/nclimate2136.
Shindell, D. T., G. A. Schmidt, R. L. Miller, and D. Rind (2001), Northern Hemisphere winter climate response to greenhouse gas, ozone, solar, and volcanic forcing, *J. Geophys. Res.*, *106*(D7), 7193–7210, doi:10.1029/2000JD900547.
Shindell, D. T., et al. (2013), Radiative forcing in the ACCMIP historical and future climate simulations, *Atmos. Chem. Phys.*, *13*, 2939–2974, doi:10.5194/acp-13-2939-2013.
Shukla, J., and Y. Mintz (1982), Influence of land-surface evapotranspiration on the Earth's climate, *Science*, *215*, 1498–1501, doi:10.1126/science.215.4539.1498.
Sigmond, M., and J. C. Fyfe (2010), Has the ozone hole contributed to increased Antarctic sea ice extent?, *Geophys. Res. Lett.*, *37*, L18502, doi:10.1029/2010GL044301.
Sigmond, M., and J. C. Fyfe (2014), The Antarctic sea ice response to the ozone hole in climate models, *J. Clim.*, *27*, 1336–1342, doi:10.1175/JCLI-D-13-00590.1.
Sigmond, M., J. F. Scinocca, V. V. Kharin, and T. G. Shepherd (2013), Enhanced seasonal forecast skill following stratospheric sudden warmings, *Nat. Geosci.*, *6*(2), 98–102, doi:10.1038/ngeo1698.
Simmons, A., C. Uppala, D. Dee, and S. Kobayashi (2007), ERA-Interim: New ECMWF reanalysis products from 1989 onwards, *ECMWF Newslett.*, *110*, 25–35.
Simmonds, I., and T. H. Jacka (1995), Relationships between the Interannual Variability of Antarctic Sea Ice and the Southern Oscillation, *J. Clim.*, *8*, 637–647, doi:10.1175/1520-0442(1995)008<0637:RBTIVO>2.0.CO;2.
Simpson, I. R., M. Blackburn, and J. D. Haigh (2009), The role of eddies in driving the tropospheric response to stratospheric heating perturbations, *J. Atmos. Sci.*, *66*, 1347–1365, doi:10.1175/2008JAS2758.1.
Smedsrud, L. H., et al. (2013), The role of the Barents Sea in the Arctic climate system, *Rev. Geophys.*, *51*, 415–449, doi:10.1002/rog.20017.
Smith, D. M., S. Cusack, A. W. Colman, C. K. Folland, G. R. Harris, and J. M. Murphy (2007), Improved surface temperature prediction for the coming decade from a global climate model, *Science*, *317*(5839), 796–799.
Smith, D. M., R. Eade, N. J. Dunstone, D. Fereday, J. M. Murphy, H. Pohlmann, and A. A. Scaife (2010), Skilful multi-year predictions of Atlantic hurricane frequency, *Nat. Geosci.*, *3*(12), 846–849.
Solomon, S., K. H. Rosenlof, R. W. Portmann, J. S. Daniel, S. M. Davis, T. J. Sanford, and G.-K. Plattner (2010), Contributions of stratospheric water vapor to decadal changes in the rate of global warming, *Science*, *327*, 1219–1223.
Solomon, S., J. S. Daniel, R. R. Neely III, J.-P. Vernier, E. G. Dutton, and L. W. Thomason (2011), The persistently variable "background" stratospheric aerosol layer and global, *Clim. Change*, *333*(6044), 866–870, doi:10.1126/science.1206027.
Son, S. W., et al. (2010), Impact of stratospheric ozone on the Southern Hemisphere circulation changes: A multimodel assessment, *J. Geophys. Res.*, *115*, D00M07, doi:10.1029/2010JD014271.
Song, Y., and W. A. Robinson (2004), Dynamical mechanisms of stratospheric influences on the troposphere, *J. Atmos. Sci.*, *61*, 1711–25.

Soukharev, B., and L. Hood (2006), Solar cycle variation of stratospheric ozone: Multiple regression analysis of long-term satellite data sets and comparisons with models, *J. Geophys. Res.*, *111*, D20314, doi:10.1029/2006JD007107.
SPARC-CCMVal (2010), SPARC report on the evaluation of chemistry-climate models, in *SPARC Report*, *WCRP-132*, *WMO/TD-1526*, edited by V. Eyring, T. G. Shepherd, and D. W. Waugh. [Available at http://www.atmosp.physics.utoronto.ca/SPARC/ccmval_final/.]
Spracklen, D. V., K. S. Carslaw, U. Pöschl, A. Rap, and P. M. Forster (2011), Global cloud condensation nuclei influenced by carbonaceous combustion aerosol, *Atmos. Chem. Phys.*, *11*, 9067–9087, doi:10.5194/acp-11-9067-2011.
Stenchikov, G., K. Hamilton, R. J. Stouffer, A. Robock, V. Ramaswamy, B. Santer, and H.-F. Graf (2006), Arctic Oscillation response to volcanic eruptions in the IPCC AR4 climate models, *J. Geophys. Res.*, *111*, D07107, doi:10.1029/2005JD006286.
Stenchikov, G., T. L. Delworth, V. Ramaswamy, R. J. Stouffer, A. Wittenberg, and F. Zeng (2009), Volcanic signals in oceans, *J. Geophys. Res.*, *114*, D16104, doi:10.1029/2008JD011673.
Stevens, B., and G. Feingold (2009), Untangling aerosol effects on clouds and precipitation in a buffered system, *Nature*, *461*, 607–613, doi:10.1038/nature08281.
Storelvmo, T., U. Lohmann, and R. Bennartz (2009), What governs the spread in shortwave forcings in the transient IPCC AR4 models?, *Geophys. Res. Lett.*, *36*, L01806, doi:10.1029/2008GL036069.
Sutton, R. T., and B. Dong (2012), Atlantic Ocean influence on a shift in European climate in the 1990s, *Nat. Geosci.*, *5*, 788–792, doi:10.1038/ngeo1595.
Sutton, R. T., and D. L. Hodson (2005), Atlantic Ocean forcing of North American and European summer climate, *Science*, *309*(5731), 115–118.
Swinbank, R. S., and A. O'Neill (1994), A stratosphere-troposphere data assimilation system, *Mon. Weather Rev.*, *122*, 686–702.
Szopa, S., et al. (2013), Aerosol and ozone changes as forcing for climate evolution between 1850 and 2100, *Clim. Dyn.*, *40*, 2223–2250, doi:10.1007/s00382-012-1408-y.
Teng, H., W. M. Washington, G. Branstator, G. A. Meehl, and J.-F. Lamarque (2012), Potential impacts of Asian carbon aerosols on future US warming, *Geophys. Res. Lett.*, *39*, L11703, doi:10.1029/2012GL051723.
Thomas, K. (2014), *Linkages Between Arctic Warmingand Mid-Latitude Weather Patterns: Summary of a Workshop*, The National Academies Press, Washington, D. C.
Thompson, D. W. J., and S. Solomon (2002), Interpretation of recent Southern Hemisphere climate change, *Science*, *296*, 895–899.
Thompson, D. W. J., M. P. Baldwin, and J. M. Wallace (2002), Stratospheric connection to Northern Hemisphere wintertime weather: Implications for prediction, *J. Clim.*, *15*, 1421–1428.
Thompson, D. W. J., S. Solomon, P. J. Kushner, M. H. England, K. M. Grise, and D. J. Karoly (2011), Signatures of the Antarctic ozone hole in Southern Hemisphere surface climate change, *Nat. Geosci.*, *4*, 741–749.
Tietsche, S., D. Notz, J. H. Jungclaus, and J. Marotzke (2013), Assimilation of sea ice concentration in a global climate model—Physical and statistical aspects, *Ocean Sci. Discuss.*, *9*, 2403–2455.
Trenberth, K. E., and D. J. Shea (2006), Atlantic hurricanes and natural variability in 2005, *Geophys. Res. Lett.*, *33*, L12704, doi:10.1029/2006GL026894.
Tsutsui, J., K. Nishizawa, and F. Sassi (2009), Response of the middle atmosphere to the 11-year solar cycle simulated with the Whole Atmosphere Community Climate Model, *J. Geophys. Res.*, *114*, D02111, doi:10.1029/2008JD010316.
Tucker, C. J. (1979), Red and photographic infrared linear combinations for monitoring vegetation, *Remote Sens. Environ.*, *8*, 127–150.
Turner, J., J. C. Comiso, G. J. Marshall, T. A. Lachlan-Cope, T. Bracegirdle, T. Maksym, M. P. Meredith, Z. Wang, and A. Orr (2009), Non-annular atmospheric circulation change induced by stratospheric ozone depletion and its role in the recent increase of Antarctic sea ice extent, *Geophys. Res. Lett.*, *36*, L08502, doi:10.1029/2009GL037524.
United Nations Environment Programme and World Meteorological Organization (2011), Integrated assessment of black carbon and tropospheric ozone. [Available at http://www.unep.org/dewa/portals/67/pdf/BlackCarbon_report.pdf.]
Uppala, S. M., et al. (2005), The ERA-40 re-analysis, *Q. J. R. Meteorol. Soc.*, *131*, 2961–3012, doi:10.1256/qj.04.176.
van den Hurk, B. J. J. M., F. Doblas-Reyes, G. Balsamo, R. D. Koster, S. I. Seneviratne, and H. Camargo Jr. (2012), Soil moisture effects on seasonal temperature and precipitation forecast scores in Europe, *Clim. Dyn.*, *38*, 349–362, doi:10.1007/s00382-010-0956-2.
van Loon, H., and K. Labitzke (2000), The influence of the 11-year solar cycle on the stratosphere below 30 km: A review, *Space Sci. Rev.*, *94*, 259–278.
van Loon, H., and G. A. Meehl (2008), The response in the Pacific to the Sun's decadal peaks and contrasts to cold events in the Southern Oscillation, *J. Atmos. Sol. Terr. Phys.*, *70*(7), 1046–1055.
van Oldenborgh, G. J., F. J. Doblas-Reyes, B. Wouters, and W. Hazeleger (2012), Decadal prediction skill in a multi-model ensemble, *Clim. Dyn.*, *38*(7-8), 1263–1280.
van Vuuren, D. P., et al. (2011), The representative concentration pathways: An overview, *Clim. Change*, *109*(1-2), 5–31.
van Vuuren, D. P., et al. (2014), A new scenario framework for Climate Change Research: Scenario matrix architecture, *Clim. Change*, *122*(3), 373–386.
Venegas, S., and L. Mysak (2000), Is there a dominant timescale of natural climate variability in the Arctic?, *J. Clim.*, *13*, 3413–3434.
Villarini, G., G. A. Vecchi, T. R. Knutson, M. Zhao, and J. A. Smith (2011), North Atlantic tropical storm frequency response to anthropogenic forcing: Projections and sources of uncertainty, *J. Clim.*, *24*, 3224–3238, doi:10.1175/2011JCLI3853.1.
Vinje, T. (2001), Anomalies and trends of sea-ice extent and atmospheric circulation in the Nordic Seas during the period 1864–1998, *J. Clim.*, *14*, 255–267, doi:10.1175/1520-0442(2001)014<0255:AATOSI>2.0.CO;2.
Wagner, W., V. Naeimi, K. Scipal, R. de Jeu, and J. M. Fernandez (2007), Soil moisture from operational meteorological satellites, *Hydrogeol. J.*, *15*(1), 121–131.
Wallace, J. M., I. M. Held, D. W. J. Thompson, K. E. Trenberth, and J. E. Walsh (2014), Global warming and winter weather, *Science*, *343*, 729–730.
Wang, C., S. Dong, A. T. Evan, G. R. Foltz, and S.-K. Lee (2012), Multidecadal covariability of North Atlantic sea surface temperature, African dust, Sahel rainfall, and Atlantic hurricanes, *J. Clim.*, *25*, 5404–5415, doi:10.1175/JCLI-D-11-00413.1.
Wang, G., S. Sun, and R. Mei (2011a), Vegetation dynamics contributes to the multi-decadal variability of precipitation in the Amazon region, *Geophys. Res. Lett.*, *38*, L19703, doi:10.1029/2011GL049017.
Wang, M., S. Ghan, M. Ovchinnikov, X. Liu, R. Easter, E. Kassianov, Y. Qian, and H. Morrison (2011b), Aerosol indirect effects in a multi-scale aerosol-climate model PNNL-MMF, *Atmos. Chem. Phys.*, *11*, 5431–5455, doi:10.5194/acp-11-5431-2011.
Wang, Y., P. Zhao, R. Yu, and G. Rasul (2010), Inter-decadal variability of Tibetan spring vegetation and its associations with eastern China spring rainfall, *Int. J. Climatol.*, *30*, 856–865, doi:10.1002/joc.1939.
Weiss, M., B. Van den Hurk, R. Haarsma, and W. Hazelger (2012), Impact of vegetation variability on potential predictability and skill of EC-Earth simulations, *Clim. Dyn.*, *39*(11), 2733–2746.
Weiss, M., P. Miller, B. J. J. M. van den Hurk, S. Ştefănescu, R. Haarsma, L. H. van Ulft, W. Hazeleger, P. le Sager, B. Smith, and G. Schurges (2014), Contribution of dynamic vegetation phenology to decadal climate predictability, *J. Clim.*, *27*, 8563–8577, doi:10.1175/JCLI-D-13-00684.1.

White, W. B., J. Lean, D. R. Cayan, and M. D. Dettinger, (1997), Response of global upper ocean temperature to changing solar irradiance, *J. Geophys. Res.*, *102*(C2), 3255–3266.
Wilcox L., E. J. Highwood and N. Dunstone (2013), The influence of anthropogenic aerosol on multi-decadal variations of historical global climate, *Environ. Res. Lett.*, *8*, 024033, doi:10.1088/1748-9326/8/2/024033.
Williams, K. D., A. Jones, D. L. Roberts, C. A. Senior, and M. J. Woodage (2001), The response of the climate system to the indirect effects of anthropogenic sulphate aerosol, *Clim. Dyn.*, *17*, 845–856.
Winton, M. (2008), Sea ice-albedo feedback and nonlinear Arctic climate change, in *Arctic Sea Ice Decline*, pp. 111–131, AGU, Washington, D. C.
Wu, P., N. Christidis, and P. Stott (2013), Anthropogenic impact on Earth's hydrological cycle, *Nat. Clim. Change*, *3*, 807–810, doi:10.1038/nclimate1932.
Xie, W.-P., B. Lu, and B. Xiang (2013), Similar spatial patterns of climate responses to aerosol and greenhouse gas changes, *Nat. Geosci.*, *6*, 828–832, doi:10.1038/NGEO1931.
Xie, Y., Z. Sha, and M. Yu (2008), Remote sensing imagery in vegetation mapping: A review, *J. Plant Ecol.*, *1*, 9–23, doi:10.1093/jpe/rtm005.
Zeng, N., J. D. Neelin, K.-M. Lau, and C. J. Tucker (1999), Enhancement of interdecadal climate variability in the Sahel by vegetation interaction, *Science*, *286*, 1537–1540, doi:10.1126/science.286.5444.1537.
Zhang, J. (2007), Increasing Antarctic sea ice under warming atmospheric and oceanic conditions, *J. Clim.*, *20*, 2515–2529.
Zhang, J., D. R. Thomas, D. A. Rothrock, R. W. Lindsay, Y. Yu, and R. Kwok (2003), Assimilation of ice motion observations and comparisons with submarine ice thickness data, *J. Geophys. Res.*, *108*(C6), 3170, doi:10.1029/2001JC001041.
Zhang, R., and T. L. Delworth (2006), Impact of Atlantic multidecadal oscillations on India/Sahel rainfall and Atlantic hurricanes, *Geophys. Res. Lett.*, *33*, L17712, doi:10.1029/2006GL026267.
Zhang, R., et al. (2013), Have aerosols caused the observed Atlantic multidecadal variability?, *J. Atmos. Sci.*, *70*, 1135–1144.
Zhu, Z., J. Bi, Y. Pan, S. Ganguly, A. Anav, L. Xu, A. Samanta, S. Piao, R. R. Nemani, and R. B. Myneni (2013), Global data sets of vegetation leaf area index (LAI) and fraction of photosynthetically active radiation (FPAR) derived from Global Inventory Modeling and Mapping Studies (GIMMS) Normalized Difference Vegetation Index (NDVI) for the period 1981 to 2011, *Remote Sens.*, *5*, 927–948.
Zunz, V. (2014), Antarctic sea ice variability and predictability at decadal timescales, PhD thesis, Université catholique de Louvain. [Available at http://dial.academielouvain.be/handle/boreal:150599.]
Zunz, V., H. Goosse, and F. Massonnet (2013), How does internal variability influence the ability of CMIP5 models to reproduce the recent trend in Southern Ocean sea ice extent?, *Cryosphere*, *7*, 451-468, doi:10.5194/tc-7-451-2013, 2013.